NELSON MANDELA UNIVERSITY

# IL-4/ IL-13 DIRECTED MICROGLIAL ACTIVATION AND DIFFERENTIATION IN RESPONSE TO LPS-INDUCED NEUROINFLAMMATION

By

Shiraz Ackerdien

*A dissertation submitted in fulfilment of the requirements for the degree of Master of Science in Human Physiology to the School of Biomolecular and Chemical Sciences, Faculty of Science, Nelson Mandela University*

Supervisor: Dr DC Ajonijebu

Co-supervisor: Prof GB Dealtry

April 2024

NELSON MANDELA UNIVERSITY

# DECLARATION BY CANDIDATE

**NAME: Shiraz Ackerdien**

**STUDENT NUMBER: 215132572**

**QUALIFICATION:** Master of Science (MSc) in Human Physiology

**TITLE OF PROJECT:**

**IL-4/ IL-13 DIRECTED MICROGLIAL ACTIVATION AND DIFFERENTIATION IN RESPONSE TO LPS-INDUCED NEUROINFLAMMATION**

**DECLARATION**:

In accordance with Rule G5.11.4, I hereby declare that the above-mentioned treatise/ dissertation/ thesis is my own work and that it has not previously been submitted for assessment to another University or for another qualification.

**SIGNATURE:**

**DATE: March 2024**

NELSON MANDELA UNIVERSITY

**PERMISSION TO SUBMIT FINAL COPIES**

**OF TREATISE/DISSERTATION/THESIS TO THE ASSESSMENT AND GRADUATION OFFICE**

***Please type or complete in black ink***

**FACULTY:** Science

**SCHOOL/DEPARTMENT:** Human Physiology

I, (surname and initials of supervisor) Dr. Ajonijebu D.C

and (surname and initials of co-supervisor) Prof. Dealtry G.B

the supervisor and co-supervisor respectively for (surname and initials of candidate) Ackerdien S.

(student number) 215132572 a candidate for the (full description of qualification)

Master of Science (MSc) in Physiology

with a treatise/dissertation/thesis entitled (full title of treatise/dissertation/thesis):

IL-4/IL-13 directed microglial activation and differentiation in response to LPS-induced neuroinflammation.

It is hereby certified that the proposed amendments to the treatise/dissertation/thesis have been effected and that **permission is granted to the candidate to submit** the final bound copies of his/her treatise/dissertation/thesis to the examination office.

_____ 8/3/2024

**SUPERVISOR** **DATE**

***And***

_____ _____

**CO-SUPERVISOR** **DATE**

## ACKNOWLEDGEMENTS

***In the name of God, the Most Beneficent, the Most Merciful***

First and foremost, I make ***shukr*** to my Creator for granting me the ability to fulfil this goal.

To my Supervisor, Dr C Ajonijebu, and my co-supervisor, Prof GB Dealtry, for your ongoing support, assistance, and encouragement. I am thankful for the honour to have studied under your guidance. Thank you for always believing in me, I am wholeheartedly grateful.

To Prof Davids, Mrs Prahladh, Mrs Fensham, and the rest of the Faculty of Physiology for their continuous support, guidance, and friendship throughout this journey.

To Dr Melanie Pereira and Dr Maleeha Fortuin-Seedat for your constructive guidance and assistance throughout this degree, for your incredible friendship and mentorship, I wholeheartedly appreacite you both so much.

To my loving and wise father, Achmat, my encouraging mother, Mymona, and my inspiration, Riaz, for your unwavering support, encouragement, and guidance throughout my studies. Shukran for showing me what unconditional love means daily, and for being my motivation throughout life. Shukran for always reminding me that with the Almighty by my side, anything is possible. There are no words that could ever describe my love and admiration for you all.

To my loving husband and soulmate, Abu-Taliep, for your unconditional love, emotional support, comfort, and commitment throughout this journey. I am so thankful to you for always believing in me even when I couldn't, and for picking me up when I needed you the most. I am so blessed to have you as my partner in this life. Shukran for being my biggest supporter, I love you and appreciate you with all my heart.

To my friend who has become family, Ashleigh, for making the long days in the lab bearable, for being my pillar of strength, and for a friendship that will last a lifetime.

To my wonderful additional parents, Yousuf and Zainap, my sister, Taybah, and the rest of my Cassim family, for your incredible love, support, and encouragement throughout this journey.

To the rest of my Ackerdien and Cassim family, and all my friends, for all your unwavering support and guidance throughout this journey, I appreciate you all so much.

The National Research Foundation and Nelson Mandela University for their financial support in helping me obtain this goal.

## TABLE OF CONTENTS

**List of abbreviations**

- AP1 - activator protein 1
- APC - antigen-presenting cell
- Arg1 - Arginase 1
- ATK/PKB - Protein kinase B
- ATP - Adenosine triphosphate
- BBB - Blood Brain Barrier
- BCSFB - blood- cerebrospinal fluid barrier
- BDNF - Brain-derived neurotrophic factor
- BLAST - Primer-Basic Alignment Search Tool
- BSA - Bovine serum albumin
- CCL - chemokine ligand
- CCL - Chemokine ligand
- CD - Cluster of differentiation
- cDNA - Complimentary deoxyribonucleic acid
- CNS - Central Nervous System
- Cq - quantification cycle
- CREB - c-AMP-responsive element-binding protein
- CSF - cerebrospinal fluid
- DAMPS - Damage- associated molecular patterns
- DMEM - Dulbecco's modified Eagle's medium
- DNA - deoxyribonucleic acid
- dsDNA - double-stranded DNA
- ELISA - Enzyme-linked immunosorbent assay
- FBS - Fetal bovine serum
- GAPDH - glyceraldehyde-3-phosphate dehydrogenase
- HRP - Horseradish peroxidase
- Iba1 - Ionized calcium-binding adaptor molecule 1
- IFN $\gamma$ - Interferon gamma
- IL - Interleukin
- IL4R$\alpha$ - Interlukin-4R alpha chain
- iNOS - inducible nitric oxide synthase

- IRF - interferon-regulatory factor
- JAK - Janus kinase
- JAK-STAT - Janus kinase-signal transducer and activator of transcription
- LBP - Lipopolysaccharide-binding protein
- LPS - Lipopolysaccharide
- M1 - classical activation
- M2 - alternative activation
- MAVS - mitochondrial anti-viral signalling
- MyD88 - Myeloid differentiation primary response 88
- NF-$_{K}$B - Nuclear factor kappa
- NG-2 - Nerve glia antigen- 2
- NLR - Nod-like receptors
- nm - nanometers
- NQR - Normalised relative quantitates
- NTC - no template control
- PAMPS - Pathogen-associated molecular patterns
- PBS - Phosphate buffered saline
- PCR - polymerase chain reaction
- $PGE_2$ - Prostaglandin E2
- PI3K - Phosphoinositide 3-kinase
- PM - primary microglia
- PPAR - peroxisome proliferator-activated receptor
- RNA - ribonucleic acid
- ROS - Reactive oxygen species
- RT-PCR - Reverse transcriptase-polymerase chain reaction
- SEM - Standard error of mean
- STAT - signal transducer and activator of transcription
- TGF - Transforming growth factor
- Th - Helper T cell
- TLR - Toll-like receptor
- $T_m$ - melting temperature
- TMB - 3,3',5,5'-Tetramethylbenzidine

- TNFα - Tumor necrosis factor-alpha
- TRIF - TIR-domain-containing adaptor- inducing beta interferon
- TYK - Tyrosine kinase
- γC - gamma chain
- IgG - Immunoglobulin G

**List of Figures**

## List of Tables

# ABSTRACT

Microglia activation is a common hallmark of neuroinflammation that occurs during pathogen invasion or lipopolysaccharide (LPS)-induced inflammation. A neuroinflammatory response is elicited by the release of proinflammatory cytokines which stimulates microglia in an autocrine manner to be polarized into classically activated, pro-inflammatory M1 cells. Prolonged exposure to the inflammatory response can have disastrous effects on the central nervous system (CNS). However, microglia can alternatively be polarized into the activated M2 anti-inflammatory phenotype, but the exact molecular mechanism mediating this phenotypic switch remains poorly understood. Studies have shown that interleukin (IL)-4 can induce the M2 phenotype and activate the signal transducer and activator of the transcription 6 (STAT6) signalling pathway that in turn provokes a beneficial Th2 immune response. Since IL-4 and IL-13 share a common IL-4 receptor alpha (IL-4Rα) chain, it is possible that alternative microglia differentiation and its anti-inflammatory action also involve IL-13. This study aimed to investigate how IL-13 and STAT6 signalling orchestrates the microglial response and differentiation associated with LPS-induced inflammation. Furthermore, the molecular mechanisms that relieve LPS-induced neuroinflammation and neural protection through IL-13-enhanced BDNF signalling were also investigated.

C8-B4 microglial cells were induced with LPS to exhibit an M1 pro-inflammatory phenotype or stimulated with IL-4 and/or IL-13 to exhibit an M2 anti-inflammatory microglial phenotype. The cell viability following LPS, IL-4, and/ or IL-13 exposure was determined. The LPS-induced neuroinflammatory response and the anti-inflammatory response induced by IL-4 and IL-13 which promotes STAT-6 signalling were determined by measuring TNFα, IL-1β, and BDNF protein concentrations using ELISA assays. The polarising effects of LPS and IL-4/IL-13 cytokines were also examined via changes in the expression of Iba-1, CD206, CD86, and STAT-6 determined by immunofluorescence analysis. These changes were further investigated by quantifying the mRNA transcripts of TNFα, IL-1 β, Arg-1, CD206, IL-4Rα, and STAT-6 and BDNF using qRT-PCR.

Therefore, the study demonstrated that LPS is a potent pro-inflammatory mediator that can switch microglia to attain an activated proinflammatory M1 phenotype. This was confirmed by the upregulation of TNFα and IL-1β secretion and gene expression following LPS treatments, and the positive expression of CD86. Furthermore, IL-4 and IL-13 are vital components of the Th2-mediated immune response and play a functional role in the alleviation of neuroinflammation. IL-4 and IL-13 cytokines can polarise the resting microglial cells to an alternatively activated anti-inflammatory M2 phenotype. This resulted in the positive fluorescence of CD206 expression and confirmed by increased mRNA transcripts of Arg-1 and CD206. In the presence of LPS, these M2 cytokines can promote the upregulation of signalling mediators required for downstream STAT-6 signalling in the activation of the JAK/STAT pathway. A peak intensity was observed in the cells exposed to co-treatment of IL-4 and IL-13, thus confirming an increased amount of the intracellular STAT6 downstream molecule. The role of IL-4Rα in mediating the phenotypic switch from M1 to M2 was highlighted in this study, as significant increases in IL-4Rα mRNA expression were observed in almost all cell cultures exposed to separate or combined treatments of IL-4 and IL-13. Furthermore, the presence of LPS treatment on cultures following treatments with IL-4/IL-13 cytokines revealed a synergistic effect on increased BDNF expression and secretion in response to the inflammatory insults.

# CHAPTER ONE

# LITERATURE REVIEW

## 1.1 Introduction

Understanding the central nervous system (CNS) inflammatory response has provoked a great deal of interest in recent years. Neuroinflammation has a well-known association with neurodegenerative diseases, such as Parkinson's disease, Alzheimer's disease, and multiple sclerosis (Werner & Engelhard, 2007). Neuroinflammation is also considered a hallmark of a protective mechanism against pathogenic substances (Sevenich, 2018).

Under homeostatic conditions, the brain is considered an "immune privileged" site. The first source of protection is implemented by the blood-brain barrier (BBB) which acts as a source of protection from intruding pathogens. Although microglia may not contribute to the key immune functions under normal conditions in the adult brain, this does not mean they remain inactive until disease or disruption occurs. Microglia are well-known to have numerous homeostatic functions including the phagocytic capability of expelling debris within the brain and monitoring of neuronal action. Additionally, it has been shown that microglia play vital roles in CNS inflammatory responses (Yin *et al*., 2017), however, the underlying mechanism through which they elicit an anti-inflammatory response remains underexplored.

Microglial cells, similar to peripheral macrophages, can be polarised to pro-inflammatory phenotypes (M1 phenotype) when induced by lipopolysaccharide (LPS) (Kettenmann & Hanisch, 2011). Concurrently, interleukins (IL)-4 and 13 can stimulate an alternative activation and polarisation of the M2 phenotype which provokes an anti-inflammatory response (Mosser & Edwards, 2008). Therefore, the polarisation of M1/M2 microglia is important in understanding the resolution of neuroinflammation in the CNS.

IL-4 and IL-13 are functionally associated cytokines, which play a role in various immune functions such as initiating type II inflammatory responses and by investigating IL-4 and IL-13 directed microglial activation in response to LPS-induced inflammation, the underlying molecular and cellular processes involved in the M2 microglia anti-inflammatory phenotype will be revealed. Investigating the IL-4/IL-13

and signal transducer and activator of transcription 6 (STAT-6) signalling cascade events is proposed to offer deeper insights into the functional roles of T-helper 2 (Th2) immunity. Furthermore, exploring the mechanisms involved in IL-13 enhanced BDNF function in neural protection will also indicate ways to alleviate and resolve LPS-induced neuroinflammation.

## 1.2 The central nervous system

The CNS consists of two major components, the brain and spinal cord, which undertakes a significant role in monitoring and coordinating internal organs and responding swiftly to alterations in the environment (Louveau *et al.,* 2015). As a result, the CNS is one of the most well-known immune privileged locations in the body which needs protection from endogenous and exogenous threats (Ransohoff *et al*, 2003). The term ‘immune privileged site’, originated in the mid-twentieth century when multiple physiological characteristics of the CNS were believed to underlie the various immune responses in the brain.

Structurally, the CNS is safeguarded by the meninges and cerebrospinal fluid (CSF) that encompass the brain and the spinal cord (Ransohoff *et al.,* 2003). The meninges, consisting of the pia mater that conceals the parenchyma, a non- vascularised arachnoid mater, and a densly vascularised dura mater, anchors to the skull. The BBB monitors movement into the CNS by restricting admission to the brain to numerous blood-borne immune and inflammatory cells (Sevenich, 2018). Moreover, it is the role of the microglia, astrocytes, and many other resident immune cells of the CNS, to maintain tissue homeostasis and further defend against pathogenic entities (Reemst *et al.,* 2016). Hence, potentially damaging substances are unable to readily access the CNS.

## 1.3 The brain's immune system

Brain cells are divided into two types of cells: neurons and glial. Neurons are electrically excitable cells, which function by obtaining, processing, and transmitting information through chemical signals and electrical impulses (Ludwig *et al.,* 2022). Neurons interact with one another employing functional connections called synapses. Glial cells are the most populated cells residing in the CNS and perform varying

functions (Jäkel & Dimou, 2017). Their interaction does not involve direct synaptic transmission or electrical signalling but is still able to maintain synaptic connections and neuronal signalling. Glial cells contribute to structural and functional support within the CNS and can be subdivided into four main cell types: oligodendrocytes, astrocytes, microglia, and oligodendrocyte progenitor cells – nerve glial antigen-2 (NG2) (Dimou and Gallo, 2015). Oligodendrocytes carry out their function by forming myelin sheaths around neurons which influences the speed of action potential conduction (Mazuir *et al., 2021*). Astrocytes preserve a suitable chemical environment for neuronal signalling. Microglia activation and functions in overall brain homeostasis are considered to be the hallmark of numerous brain pathologies associated with neuroinflammation (Jessen, 2004). NG2-glia are capable of sensing gaps between the neuronal cells through their filopodia and when stimulated, NG2-glia cells can migrate to fill these gaps (Jessen, 2004).

### 1.4 Neuroinflammation

Inflammation has been associated with the progression and pathogenesis of numerous neurodegenerative diseases, such as Parkinson's disease, lateral sclerosis, and Alzheimer's disease (Chen *et al*., 2016). Each of these diseases exhibits complex cross-talk linking the inflammatory response in the brain and neurodegeneration. The term 'neuroinflammation' was first used in the 1990s as a phenomenon by which an inflammatory response is elicited by the brain and spinal cord as a byproduct of neurological disorders (Chen *et al*., 2016). Neuroinflammation is commonly known to be deleterious for neurological function and is frequently associated with neurodegenerative diseases, as previously mentioned (Werner & Engelhard 2007).

Lipopolysaccharide (LPS), frequently known as endotoxin, is an immunogenic molecule located in the outer surface of Gram-negative bacteria, which triggers a potent inflammatory response. Therefore, LPS is widely used as an effective pro-inflammatory agent applied in both *in vivo* and *in vitro* studies. Living organisms are continuously exposed to pathogenic or non-pathogenic bacteria, and Gram-negative bacteria can result in the onset of many infectious diseases, such as salmonellosis and brucellosis (Gorman & Golovanov, 2022). Exposure to LPS can result in the

disruption of the BBB, allowing inflammatory immune cells to enter the CNS. Prolonged exposure to LPS molecules results in the activation of microglia, which can recognise LPS induced neuroinflammatory cells by the presence of Toll-like receptor 4 (TLR4) on the exterior of microglia (Ranoa *et al.,* 2013). When circulatory LPS molecules enter the CNS, they are entrapped by acute-phase proteins called lipopolysaccharide-binding protein (LBP) and transmitted to the cluster of differentiation-14 (CD14) molecule on the surface of certain cells, which displays the LPS molecule to TLR4. As a result, TLR4 binds the ligand, and homodimerization of TLR4 occurs, activating downstream signalling pathways, namely, both TIR-domain-containing adaptor-inducing beta interferon (TRIF) and myeloid differentiation primary response 88 (MyD88) dependent pathways (Peri & Calabrese, 2014). When TLR4 is expressed on the surface of the cell, signalling of the MyD88-dependent pathway occurs. Additionally, upon ligand binding, TLR4 exhibits the ability to be endocytosed. Once internalization to an endosome occurs, TLR4 signals via the TRIF-dependent signalling pathways are activated. The dual activation pathways simultaneously provide an effective pro-inflammatory response to the bacterial infection. Overall, TLR4 stimulation promotes the generation of cytokines and chemokines such as IL-6, IL-1β, IL-8, tumor necrosis factor alpha (TNFα), reactive oxygen species (ROS), prostaglandin E2 ($PGE_2$), nitric oxide (NO) and type I interferons (Kany *et al.,* 2019).

Excessive exposure to pro-inflammatory cytokines and ROS can lead to oxidative stress and neuronal damage, leading to the onset of neurodegeneration (Cobb & Cole, 2015). Furthermore, neuroinflammation can disrupt the balance of neurotransmitters in the brain, resulting in excitotoxicity, which may result in overstimulation of neurons and consequent cell death. Chronic neuroinflammation results in the accumulation of abnormal protein aggregates, such as amyloid-beta and tau, both hallmark characteristics of neurodegenerative conditions such as Parkinson's and Alzheimer's disease.

However, inflammation concurrently acts as a protective mechanism against different pathologies in the CNS (Sevenich, 2018). Thus, neuroinflammation serves as a fundamental local immune reaction to shield the body from infectious pathogenic substances or tissue injury that may have infiltrated the CNS (Sevenich, 2018).

At the initial stages of neurodegenerative diseases, neuroinflammation enables cells residing in the CNS to clear infection and manage the disease progression (DiSabato *et al.,* 2016). The neuroinflammatory response is elicited by the release of proinflammatory cytokines, chemokines, and ROS, activated by microglia and astrocytes (Kempuraj *et al*., 2016). Once the inflammatory response is initiated, the microglia and astrocytes secrete neuropeptides and anti-inflammatory cytokines, to safeguard neurons against neuroinflammation, and further lessen the symptoms of neurodegenerative diseases (More *et al*., 2013).

Due to the detrimental effect of neurodegenerative disease on the brain, inflammatory mediators can intersect the defective BBB and enter the periphery to recruit immune cells to the brain which further promotes neuroinflammation (Kempuraj *et al*., 2016). Thus, it is now well-recognised that various innate and adaptive inflammatory processes occur both in the brain and the periphery, though the precise mechanisms and their role in disease progression are still poorly understood and thus further work is required to identify these issues (Kempuraj *et al*., 2016).

### 1.5 Mechanisms of protective immunity in the CNS

There exists a range of physical injuries to the CNS and pathogenic microbes that enter the CNS, which may result in significant morbidity and mortality. For this reason, the arrangement of the CNS allows it to be protected by a physical structure against pathogenic entities. As mentioned previously, the CNS is safeguarded from injury by skeletal structures; the cranium and vertebrae, which is encompassed by the meninges and enveloped by CSF. The meninges (Figure 1) consist of the outer dura mater, arachnoid mater, and inner pia mater (Engelhardt & Ransohoff, 2012). The subarachnoid space, which divides the arachnoid mater and pia mater, contains CSF produced by the choroid plexus located in the ventricles of the brain. The CSF functions in mechanical support, regulates ionic composition, and governs chemical stability (Weller, 2013).

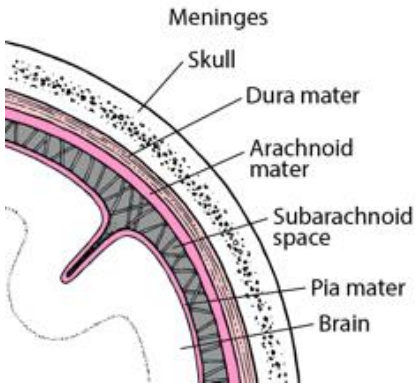


**Fig. 1: Meninges consisting of the dura mater, arachnoid mater, and pia mater**
(Greenlee, 2023)

The multifaceted operations of the brain are reliant on homeostatic systems that maintain the ionic balance of the surrounding environment. The regulation of homeostatic control is governed by two cellular barriers that divides the CNS from systemic circulation (Takeshita & Ransohoff, 2012). The presence of these barriers, the BBB and the blood-cerebrospinal fluid barrier (BCSFB) safeguards the brain from changes in blood composition, controls nutrient delivery and removal of metabolites, and protects the CNS from microbe invasion (Archie *et al.,* 2021). The arrangement of the BBB consists of endothelial cells that line the cerebral micro-vessels correlating to the astrocytes, pericytes, and basement membrane (Geier *et al.,* 2013). The pericytes and astrocytes, both form the adjoining membrane barrier.

The formation of a physical barrier is accomplished by complex junctions at the inter-endothelial cleft that tightly regulate the channel of ions and molecules from systemic circulation. The complex junction at the inter-endothelial cleft is composed of adherens and tight junctions, which encompass the BBB. These junctions function by obstructing the transport of certain molecules and restricting paracellular permeability across the BBB (Archie *et al*., 2021).

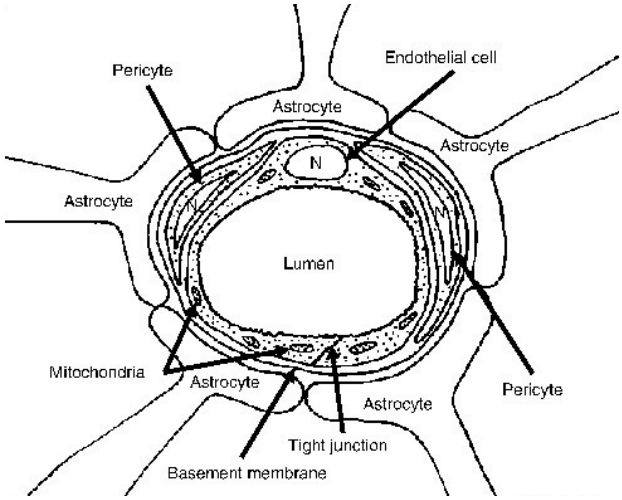


**Fig. 2: Complex junctions at the inter-endothelial cleft encompassing the BBB**
(Adopted from Avraham*, et al*., 1970)

Additionally, resident cells of the CNS can elicit numerous immune responses against invading pathogens. Varying neural cell types, such as astrocytes, neurons, oligodendrocytes, and microglia, proficiently elicit and respond to inflammatory detection as a result of infection (Nair & Diamond, 2015). As mentioned previously, the electrically excitable neurons process and convey information by chemical and electircal signalling. The glial cells, namely the astrocytes, and oligodendrocytes, maintain CNS homeostasis, assist and safeguard neurons, and improve neurotransmission through chemical and physical insulation. The ontogenetically well-defined microglial cells, composed of the reticuloendothelial system that operates as macrophages in the CNS, are resident cells that act as the first responders to pathogenic invasion (Drokhlyansky *et al*., 2017). Together, these resident CNS cells display TLR, Nod-like receptors (NLR), and mitochondrial anti-viral signalling (MAVS), which upon activation, promotes the defence against viral pathogens in the CNS (Reinert *et al.,* 2016).

## 1.6 Roles of microglia in CNS immunity

Microglia are a heterogeneous population of brain-resident immunocompetent cells. Along with the CNS-infiltrating macrophages, microglia serve as the initial line of defense against pathogenic invasion and regulate a variety of important immunological programs involving both innate and adaptive immunity (Yin *et al.,* 2017). While mediating responses to pathogens and injury, microglia can become

active and alter their transcriptional form to exhibit phagocytic clearing ability, and propagate inflammatory signals, including cytokines (such as TNF-α, IL-1β), chemokines and redox proteins that help defend neuronal tissue (Kempuraj *et al*., 2016; Frank-Cannon *et al.,* 2009; Colton 2009). Usually, microglial-mediated adaptive host responses to insults are considered normal and beneficial, except when they become primed and provoke inflammatory responses that significantly interrupt brain homeostasis, which may lead to severe neurodegenerative and/or neurobehavioral complications (Norden *et al.,* 2016). According to Colton (2009), microglia can restore tissue homeostasis by altering their functional phenotype to decrease pro-inflammatory signals and promote the secretion of anti-inflammatory cytokines, and other brain-specific cytoactive repair factors.

In general, microglia maintain their residence in the CNS by self-renewal and require minimal contribution from blood cells (Ginhoux *et al.,* 2010). In recent years, it has been discovered that microglial cells emerge from embryonic yolk sac mesodermal precursors, and both microglia and macrophages stem from myeloid cells such as monocytes. Hence, microglia and macrophages share phenotypic characteristics (Li & Barres, 2018). Microglia also functions significantly in immune surveillance, monitoring neuronal health by synaptic scanning, controlling synaptic transmission, and stimulating neurogenesis by discharging apoptotic neurons that are unable to assimilate into the complex neuronal network (Ekdahl *et al.,* 2009).

Furthermore, microglia functions in immune surveillance and motility. A study conducted by Nimmerjahn *et al*. (2005) using *in vivo* two-photon imaging of the neocortex, found that microglia can actively respond even when induced in their resting state. They can monitor subtle changes through a variety of surface receptors and continuously keep their microenvironment under immune surveillance using motile protrusions (Nimmerjahn *et al.,* 2005). When a disruption in the BBB or a change in brain homeostasis is detected, adjacent microglia are immediately activated and deploy themselves to the site of injury. Microglia then demonstrate a neuroprotective function, in which they shift their patrolling actions to shield the wounded site. This was demonstrated in an ischemic brain model, which displayed that microglia protrusions created a barrier between the unaffected and injured tissue (Wake *et al.,* 2009).

## 1.7 M1/ M2 Polarization of macrophages and microglia

When infection arises, circulating monocytes together with tissue-resident precursors give rise to macrophages, that migrate to sites of inflammation, and immune cells are recruited to relieve the inflammatory state (Geissmann *et al*., 2013). Macrophages are highly specialized and display phenotypic heterogeneity, allowing them to react differently according to different biological stimuli (Fortuin-Seedat *et al*., 2018; Daigneault *et al*., 2010). Hence, their function may vary depending on the tissue they reside in. Additionally, they can alter their gene expression profile on exposure to new tissue environments (Gordon & Martinez-Pomares, 2017).

Pathogen-associated molecular patterns (PAMPS) or damage-associated molecular patterns (DAMPS) can promote the stimulation of resting macrophages via activation of Adenosine triphosphate (ATP) receptors or TLRs. Consequently, activation of resting macrophages leads to classically active M1 macrophages when exposed to LPS, and interferon (IFN)-γ (Caballero-Herrero *et al*., 2023). M1 macrophages yield pro-inflammatory chemokines and cytokines such as ROS, NO, chemokine ligand 2 (CCL2), IL-1β and TNFα, and play a key role in maintaining tissue homeostasis, tissue remodeling, immune surveillance, elimination of pathogenic entities and inflammatory regulation (Chen *et al*., 2023). Additionally, Th2-derived cytokines, such as IL-4 and IL-13, may stimulate the alternative activation of M2 macrophages (Chen *et al*., 2023). On the cell surface, M2 macrophages express arginase-1 (Arg-1), CD36, CD163, and CD206 and elicit the anti-inflammatory cytokine IL-10 which can suppress M1 macrophage-mediated inflammatory response (Chen *et al*., 2023).

Vital players involved in macrophage polarization are transcription factors such as signal transducers and activators of transcription (STAT)s, interferon-regulatory factor (IRFs), peroxisome proliferator-activated receptor (PPAR)-γ, c-AMP-responsive element-binding protein (CREB), nuclear factor (NF)-κB, and activator protein 1 (AP1). When these molecules interact, they stimulate macrophage phenotypic switching on various inflammatory diseases (Li *et al.,* 2018).

Numerous macrophage-associated markers are expressed by microglial cells, namely, CD11b, CD14, CX3C chemokine receptor 1 (CX3CR1, fractalkine receptor), and ionized calcium-binding adaptor molecule-1 (Iba-1) (Franco-Bocanegera *et al.,*

2019). Microglial cells, as opposed to other CNS resident cells, are derived from hematopoietic stem cells in the yolk sac and act as the first responders for pathogen invasion or injuries in the CNS (Casli & Reed-Gaeghan, 2021). Hence, microglia act similarly to macrophages to sustain and promote tissue homeostasis and protect the CNS against infection and injury. (Casli & Reed-Gaeghan, 2021).

As shown in Figure 3, microglial cells respond similarly to macrophages and can polarise the resting mycroglia to exhibit the M1 phenotype following stimulation with LPS and IFN-γ, resulting in the production of pro-inflammatory cytokines, namely, TNFα, IL-6, IL-1β, CCL2, ROS, and NO (Franco-Bocanegera *et al.,* 2019). Furthermore, IL-4 and IL-13 can induce alternative activation and polarization of M2 microglia which stimulate M2 markers and the anti-inflammatory cytokine, IL-10 (Scott *et al.,* 2023). Therefore, the M1/M2 polarization of microglia is vital in understanding the balance between resolution or promotion of neuroinflammation in the CNS.

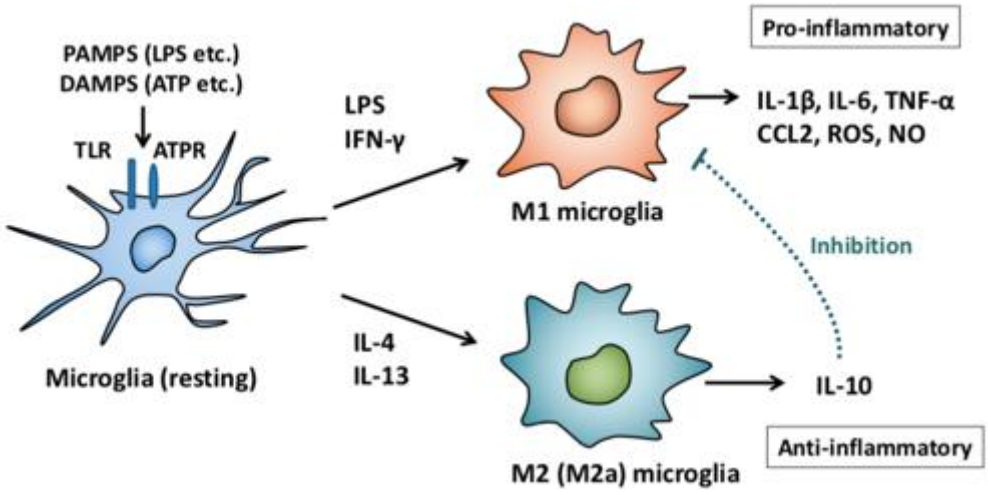


**Fig. 3: Immunoregulatory functions of M1/M2 microglial polarization** (adapted from Nakagawa and Chiba, 2014)

### 1.7.1 Pro-inflammatory M1 stimulation

LPS, a bacterial endotoxin, is the essential structural component of the outer membrane of gram-negative bacteria and operates as a powerful virulent influence. Classical and alternative macrophage activation represent two complementary and overlapping functional states. A previous study has shown that IFN-γ, with the

deactivation of transforming growth factor (TGF)-β and IL-10, activated the classical activation of M1 macrophages (Maldonado *et al.,* 2016). This is distinct from the alternative M2 activation induced by anti-inflammatory IL-4 or IL-13 cytokines that ultimately promote wound healing (Maldonado *et al.,* 2016).

Various experimental models have indicated that the M1 response is characterised by exposure to products derived from bacterial substances such as LPS, which induce inflammation (Martinez & Gordon, 2014). Thus, LPS is commonly used in experimental models to induce neuroinflammation, which results in increased microglial activation. (Fan *et al*., 2015). The pro-inflammatory LPS stimulation promotes microglial activation through the TLR-4 where, in the CNS, TLR4 is a specific LPS receptor as well as primarily expressed in the microglia (Schafer *et al.,* 2013). Upon stimulation, microglia phenotypically change from resting branched cells to the phagocytic amoeboid form, initiating transcriptional activation of microglial growth factors, phagocytic markers, cytokines, NO, and free radicals, which contribute to the immune response to inflammation or injury of the CNS (Maguire *et al*., 2022).

### 1.7.2 Anti-inflammatory M2 activation

The M2 anti-inflammatory phenotype expresses receptors with the ability to safeguard the immune system and its supporting tissues from inflammation by aiding the release of protective and trophic factors which can further stimulate anti-inflammatory and immunosuppressive responses (Park *et al.,* 2016). Studies have shown that the M2 phenotype exhibits an array of proteins differentially expressed, which apart from its anti-inflammatory wound healing properties, promote the Th2 immune response. Concurrently with the pro-inflammatory M1 response, M2 microglia enhances the activities of anti-inflammatory mediators, contributing both to wound healing and clearing of debris by phagocytosis (Alvares *et al.,* 2016).

A specific M2 markers such as CD206, which consists of a receptor focused on endosomal and cellular and membranes, function in endocytosis by detecting pathogenic polysaccharide chains and glycoproteins (Ohgidani *et al.,* 2017). The M2 phenotype results in the secretion of anti-inflammatory cytokines such as IL-4, IL-13 TGFβ, and IL-10, as well as IL-4 and IL-13 receptor antagonists (IL-4Ra). The M2 phenotype further promotes the release of chemokines such as CCL2, CCL22,

CCL17, and CCL24, which together with the secreted cytokines, aim to relieve the inflammatory insult (Biswas & Mantovani, 2010).

As seen in Figure 4, a cell surface maker specific to the M2 phenotype is the enzyme Arg1, which contributes to wound healing (Rossi *et al*., 2018). Arg1 is an enzyme which converts arginine, an mino acid into ornithine and urea, which are then metabolised to polyamides and proline, required for wound healing and tissue repair (Rossi *et al*., 2018). Arg 1 has been shown to outcompete inducible nitric oxide synthase (iNOS) and competitively downregulate the production of nitric oxide.

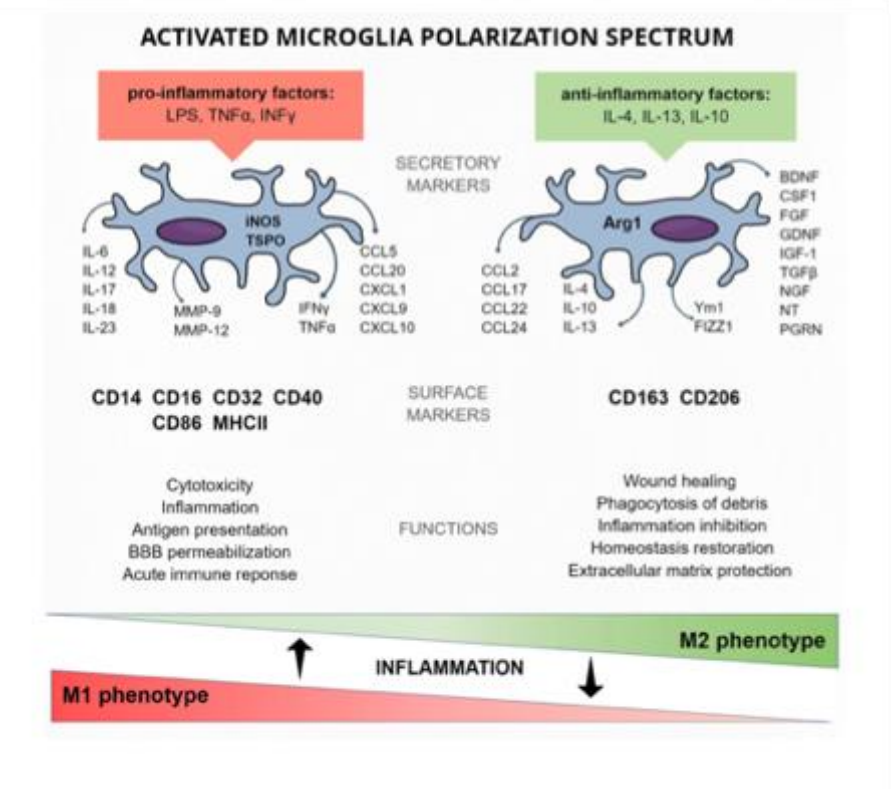


**Fig. 4: Activated microglial pro-inflammatory M1 and anti-inflammatory M2 markers** (Adopted from Jurga *et al*., 2020)

## 1.8 IL-4/ IL-13 receptor complex and induction of alternate M2 phenotype.

IL-4 and IL-13 are closely linked structurally and functionally associated cytokines, involved in various immune functions such as initiating the type II inflammatory response (McCormick & Heller, 2015). Both IL-4 and IL-13, form a short four α-helix bundle sharing a 25% sequence similarity (McCormick & Heller, 2015), encoded by bordering genes with mutual *cis*-acting transactivating regulatory domains (Bao & Reinhardt, 2015). These two cytokines share receptor subunits and signalling

molecules, stimulating coinciding, yet distinct, biological reactions during the type 2 immune response. The signalling of IL-4 and IL-13 occurs via cell surface receptor consisting of heterodimeric structure. Countless cell signalling mediators and transcription factors, associate to facilitate the physiological and pathophysiological effects of these cytokines.

The IL-4/ IL-13 signalling arises from two heterodimeric transmembrane receptor complexes; the type I receptor, which binds soley to IL-4 and includes the IL-4Rα and common gamma chain (γC) subunits; and the type II receptor, which binds both IL-4 and IL-13 and consists of the IL-4Rα and IL-13Rα1 subunits (McCorrnick & Heller, 2015). Therefore, the limited presence of the type I receptor on a specific cell restricts responsiveness to IL-4, however the type II receptor facilitates signalling for both IL-4 and IL-13 (Heller *et al.,* 2012). Therefore, the binding of IL-4 to IL-4Rα occurs in a highly precise, species -specific manner with a high affinity ($K_D$ = 20–300 nM) (McCorrnick & Heller, 2015), recruiting either the common γC or IL-13Rα1. Comparatively, the γC and IL-13Rα1 subunits exhibit a lower affinity in comparison to the IL-4-IL-4Rα complex ($K_D$ = 500 nM) (Gour & Wills-Karp, 2015). Hence, the signalling pathway activated in responding cells is determined by the presence of the chain on each cell surface.

The expression of IL-4Rα and IL-13Rα1 chains are expressed at minimal levels across most cell types, where the γC chain is predominantly situated on hematopoietic immune cells. The binding of IL-4 to the type I receptor complex triggers Janus kinase (JAK)1/3 phosphorylation, subsequently phosphorylating tyrosine in the IL-4Rα cytoplasmic domain (Seif *et al.,* 2017). This sequence of events creates docking sites for STAT6 and/or insulin receptor substrate 2 (IRS-2) (Figure 3). Thus, STAT6 and IRS-2 are recognized as the principal pathways involved in IL-4/-13 responsiveness, although other cell types activate STAT3 and other STATs. The tyrosine phosphorylation of STAT6 stimulates STAT6 homodimerization, gene transcription, and nuclear translocation. Additionally, IRS-2 tyrosine phosphorylation activates phosphoinositide 3-kinase (PI3-K) (Ruckerl *et al*., 2012), protein kinase B (AKT) (Landis *et al.,* 2014), and NF-κB-driven activation of the cell cycle, gene transcription, survival and proliferation (Jenkins *et al.,* 2013).

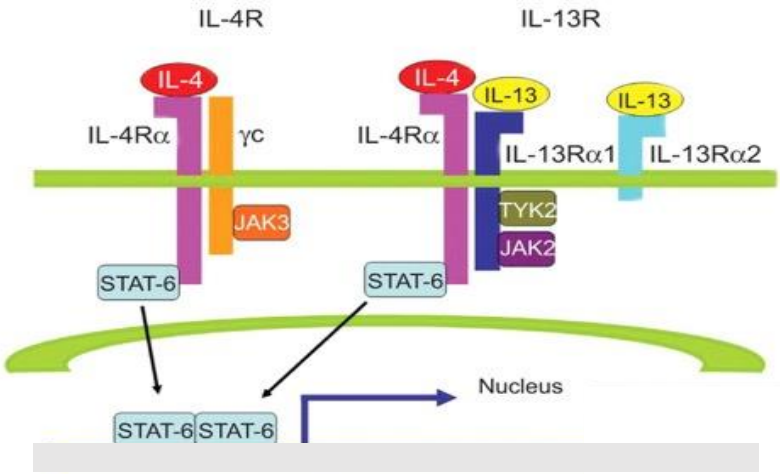


**Fig. 5: The IL-4 and IL-13 receptor complex** (Adapted from Oh *et al.,* 2010)

Additionally, to functioning as the subunit for the type II IL-4 receptor, IL-13Rα1 also serves as a subunit responsible for binding IL-13. IL-13 binds IL-13Rα1 with moderate affinity ($K_D$ = 30 nM), inducing the recruitment of the IL-4Rα subunit. Consequently, when IL-13 binds to the type II receptor, it promotes the activation of Janus kinase 2/Tyrosine kinase 2 (JAK2/TYK2), along with STAT6, STAT3, and STAT1. This activation leads to STAT dimerization and nuclear translocation leading to gene transcription activation (Figure 3).

The binding of STAT-6 to the phosphorylated receptor enables the activated kinases to phosphorylate its C-terminal domain, initiating downstream intracellular signalling cascade events (Hu *et al*., 2021). Once activated, STAT-6 is released from binding to the receptor, and via interactions with the phosphorylated C-terminal domain, forms homodimer components (Hu *et al*., 2021). The STAT-6 homodimers then travel to the nucleus and bind to distinct DNA motifs in the promotors of responsive genes, enhancing transcription. Additionally, signalling of IL-4 via the IL-4Rα chain promotes the PI3K pathway and the IRS signalling pathway and further provokes microglia/macrophage differentiation (Keegan *et al.,* 2018).

This in turn enhances phagocytosis, upregulation of Arg 1, and inhibition of NF-κB induced by classical macrophages (Sica & Mantovani, 2012). Despite this well-known role of the IL-4/IL-4Rα signalling pathway in the stereotypical induction of anti-inflammatory M2 phenotype, the exact contribution by IL-13 to this phenotypic

switching remains underexplored. A recent study validated that immune-driven cognitive functions are not only limited to IL-4 producing T cells; but rather involve a complex cascade of immunological signalling that includes the recruitment of IL-13 for optimal acquisition of learned tasks (Brombacher *et al.,* 2017). It is further believed that both sister cytokines share complementary functions in facilitating astrocytes in producing brain-derived neurotrophic factor (BDNF) (Brombacher *et al.,* 2017; Derecki *et al.,* 2010), vital for cellular survival and growth as well as cellular plasticity (Bathina & Das, 2015). Having established the importance of IL-4/IL-4Rα/STAT6 signalling in the induction of the alternative M2 phenotype, it remains unclear how IL-13/BDNF signalling via the STAT-6 intracellular pathway mediates cellular protection and enables the anti-inflammatory modality of microglia, the parenchymal macrophages.

## 1.9 Problem Statement

Microglia and CNS infiltrating macrophages are mononuclear phagocytes that are increasingly recognized for their importance in neural development, homeostasis, and neurodegenerative disorders. During the pathogenic invasion of the CNS parenchyma or LPS-induced inflammation, microglia become activated and plastically change form (Rossi *et al.,* 2018). Microglia differentiation from the pro-inflammatory M1 phenotype to the protective M2 phenotype now constitutes the focus of most prominent therapies used to revert or halt the progression of neurodegeneration or neuroinflammatory-related diseases (Jeong, *et al.,* 2013). Despite this, the phenotypic alteration of microglia phenotype in response to inflammatory insult appears complex and is not well understood. Even though studies have implicated IL-4 in the resolution of local inflammation via induction of the anti-inflammatory M2 phenotype, less is known about the Th2 effector response involving IL-13 which shares a common heterodimeric IL-4Rα chain with lL-4. Since it has also been established that STAT6 deficiency favours the shift of microglia towards the adverse phenotype (Cai *et al*., 2019), the exact molecular mechanism linking the STAT6 signalling pathway to the anti-inflammatory modality of microglia dependent on IL-13/ BDNF neuroprotective responses remains unresolved.

## 1.10 Study Rationale

Neuroinflammation has a dual role in the CNS by eliciting both beneficial and harmful effects (DiSabato *et al.,* 2016). Attributes of neuroinflammation vary depending on the course and duration of the inflammatory response. This is vital in understanding the physiological, biochemical, and behavioral consequences that may occur as a result. Microglia are considered the innate immune cells of the CNS and function in mediating the inflammatory response (DiSabato *et al.,* 2016). However, evidence has shown that microglia can also be polarized into the M2 anti-inflammatory phenotype involved in resolving the inflammatory response. The underlying molecular mechanisms and signalling pathways stimulating the microglial M2 anti-inflammatory response remain unclear and therefore need to be investigated (Kaminska *et al.,* 2016).

### 1.11 Aims and Objectives

This study aims firstly to investigate how IL-4/13 and STAT6 signalling orchestrates microglia response activation and differentiation to LPS challenge. Secondly, the underlying molecular mechanisms involving the resolution of LPS-induced inflammation and neural protection through IL-13 enhanced BDNF signalling will also be investigated.

The following objectives have been formulated to achieve the aims:

1. To culture and maintain the murine C8-B4 microglia cell line.
2. To investigate the effects of IL-4 and IL-13 stimulation on LPS-treated and untreated C8-B4 microglial cells and examine the cells' response through endogenous production of TNFα, IL-1β, and BDNF using the ELISA technique.
3. To examine LPS-induced inflammatory changes in C8-B4 cells and possible polarizing effects of exogenous IL-4 and IL-13 cytokines via expression of Iba1, CD206, CD86, STAT6, and related cell surface markers by immunohistochemistry.
4. To identify and compare the IL-4 or IL-13 induced alternative M2 phenotype through molecular quantification of mRNA transcripts of TNFα, IL-1 β, Arg1, CD206, IL-4Rα, and STAT-6 in LPS treated and untreated cells using the reverse transcriptase-polymerase chain reaction (RT-PCR). Also, the linkage of this phenotypic expression to neuroprotection or neuroinflammation will be determined by examining BDNF transcripts in the cells.

## 1.12 Potential benefits of this study

1) Novel therapeutic agents: The investigation of IL-4 and IL-13 mediated anti-inflammatory responses may identify potential therapeutic targets for novel anti-inflammatory drug development. Identifying the molecular downstream IL-4/13/ STAT-6 signalling pathways at the cellular level is vital for the development of therapeutic interventions in mediating the anti-inflammatory response.
2) Neuroprotective effects: Understanding the effect of IL-4 and IL-13 induced M2 microglia may uncover neuroprotective effects, which could promote neuronal survival and reduce neurotoxicity by investigating the response through BDNF secretion.
3) Validation of *in vitro* models: Using the C8-B4 murine microglial cell line as an *in vitro* model for understanding neuroinflammation and cytokine-directed responses contributes to the refinement of experimental models. This promotes the reproducibility and reliability of future studies.
4) Pre-clinical screening for therapeutic agents in reducing inflammation: The use of in vitro studies using the microglial cell line can form the basis for screening potential therapeutic agents that target microglial activation in the CNS.
5) Foundation for future studies: Understanding the LPS induced neuroinflammatory effects and the counteractive IL-4/ IL-13 mediated anti-inflammatory response can provide insight for future *in vivo* investigations. This includes the use of animal models to validate and expand the findings in a more complex biological context.

# CHAPTER TWO

# MATERIALS AND METHODS

## 2.1 Murine C8-B4 microglial cell line

Biomedical research exploring microglia's role in neurodegeneration, toxicology, and immunity is a growing area of research which requires extensive animal use. To expedite research and reduce the need animal experimentation, using a microglial cell line is essential, provided that the cell line accurately replicates the primary microglia (PM) with high fidelity (Slanzi *et al*., 2020). Among many widely used rodent microglial cell lines, the C8-B4 microglia cell line is the most prevalent, displaying reported similarities in characteristics to primary microglia (Figuera-Losada *et al.,* 2014). Therefore, in this study, the C8-B4 microglial cell line was used.

Microglia are generally considered to be intraparenchymal brain macrophages which constitute a major component of the CNS, as they compose 10% of all cell types in the adult mouse brain (Ochacka & Kaminska, 2021). Derived from monocytes, microglia are colonised by circulating monocytes infiltrating the brain on pathological incidents such as neuron apoptosis. Therefore, it is commonly viewed that microglial cells are derived from the same hemopoietic lineage as peripheral macrophages (Geissmann *et al.,* 2010).

The presence of ameboid microglia occurs during post-natal days 6–8 of development, and these develop into branched microglial cells. Therefore, microglia are characterised as of mesodermal origin (Giessmann *et al.,* 2010).

The clonal murine C8-B4 microglial cell line was obtained from explant 8-day postnatal mouse cerebella cultures, undergoing spontaneous *in vitro* transformation. This multistage derivation involved the appearance of slowly proliferating foci with diverse morphologies, which appeared after 4 months, and became an increasingly enriched population exhibiting a homogenous microglial appearance.

### 2.1.1 Retrieving cells from cryopreservation.

Cryopreserved C8-B4 microglial cells were removed from storage in liquid nitrogen and thawed on ice. The cells were transferred to a 15 mL tube (LabSelect, SA) and

centrifuged using the Eppendorf Prism Micro Centrifuge (Labnet, USA) at 1300 rpm for 5 minutes. The supernatant was removed, and cells were resuspended in 1 mL of pre-warmed complete growth medium. The cell suspension was pipetted up and down for accurate mixing and transferred dropwise to a 25 $cm^2$ flask containing 6 mL pre-warmed media, or a 75 $cm^2$ flask containing 14 mL pre-warmed media. To remove all cells from the cryopreservation vial, the vial was washed with 1 mL pre-warmed media, and this was transferred to the culture flask. Thereafter, the cells were placed in a humidified incubator (Spellbound Laboratory Solutions, SA) incubated at 37°C with an atmosphere of 5% $CO_2$ and 95% air.

### 2.1.2 Cell culture maintenance

The C8-B4 murine microglial cell line (Passage 6) (ATCC, SA) was routinely maintained as a monolayer culture in 25 $cm^2$ or 75 $cm^2$ tissue culture-treated flasks (LabSelect, SA) enabling the cells to adhere to the base of the flask. The cells were grown in complete growth medium consisting of high glucose Dulbecco's Minimal Essential Medium (DMEM) (Biowest, SA) supplemented with 10% heat-inactivated foetal bovine serum (FBS) (Biowest, SA). The cells were routinely sub-cultured three times a week, maintained between a cell density of $1 \times 10^5$ and $1 \times 10^6$ cells $mL^{-1}$, and were grown at 37°C in a humidified incubator with an atmosphere of 5% $CO_2$ and 95% air.

When cells attained 80% confluency, viewed under a light microscope (Analytical Solutions), the media was aspirated, and the culture was rinsed with 2 mL phosphate-buffered saline (PBS) to remove the residual medium. The flask was gently swirled, PBS aspirated, and 1 mL of 1x trypsin (Biowest, SA) was added to the cells and incubated at 37°C for 5 minutes. Following observation using the light microscope, once the cells appeared rounded up and began detaching from the flask surface, 1 mL of growth medium was added to the flask to inactivate the trypsin. The contents of the flask were gently pipetted up and down five times to prevent clumping of the cells to produce a consistent cell suspension. The cell suspension was then added to a sterile 15 mL tube and centrifuged using Eppendorf Prism Micro Centrifuge (Labnet, USA) at 1300 rpm for 5 minutes. Thereafter, the supernatant was removed and the pellet was resuspended in 5 mL complete media. 20 µL of the resuspended cell culture was pipetted into a sterile 1.5 mL Eppendorf tube (Labselect, SA) for cell counting, to

produce the correct cell density for future experimental seeding and to split and maintain the cell cultures at desired densities.

### 2.1.3 Cell counting

The trypan blue exclusion assay is a simple, rapid technique used for cell counting and measuring cell viability and mortality (Strober, 2015). The principle of this assay is based on the fact that viable live cells possess intact cell membranes that exclude certain dyes, such as trypan blue, whereas non-viable cells do not. Exposure of the cell suspension to the dye visually displays viable cells' appearance as colourless with clear cytoplasm due to the intact cell membrane. A nonviable cell will have blue cytoplasm, due to fragmented membrane structure which allows the trypan blue dye to enter the cell, appearing dark blue under light microscopy (Strober, 2015).

Cell counts were completed using the Countess® II automated cell counter (Invitrogen, USA) where cells were diluted 1:1 with trypan blue stain (0.4% w/v trypan blue in 0.1M PBS, pH 7.4). A final 10 µL aliquot was pipetted into a Countess® cell counting chamber slide. The slide was inputted into the automated cell counter to enable measurement of the number of cells in the cell suspension, as well as the number of live (clear) and dead (dark blue) cells.

## 2.2 Cell Treatment

The resting C8-B4 microglial cells were routinely sub-cultured (as described in section 2.1.3) until confluency was reached. As seen in Figure 6 below, the cells were either stimulated with LPS for 24 hours to induce the M1 pro-inflammatory response or stimulated with IL-4 and/or IL-13 for 24 hours to promote the M2 anti-inflammatory response. The LPS treated groups were then further stimulated with IL-4 and or IL-13 for 24 hours to investigate the effects of IL-4/IL-13 mediated anti-inflammatory response. The treatment groups were as follows:

1. Untreated C8-B4 microglia
2. LPS M1 stimulated
3. IL-4 M2 stimulated
4. IL-13 M2 stimulated
5. IL-4 + IL-13 M2 stimulated
6. LPS + IL-4

7. LPS + IL-13
8. LPS + IL-4 + IL-13

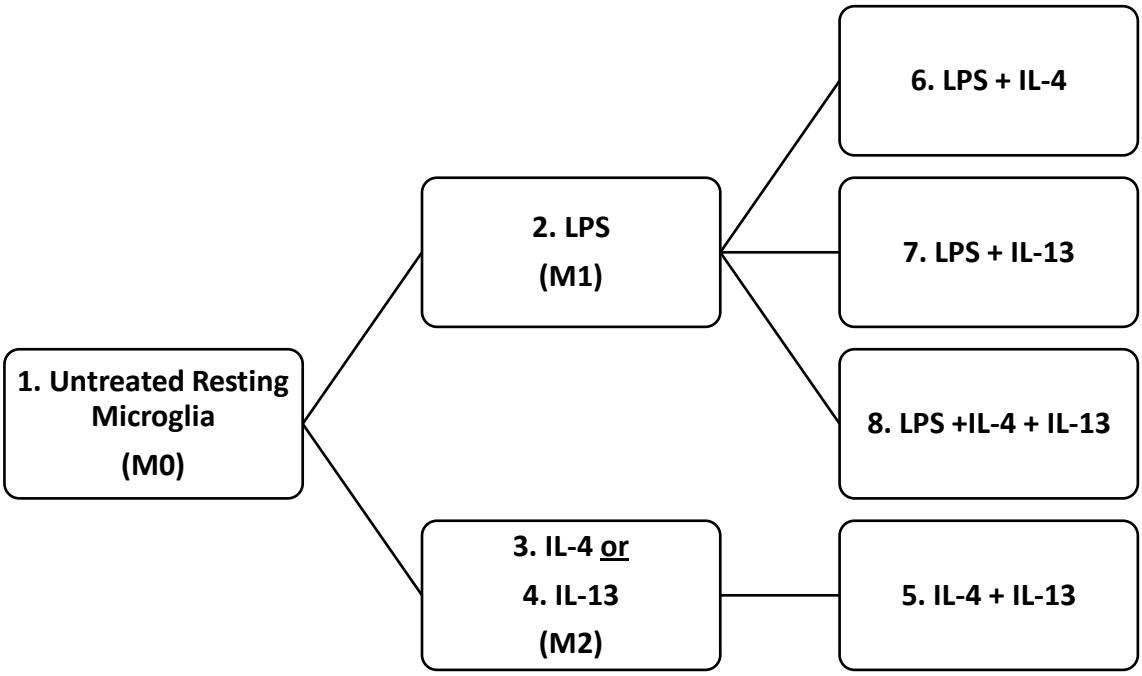


**Fig. 6: Flow diagram depicting treatment groups to investigate the effect of IL-4 and IL-13 on LPS induced neuroinflammation.**

### 2.2.1 M1 microglial polarisation

Resting M0 C8-B4 microglial cells were stimulated to become M1 microglia with LPS (Sigma-Aldrich, SA). Stock solutions of LPS were prepared at 10 ng $mL^{-1}$ with PBS (8.0 g NaCl; 0.2 g KCl; 1.44 g $Na_2HPO_4$; 0.24 g $KH_2PO_4$) to obtain a working solution of 10 ug $mL^{-1}$ LPS and treated for 24 hours. On the day of the experiment, dilutions were made using the complete growth medium from the stock solutions.

### 2.2.2 IL-4/IL-13 M2 preparation

Resting M0 C8-B4 microglial cells were treated with IL-4, IL-13, or both (Biolegend, USA) for 24 hours in the absence or presence of LPS, to activate the cells to become M2 microglia. Stock solutions of IL-4 and IL-13 were prepared at 0.1 mg $mL^{-1}$ with 0.1% BSA (HyClone, SA) to obtain a working concentration of 20 ng $mL^{-1}$. Dilutions

were prepared on the day of experimentation from the stock solutions with complete growth medium.

## 2.3 Cell viability

In this study, the WST-1 assay kit was used for spectrophotometric quantification of cell proliferation, viability, and growth of cultured cells in a 96-well plate.

Briefly, the WST assay employs a colorimetric approach to assess the viable cells through the cleavage of tetrazolium salts within a culture medium (Protocol guide, Sigma Aldrich). The cellular enzymes act on the tetrazolium salts by cleavage to form formazan as shown in Figure 6. Once exposed to viable cells, the overall activity of mitochondrial dehydrogenases increases in the sample, leading to increased formazan dye production. A spectrophotometer was used to quantify the formazan dye generated by metabolically active cells.

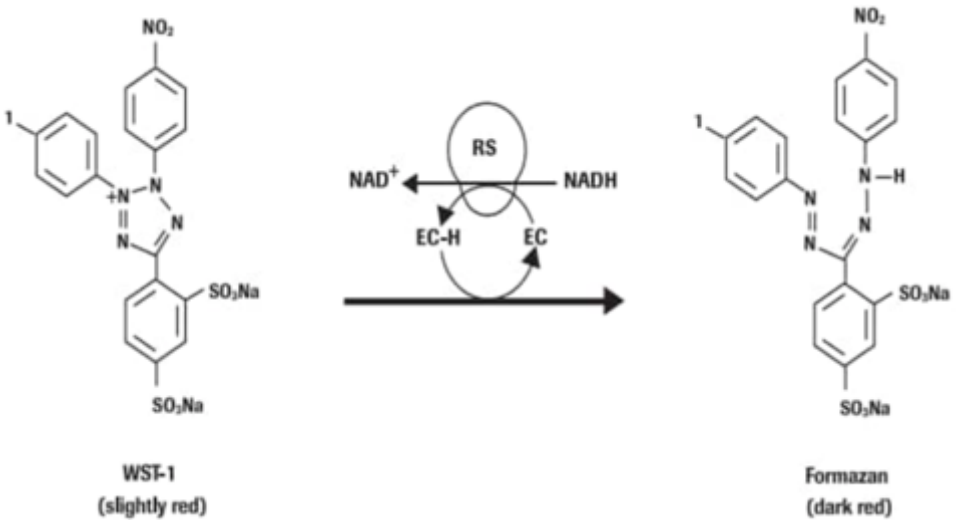


**Fig. 7: Measurement of cell viability- WST-1 reagent** (Adopted from Rahman *et al.* 2015).

WST-1 (Cell Biolabs, USA) stock solution was prepared by dissolving 5 mg of the reagent in 1 mL 1 x PBS with filter sterilization to remove potential insoluble residue. A working solution of WST-1 was prepared from the stock solution at a dilution of 1 in 10 in complete medium.

C8-B4 microglia were seeded at a density of 1 x $10^4$ cells per 100µL in a 96-well plate to determine the cytotoxic effects of the treatments. For the treatment of resting

microglia, the medium was replaced with the fresh complete medium on the day of experimentation. The cells were then treated with or without 10 ng $mL^{-1}$ LPS and placed at 37°C in a humidified 5% $CO_2$ incubator for 24 hours. Thereafter, the cells were treated with or without 20 ng $mL^{-1}$ IL-4 and/or IL-13 for 24 hours under the same conditions. To determine the antiproliferative effects of the treatments, 10 µL of the WST-1 reagent was added to each well of the 96-well plate. Cells were incubated at 37°C in a humidified 5% $CO_2$ incubator for 2 hours. The absorbance was then obtained using a Multiscan-go micro plate-reader (ThermoScientific, SA) at 450 nm. The percentage cell viability was calculated as follows:

$$\%\ cell\ viability\ = \frac{Sample\ (OD) - Background\ (OD)}{Control\ (untreated)(OD) - Background\ OD)}\ x\ 100$$

## 2.4 Enzyme-linked Immunosorbent Assay

The levels of BDNF and inflammatory cytokines TNFα and IL-1β in the cultured samples were quantified using a sandwich mouse Enzyme-linked immunosorbent assay (ELISA) kit (Elabscience, SA).

### 2.4.1 Preparation of reagents and standards

All reagents were brought to room temperature (18-25 °C). The wash buffer was prepared by diluting 30 mL of the wash buffer concentrate with 720 mL of deionized water. For the standard working solution, the reference sample was centrifuged in an Eppendorf Prism Micro Centrifuge (Labnet, USA) at 10,000 x g for 1 minute. Thereafter, 1 mL of the standard solution and sample diluent were added and kept at room temperature for 10 minutes with gentle mixing. Once dissolved, the standards were mixed thoroughly with a pipette, forming a working solution of 500 pg $mL^{-1}$. Serial doubling dilution produced concentrations of 500, 250, 125, 62.5, 31.25, 15.63, 7.81, and 0 (diluent only) pg $mL^{-1}$. To obtain a Biotinylated Detection Antibody (Ab) working solution, 100 µL concentrated biotinylated detection antibody was added to 9.9 mL biotinylated detection antibody diluent (1:100 dilution) to obtain a 1x working solution. To obtain a concentrated Horseradish Peroxidase (HRP) conjugate working solution,

100 µL concentrated HRP conjugate was added to 9.9 mL concentrated HRP conjugate diluent (1:100 dilution) to obtain a 1x working solution.

### 2.4.2 Assay protocol

A 96-well microplate pre-coated with a monoclonal antibody specific to mouse TNFα, IL-1β or BDNF was used. Duplicates of the relevant standard working solution, with a volume of 100 µL per well, were added to the first two columns of the microplate. Thereafter, 100 µL per well of the samples was added to complete the plate. The plate was covered with a plate seal and incubated at 37 °C for 90 minutes. The liquid was then removed from each well, and 100 µL biotinylated detection antibody working solution was added. Thereafter, the plate was covered with a seal, mixed gently, and incubated at 37 °C for 1 hour. The obtained solution was decanted and 350 µL wash buffer was added to each well. After 2 minutes, the liquid was removed, and the plate was dried on absorbent paper the wash steps were repeated three times. Once all the liquid was removed, 100 µL HRP conjugate working solution was added to each well, covered with a plate sealer, and incubated at 37 °C for 30 minutes. After removing the solution, the wash step was repeated five times. Once thoroughly washed, 90 µL substrate reagent was added to each well, covered with a new plate seal, and incubated at 37 °C for 15 minutes, while protected from light. After incubation, 50 µL stop solution was added to each well. Thereafter, absorbance was read at 450 nm using a Multiscan-go microplate reader (ThermoScientific, SA).

## 2.5 Immunofluorescence staining

Cultured microglial cells were processed using an immunofluorescence technique to detect STAT-6, Iba-1, CD206, or CD86 antigens in the treated cells.

Cultured cells were fixed in 200 µL 100% methanol (LiChrosolv, SA) for 5 minutes and further fixed in 4% paraformaldehyde in PBS for 10 minutes at room temperature. Thereafter, the cells were washed three times in PBS and blocked in 200 µL blocking buffer (2.5 mL PBS; 0.25 g bovine serum albumin (BSA); 0,1% Triton-X solution) to avoid non-specific antibody binding and incubated for 1 hour at room temperature. After incubation, the cells were stained with anti-STAT 6 (Abcam, SA), anti-Iba-1 (Abcam, SA), anti-CD-206 (Elabscience, SA), or anti-CD86 (NOVUS™, SA) rabbit

primary monoclonal antibody (1:100 dilution in PBS/BSA) for 1 hour at 37 °C. After incubation, the cells were washed three times in 200 µL PBS and stained with a secondary goat anti-rabbit Immunoglobulin G (IgG) Alexa Flour 488 conjugated antibody (1:100 diluted in blocking buffer) for 90 minutes at 37 °C. The cells were washed three times in PBS and counterstained with 200 µL Hoechst 33258 pentahydrate (bis-benzamide) (Molecular Probes, Life Technologies, USA) (10 mg $mL^{-1}$) and incubated at 37 °C for 30 minutes. The cells were washed again three times with 100 µL of PBS. The plate was viewed under an Axio Vertical A1 fluorescent microscope (Zeiss, USA) and images were captured for analysis using Zen Lite Blue 3.4 image and analysis software (Zeiss, USA). The wavelength for cell excitation was measured at 499nm and fluorescence emission at 520 nm.

## 2.6 Quantitative Reverse Transcriptase Polymerase Chain Reaction (qRT-PCR)

### 2.6.1 Sample preparation

The C8-B4 microglial cells were seeded at a cell density of 1 x $10^6$ cells in 10 mL complete medium in 100 mm cell culture dishes (Thermofisher Scientific, SA).
The resting M0 microglial cells were polarised into M1 or M2 microglia by treating the cells with either 10 ng $mL^{-1}$ LPS or 20 ng $mL^{-1}$ IL-4 and/or IL-13 for 24 hours, respectively. After treatment, the medium was aspirated and discarded. The treated cells were then washed with 2 mL sterile 1 x PBS to discard residual cell debris. The adherent cells were then gently scraped off the plate using a cell scraper (BioRad, SA), added to FACS tubes (Lasec, SA), and centrifuged at maximum speed for 2 minutes using a microcentrifuge (Eppendorf, Germany). The supernatant was discarded, and the remaining PBS was removed by blotting the tube on an absorbent paper towel.

### 2.6.2 RNA extraction

Aurum Total RNA Mini Kit (Bio-Rad, USA) was used to extract RNA from the treated C8-B4 cells following the manufacturer's instructions. The RNA extraction kit contained the following items:

- RNA binding column which selectively binds to mRNA
- Lysis solution (supplemented with 1% β-mercaptoethanol)
- Low stringency wash solution (supplemented with 70 mL molecular grade ethanol)
- High stringency wash solution
- DNase 1 (reconstituted in 250 µL 10 mM Tris pH 7.5)
- DNase dilution solution
- Elution solution

Before extraction, Ambion RNaseZap (Life Technologies, USA) was used to elimate any RNase contamination from the benchtop, all pipettes centrifuges and equipment that were used. Once the supernatant was removed, the cells were lysed by adding 350 µL lysis solution to each tube with thorough pipetting up and down, repeated 30 times. An equal volume (350 µL) of 70% ethanol was then added to each tube and vigorously mixed again by pipetting 30 times to ensure no bilayer was viable and to confirm the degradation of any remaining DNA. The homogenized lysate was then inserted into a 2 mL capless wash tube containing an RNA binding column and centrifuged at 13 400 rpm for 30 seconds in a microcentrifuge (Eppendorf MiniSpin, Germany) at room temperature. Once centrifuged, the filtrate was discarded from the wash tube and the binding column was inserted again. Thereafter, 700 µL of low stringency wash solution was added to the RNA binding column and centrifuged at 13 400 rpm for 30 seconds. The remaining low stringency wash solution was then discarded. Thereafter, 80 µL DNase 1 (diluted 1:20) was added to the center of the membrane of each RNA binding column and incubated at room temperature for 15 minutes. After incubation, 700 µL high stringency wash solution was added to the RNA binding column and centrifuged for 30 seconds at 13 400 rpm. The residual high stringency wash solution was discarded, and the wash tube was replaced. Thereafter, 700 µL low stringency wash solution was added to the RNA binding column and centrifuged at 13 400 rpm for 30 seconds as previously mentioned. The RNA binding column was further centrifuge for 2 minutes at 13 400 rpm to ensure the removal of any remaining wash solution. Thereafter, 30 µL elution solution which was heated prior to 70°C, was added onto the RNA binding column and incubated for 1 minute for the elution solution to saturate the membrane. To elute the RNA, the binding column was centrifuged at 13 400 rpm for 2 minutes at room temperature and the eluted RNA was collected, labeled and stored at -80°C.

### 2.6.3 Quantification of RNA

RNA purity and concentration were determined photometrically using a Thermo Scientific µDrop Plate (Thermo Fischer Scientific, SA). This method is based on Lambert Beer's equation which assumes that nitrogenous bases in nucleotides have a maximum absorption at 260nm (Sharma and Changotra, 2018). 2 µL of the eluted RNA was added to each well on the µDrop Plate and inserted into the Multiscan-go micro-plate reader (ThermoFisher Scientific, SA). Absorbance was measured at 260 nm and 280 nm and RNA concentration was calculated as follows:

$$[RNA] = \frac{Absorbance\ 260}{E\ (0{,}025)\ x\ I\ (pathlength)}$$

The isolated RNA concentration of each sample is shown in Table 1.

**Table 1: RNA concentrations for each experimental sample**

| Sample | RNA concentration (µg/ µL) | A 260/280 |
|---|---|---|
| **Untreated** | 0,424 | 1,935 |
| **LPS** | 0,7976 | 2,135 |
| **IL-4** | 0,861 | 2,109 |
| **IL-13** | 0,666 | 2,093 |
| **IL-4 + IL-13** | 0,915 | 2,159 |
| **LPS + IL-4** | 0,797 | 2,114 |
| **LPS + IL-13** | 0,8 | 2,126 |
| **LPS + IL-4 + IL-13** | 0,919 | 2,120 |

### 2.6.4 Synthesis of complementary DNA

The first step in the two-step reverse transcription process for qRT-PCR involved synthesizing first-strand complementary DNA (cDNA) form the RNA template, using an iScript cDNA synthesis kit (Bio-Rad, USA). This kit used an RNase H+ iScript reverse transcriptase to ensure high sensitivity and consistent cDNA synthesis across

a broad range of input RNA. Additionally, the iScript reverse transcriptase was obtained pre-blended with an RNase inhibitor to inhibit RNA degradation. The iScript reaction mix contains a combined blend of oligo (dT) and random hexamer primers optimized for the production of targets less than 1kb (iScript cDNA Synthesis Kit, Bio-Rad, product information manual)

**Table 2: cDNA reaction mix and relative volumes for each component**

| Components | Volume per reaction |
|---|---|
| **5x iScript Reaction mix** | 4 µL |
| **iScript Reverse transcriptase** | 1 µL |
| **RNA** | x µL |
| **Nuclease free water** | x µL |
| **Total volume** | 20 µL |

The previously quantified RNA was adapted to yield a 1 µg total RNA using RNase-free water (Ambion, USA). As seen in Table 2, the diluted RNA was added to 1 µL iScript™ Reverse Transcriptase and 4 µL iScript™ reaction mix to yield a volume of 20 µL total reaction mix. Priming was completed when the mix was incubated for 5 minutes at 25°C. For the reverse transcription reaction to occur, the reaction mix was incubated for 20 minutes at 46°C. To inactivate the reaction, the mix was incubated for 1 minute at 95°C in a Thermal Cycler (Bio-Rad, USA). The cDNA was aliquoted into 1.5 mL Eppendorf tubes and stored at -20°C for.

### 2.6.5 Primer selection and PCR amplification

The primers encoding microglial cell surface receptors, pro-inflammatory and anti-inflammatory cytokines, and the reference gene were chosen based on published literature, and their oligonucleotide sequences underwent validation using the Primer-Bacid Local Alignment Search Tool (BLAST) program within GenBank database (Ye *et al.*, 2012).

Each gene's primer pair, as seen in Table 4-6, were synthesized by Inqaba Biotech (South Africa). Prior to use, the primers underwent pulse spinning using a vortex (Iso Lab, B&M Scientific, SA) and were reconstituted in nuclease-free water (Ambion,

USA) to prepare a 100µM stock solution. On the day of the experiment, the primers were diluted to a concentration of 10 µM for both forward and reverse primers using nuclease-free water. The qPCR mastermix was then prepared under sterile conditions and on ice, as detailed in Table 3.

The reference gene selected in this study was glyceraldehyde-3-phosphate dehydrogenase (GAPDH). GAPDH is a well-established reference gene used in PCR reactions to normalize gene expression data. GAPDH expression can remain stable under varying experimental conditions and is a reliable, consistent housekeeping gene for qPCR analysis (Zainuddin *et al.,* 2010).

**Table 3: qPCR mix and volumes used for each reaction.**

| **Components** | **Volume per reaction** | **Volume for duplicate reactions** |
|---|---|---|
| **1x iTaq Universal SYBR Green Supermix** | 10 µL | 20 µL |
| **Forward primer** | 1 µL | 2 µL |
| **Reverse Primer** | 1 µL | 2 µL |
| **cDNA** | 1 µL | 2 µL |
| **RNase-free PCR Grade Water** | 7 µL | 14 µL |
| **Total volume** | 20 µL | 40 µL |

PCR amplification was performed on the QuantioStudio™ 3.0 real-time PCR system (Thermo Fischer Scientific, USA) using 40 µL total reaction volume that consisted of the items listed in Table 3. Prepared samples were subjected to the following PCR cycling conditions: 3 minutes polymerase activation at 95°C, followed by 40 cycles of 95°C for 30 seconds, and 72°C for 30 seconds. Each reaction was carried out in duplicate, and each run included water in replacement of the sample as a no template control (NTC). Once the ideal annealing temperature for the paired primers was obtained, the PCR efficiency for the genes of interest was assessed.

For PCR efficiency, a standard curve establishes the sensitivity, efficacy, and consistancy of the assay (Larionov *et al.*, 2005). As recommended by Bivins *et al,.* (2021) a PRC efficiency between 90% - 110% is recommended. To establish this, a

standard curve was generated using 10-fold serial dilution of template cDNA. The cocktail mix comprised of 1µL cDNA from samples of untreated resting M0 microglia, M1 and M2 polarised microglia treated with or without LPS and, IL-4 and/ or IL-13.

**Table 4: Primer pair used for the reference gene.**

| Housekeeping Gene | Accession Number | Primer | Primer sequence (5' to 3') | Primer length | Annealing Temp | Reference paper |
|---|---|---|---|---|---|---|
| GAPDH | NM_001411843.1 | Forward | GTGGCAAAGTGGAGATTGTTG | 21 | 60ºC | (Modarresi *et al*., 2021) |
| | | Reverse | ACCAGTAGACTCCACGACATA | 21 | | |

**Table 5: Target gene primer pairs for inflammatory cytokines and transcription factors activated during M1 microglial polarization.**

| Target Genes | Accession Number | Primer | Primer sequence (5' to 3') | Primer length | Annealing Temp | Reference paper |
|---|---|---|---|---|---|---|
| TNFα | NM_013693.3 | Forward | GCCTCTTCTCATTCCTGCTTGTGGCAG | 27 | 60ºC | (Doorn *et al*., 2015) |
| | | Reverse | GACGTGGGCTACAGGCTTGTCACTCG | 26 | | |
| IL-1ß | NM_008361.4 | Forward | CCTGTCCTGTGTAATGAAAGCGG | 24 | 60ºC | (Arno *et al.*, 2014) |
| | | Reverse | TGTCCTGACCACTGTTGTTTCCC | 23 | | |
| Arg-1 | NM_007482.3 | Forward | GCAGCAGCCGCTGGAACCCAG | 21 | 60ºC | (Rossi *et al*., 2018) |
| | | Reverse | GTCCCCGTGGTCTCTCACGTC | 21 | | |

**Table 6: Target gene primer pairs for cell surface receptors activated during M2 microglial polarisation.**

| Target Genes | Accession Number | Primer | Primer sequence (5' to 3') | Primer length | Annealing Temp | Reference paper |
|---|---|---|---|---|---|---|
| IL-4Rα | NM_000418 | Forward | GAGTGAGTGGAGTCCTAGCATC | 22 | 60ºC | Jakubzick *et al.*, 2003) |
| | | Reverse | GCTGAAGTAACAGAACAGGC | 20 | | |
| STAT6 | NM_00117807.8 | Forward | TGCTCTGCCCTGTTCAAGAAC | 21 | 60ºC | (Glenn *et al.*, 2019) |
| | | Reverse | CGCACTTCTCCTCTGTGACAG | 21 | | |
| CD206 | NM_008625.2 | Forward | CCACTCTATCCACCTTCACTGATG | 24 | 60ºC | (Abdul *et al.*, 2020) |
| | | Reverse | CCTGCTCGTCCACAGTCCACCG | 22 | | |
| BDNF | NM_001316310.1 | Forward | TGCCGCAAACATGTCTATGAGG | 22 | 60ºC | (Mizobuchi *et al.*, 2020) |
| | | Reverse | GCTGTGACCCACTCGCTAATAC | 22 | | |

## 2.7 Statistical Analysis

Cell viability data was measured on the Multiscan Go plate reader (Thermofisher Scientific) and analysed on the Skanit ™ 6.1.1 software. Data was processed in GraphPad Prism 9 (GraphPad Software, USA). Data are represented as the mean ± standard error of mean (SEM) of three independent experiments. Statistical significance was determined using One-Way ANOVA with Tukey's post hoc test.

The images obtained for immunofluorescence were captured using a x40 objective on the Axio Vertical A1 fluorescent microscope (Zeiss, USA) the images and mean fluorescence intensity were obtained using the Zen Lite Blue 3.4 image and analysis software (Zeiss, USA). The mean fluorescence intensity was determined using GraphPad Prism 9 (GraphPad Software, USA). Data are represented as the mean ± SD of three independent experiments. Statistical significance was determined using One-Way ANOVA with Tukey's post hoc test.

qRT-PCR data obtained from the QuanStudio™ Real-Time PCR detection system (Thermo Fisher Scientific, SA) were imported into the Quanstudio™ Design and Analysis RT-PCR analytical program. Normalisation using the GAPDH reference gene was performed, and normalised relative quantitates (NRQ) with standard error of the mean (SEM), were exported from Quanstudio™ into GraphPad Prism 9 (GraphPad Software, USA). Data represented as mean ± SEM for M1 and M2 polarised microglia, treated with or without LPS in the presence or absence of IL-4 and IL-13, were compared to the values for untreated resting microglia using unpaired Student’s t-test and One-Way ANOVA (with Tukey’s multiple comparison test).

# CHAPTER THREE

# RESULTS

## 3.1 Effects of IL-4/13 stimulation on LPS-induced changes in viability of M2 cells.

The C8-B4 microglial cells were treated with or without LPS in the presence or absence of IL-4 and/or IL-13 for 24 hours for cell viability analysis, using the WST-1 assay kit. As shown in Fig. 8, cells treated with LPS only or combined treatments of LPS and IL-4 exhibited a small, but significant decrease in percentage viability ($p<0.001$), compared to the M0 untreated control group that maintained a desired metabolic activity with 100% viability. Further analysis revealed that all groups that received separate or combined treatments of IL-4 and IL-13, with or without LPS, had a significantly increased population of viable cells compared to the group that received only LPS ($p<0.001$, Fig. 8).

.

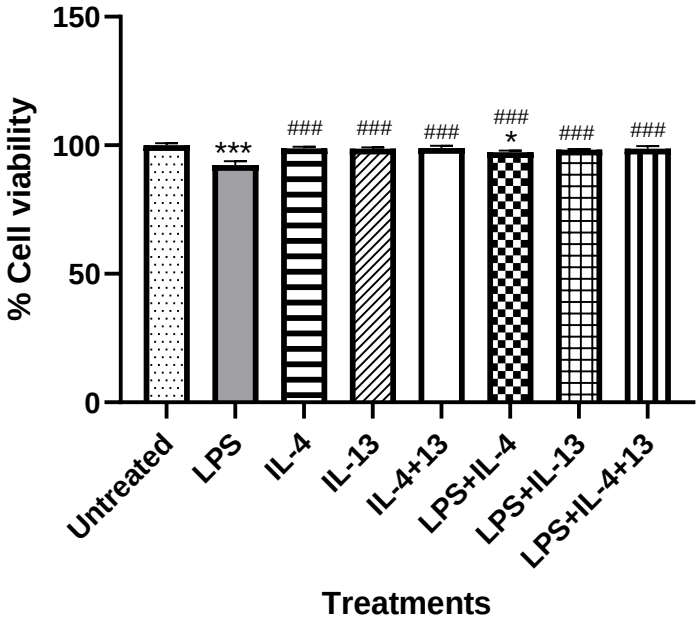


**Fig. 8: The effect of bacterial LPS on C8-B4 microglial viability after 24 hours.C8-B4 microglia were treated with LPS in the presence or absence of IL-4 and/or IL-13.** After 24 hours, the cell viability was determined using the WST-1 assay. Data are represented as the mean ± SEM from three independent experiments. Statistical significance was determined using One-Way ANOVA with Tukey's post hoc test and Student t-test: * = $p<0.05$; ** = $p<0.01$, *** = $p<0.001$ compared to untreated resting (M0) microglial control; ###= $p<0.001$ compared to LPS

## 3.2 IL-4/13-induced polarising effects on TNFα, IL-1β, and BDNF expression in microglial cells.

To investigate the effects of IL-4 and IL-13 stimulation on endogenous production of BDNF and proinflammatory cytokines TNFα and IL-1β in LPS-treated and untreated microglial cells, the levels of these protein molecules were quantified at 12 hours and 24 hours post treatment using ELISA.

### 3.2.1 TNFα levels

TNFα is a prominent pro-inflammatory cytokine that plays a vital role in promoting inflammation and is produced by immune cells such as macrophages and T cells. TNFα further triggers the release of numerous proinflammatory cytokines which further amplifies a cascade of immune responses (Zhang & Jianxiong, 2007). Hence, the expression TNFα was determined as a result of the treatments inflicted on the microglial cell line.

As seen in Fig. 9A, 12 hours post treatment, when compared to the untreated control, the TNFα concentration in the LPS treated cells was significantly increased ($p<0.001$). This indicated a robust pro-inflammatory response induced by LPS stimulation, as TNFα is a vital cytokine involved in inflammation and activation of immune responses. As mentioned previously, IL-4 and IL-13 are anti-inflammatory cytokines involved in tissue repair and alleviating allergic responses. Both IL-4 and IL-13 treated cultures displayed no significant difference in TNFα when compared to the untreated control group. However, when the cells were initially treated with LPS to induce M1 phenotypic heterogeneity, and then stimulated to M2 with IL-4/IL-13, a significant upregulation of TNFα ($p<0.001$) was detected when compared to the untreated control. When M2 treatments were compared to LPS treated cells, TNFα production by both IL-4 and IL-13 treated cells was significantly decreased.

In Fig. 9B 24 hours post treatment, when compared to the untreated control, the TNFα secretion was significantly increased in cells treated with LPS. Similarly, to the results shown in Fig 9A, cells treated with LPS and co-stimulated with IL-4 and IL-13 significantly increased TNFα concentration when compared to the untreated cell group ($p<0.001$, Fig. 9B). However, when cells were stimulated independently with IL-4 and IL-13, there was no significant difference in the TNFα concentration. The data shows that when cells were initially induced with LPS and stimulated with IL-4 and IL-13, the concentration of TNFα was significantly increased in comparison to the

cultures of cells treated with IL-4 and IL-13 independently ($p<0.001$). Furthermore, when compared to the LPS treated cells, LPS stimulated cells with IL-4/IL-13 treatment produced a significantly decreased amount of TNFα, displaying the pro-inflammatory action of LPS, as well as the anti-inflammatory influence of IL-4 and IL-13.

Overall, in comparison to the M0 untreated control, the LPS treated cultures showed highly significant upregulation of TNFα both 12 hours and 24 hours post treatment. LPS treated cells co-stimulated with IL-4/13 exhibited an increase in TNFα expression when compared to cells only treated with IL-4 and IL-13 ($p<0.001$).

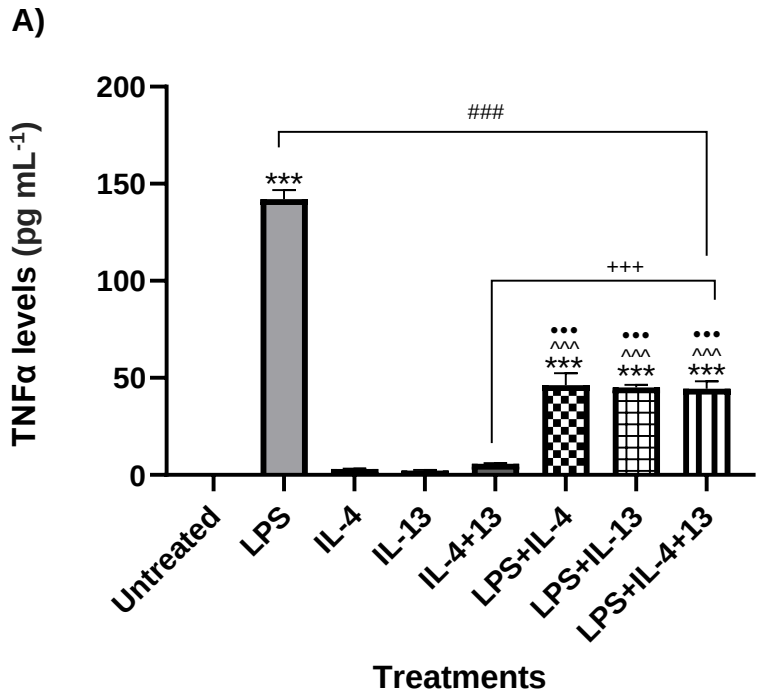

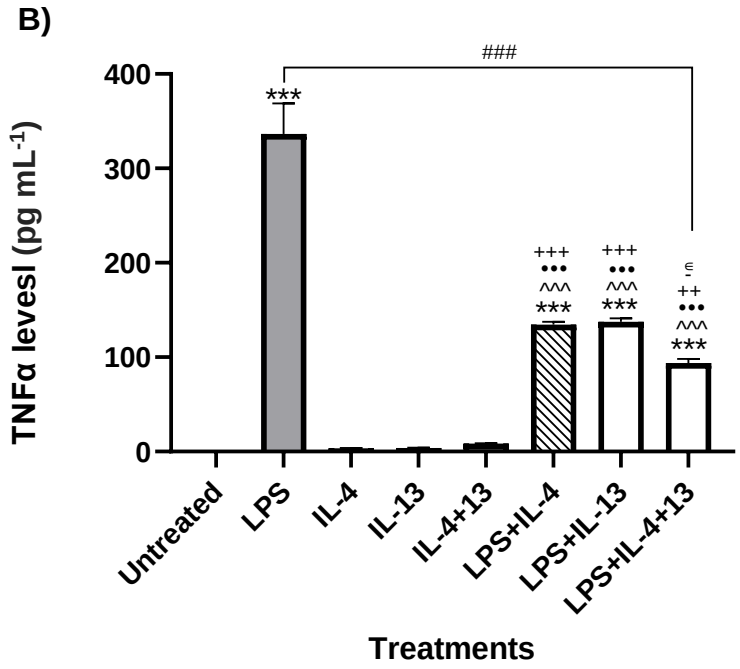


**Fig. 9**: **Protein concentration (pg mL$^{-1}$) of TNFα determined using an ELISA of resting C8-B4 microglia (M0) with or without LPS, in the presence of IL-4/ IL-13. A) 12 hours post treatment B) 24 hours post treatment.** *Data are represented as the mean ± SEM of three independent experiments. Statistical significance was determined using One-Way ANOVA with Tukey's post hoc test. ***= p≤ 0.001 vs Untreated, ###= p≤0.001 vs LPS; ^^^=p≤ 0.001 vs IL-4;••• =p≤ 0.001 vs IL-13; +++=p≤ 0.001; += p≤ 0.01 vs IL-4+IL-13; - = p<0.05 vs LPS+IL-4; ∈ = p<0.05 vs LPS+IL-13.*

### 3.2.2 IL-1β levels

IL-1β is a crucial cytokine with multifaceted roles in the inflammatory response. As a result, the protein concentration of IL-1β was measured to assess the levels of pro-inflammatory cytokines released 12 hours and 24 hours post treatment of the C8-B4 microglial cells.

In Fig. 10A, 12 hours post treatment, in comparison to the untreated control, LPS treated cells displayed a significant increase in IL-1β secretion (p<0.001). Individual treatments of IL-4 and IL-13 to the cells presented no significant difference. When compared to the positive control i.e., the LPS treated cells, IL-4 and IL-13 treated cells showed a significant decrease in IL-1β secretion. Secretion of IL-1β by cells collectively treated with LPS then IL-4 and IL-13 was also significantly decreased when compared to the cultures treated with LPS alone. However, the cultures treated with LPS and collectively treated with IL-4/ IL-13, showed a significant increase in IL-

1β in comparison to the cells treated with IL-4 and IL-13 only ($p<0.001$), confirming that IL-1β is a key mediator of the inflammatory response.

Fig. 10B, 24 hours post treatment, shows a similar response was observed to that seen in the 12-hour post treatment. In comparison to the C8-B4 resting untreated M0 microglial cells, the LPS treated cells significantly increased IL-1β secretion ($p<0.001$). Cultures treated with IL-4 and/or IL-13 showed no significant difference in comparison to the untreated control. However, when cells were treated with LPS and stimulated with IL-4 and/or IL-13, a significant increase in IL-1β secretion ($p<0.001$) was detected in comparison to the untreated cells. When compared to the individually treated LPS cells, there was a significant decrease of released IL-1β in the cultures treated with IL-4 and IL-13 individually, and when treated collectively with LPS ($p<0.001$). In contrast, the cells treated with IL-4 and IL-13 showed a significant decrease of IL-1β when compared to the cultures collectively treated with LPS, IL-4, and IL-13 ($p<0.001$), consistent with the association of IL-4 and IL-13 with anti-inflammatory properties.

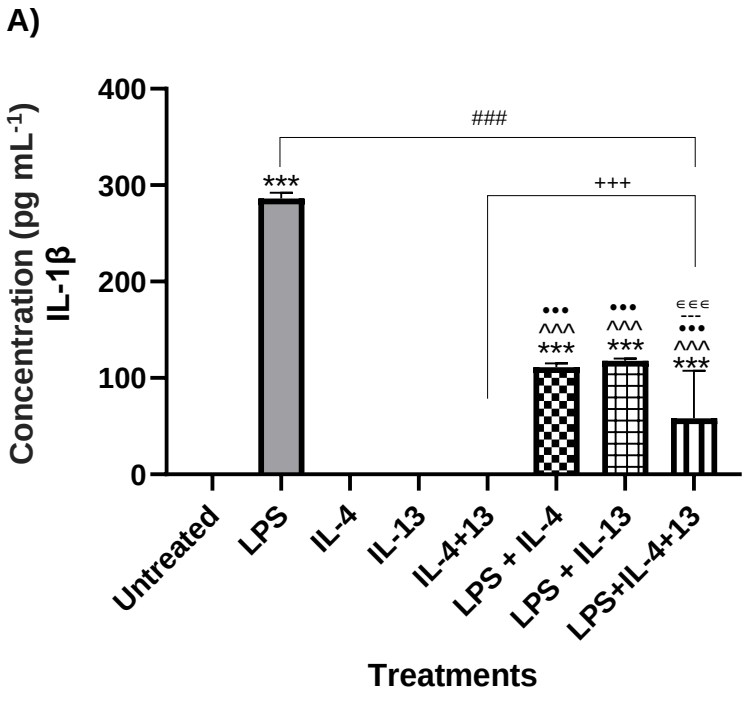

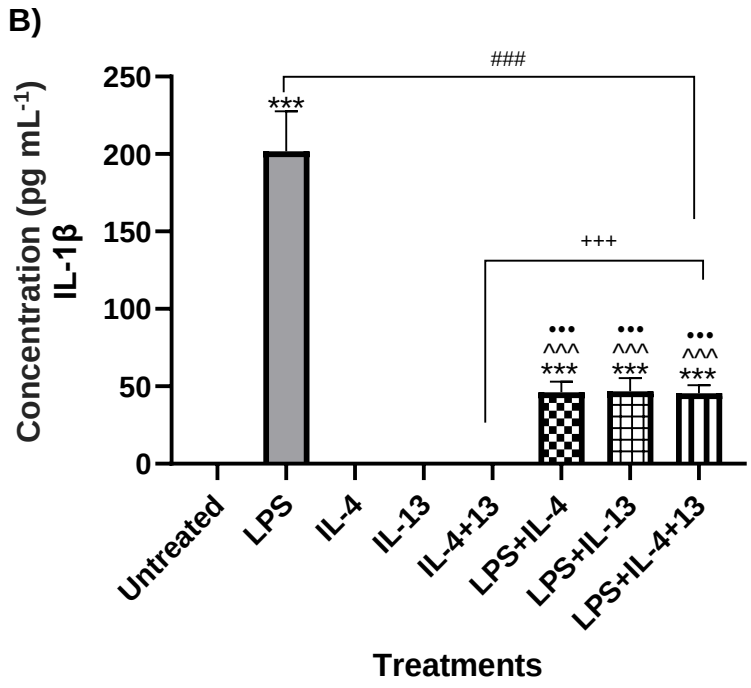


**Fig. 10: Protein concentration (pg mL$^{-1}$) of IL-1β, determined by means of an ELISA of resting C8-B4 microglia (M0) with or without LPS, in the presence of IL-4/ IL-13. A) 12 hours post treatment B) 24 hours post treatment.** *Data are represented as the mean ± SEM of three independent experiments. Statistical significance was determined using One-Way ANOVA with Tukey's post hoc test. ***= p≤ 0.001 vs Untreated, ###= p≤0.001 vs LPS; ^^^=p≤ 0.001 vs IL -4;••• =p≤ 0.001 vs IL-13; +++=p≤ 0.001 vs IL-4+IL-13.*

### 3.2.3 BDNF levels

BDNF is widely expressed in the CNS and plays a vital role in promoting neural growth and survival. BDNF is a neurotransmitter modulator, involved in neuronal plasticity, fundamental for learning and memory (Bathina & Das, 2015). BDNF expression levels were measured using a sandwich ELISA,12 hours and 24 hours post treatment.

In Fig 11 A, 12 hours post treatment when compared to the M0 untreated control, cells treated with LPS revealed a significant increase in BDNF secretion ($p<0.01$). Cells treated with individual and combined doses of IL-4 and IL-13 indicated minuscule secretions of BDNF and were significantly decreased when compared to LPS treated cells. Interestingly, when cultures were treated with LPS and co-stimulated with IL-4 and/or IL-13, the ELISA results displayed the most significant upregulation when compared to the untreated control and to the LPS stimulated cultures ($p<0.001$), indicating a potential upregulation of neurotrophic responses in response to inflammatory stimuli.

The expression of BDNF revealed a notable difference in the 24-hour post-treatment analysis (Fig. 11B). No significant differences were detected between the cultures treated with LPS and the untreated control ($p<0.001$). Yet, when cells were treated with LPS and co-stimulated with IL-4 and IL-13, a significant upregulation of BDNF secretion was measured when compared to cells treated solely with LPS, and when compared to the untreated culture ($p<0.001$). Furthermore, cells treated with IL-4 and IL-13 likewise indicated a significant increase in BDNF expression when compared to the untreated control ($p<0.001$). Intriguingly, the cultures stimulated with IL-4 and IL-13 indicated a significant increase when compared to all remaining treated samples ($p<0.001$).

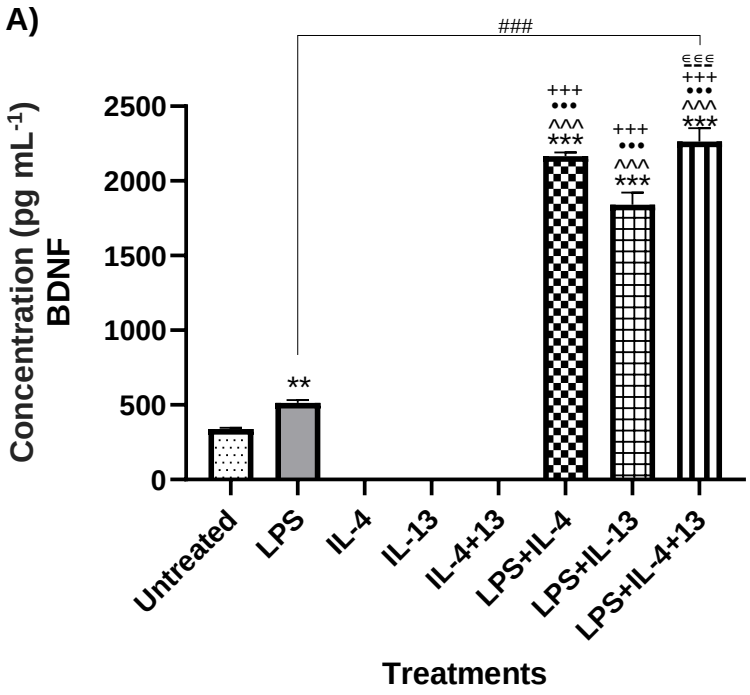

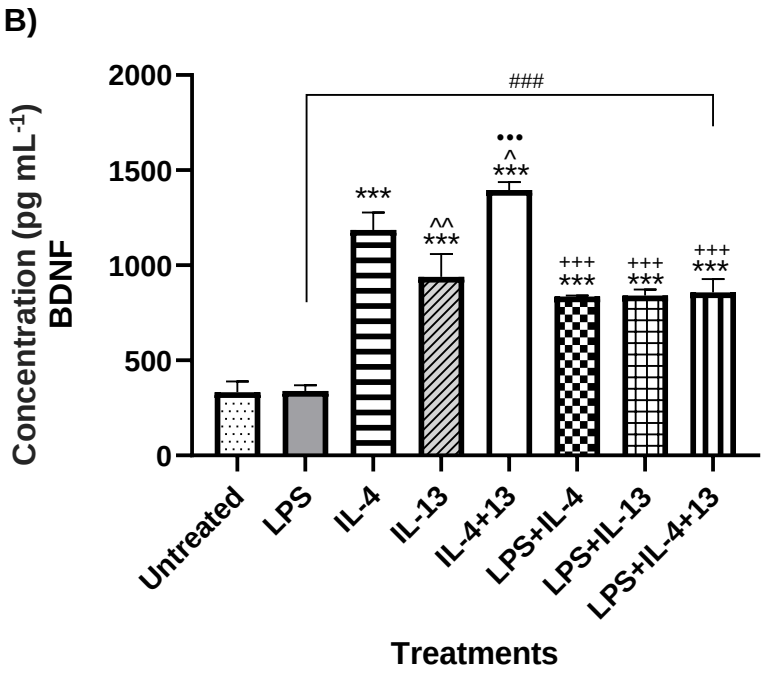


**Fig. 11: Protein concentration (pg mL$^{-1}$) of BDNF, determined by means of an ELISA of resting C8-B4 microglia (M0) with or without LPS, in the presence of IL-4/ IL-13.A) 12 hours post treatment B) 24 hours post treatment.** *Data are represented as the mean ± SEM of three independent experiments. Statistical significance was determined using One-Way ANOVA with Tukey's post hoc test. ***= p≤ 0.001, **= p≤ 0.01 vs Untreated, ###= p≤0.001 vs LPS; ^^^=p≤ 0.001, ^^=p≤ 0.01, ^=p< 0.05 vs IL-4;••• =p≤ 0.001 vs IL-13; +++=p≤ 0.001 vs IL-4+IL-13; --- = p ≤0.001 vs LPS+IL-4; ∈ ∈ ∈ = p ≤ 0.001 vs LPS+IL-13.*

Overall, the results obtained from the ELISA assays indicate significant changes in TNFα, IL- 1β, and BDNF expression in response to a range of treatments, acquired at different time points. This highlights the complex interaction between immune factors in microglial cells. The time course study further uncovered a dose-response correlation 12 hours and 24 hours post treatment which emphasized that cytokine release can be affected by factors such as cell stimulation, activation, or stress.

### 3.3 Immunofluorescence detection of Iba1 in C8-B4 cells reveals morphological diversities following LPS challenge and IL-4/IL-13 stimulation

Iba1 was used as a biomarker for tracking microglial activity in response to LPS-induced inflammatory changes and IL-4/13 stimulation. To quantify microglial activation in the cell culture, C8-B4 cells were stained with FITC-conjugated anti-Iba1 antibody and counter-stained with Hoechst 33258. Thereafter, the mean fluorescent intensity was determined for cultures with each treatment group to evaluate Iba1

expression (Fig. 12). The control culture was the untreated resting M0 macrophages (Fig. 12A). Cells were induced with LPS (Fig. 12 B) or treated with IL-4 (Fig. 12 C), IL-13 (Fig. 12D), IL-4 and IL-13 (Fig. 12E), LPS and IL-4 (Fig. 12F), LPS and IL-13 (Fig. 12G) and LPS co-stimulated with IL-4 and IL-13 (Fig. 12H). Fig. 12 (A-I) shows that Iba1 expression was significantly higher in all treated cultures compared to the untreated M0 control ($p<0.001$). However, the fluorescence intensity of Iba1 in cells that received co-stimulation of IL-4 and IL-13 was more significantly increased than with other treatments ($p<0.001$, Fig. 12E, I). Interestingly, it was further observed that most cells exposed to separate or combined treatments of LPS, IL-4 or IL-13 exhibited morphophysiological diversities. The cell bodies appeared elongated in shape indicative of the M2 phenotypic profile of activated microglia (Fig. 12B-H). Moreover, cells stimulated with LPS only displayed an amoeboid-like shape, which appeared slightly larger and rounder in shape indicating the M1 phenotypic expression (Fig. 12B). In contrast, cells treated with IL-4 and IL-13 displayed an elongated M2 phenotypic profile (Fig. 12E).

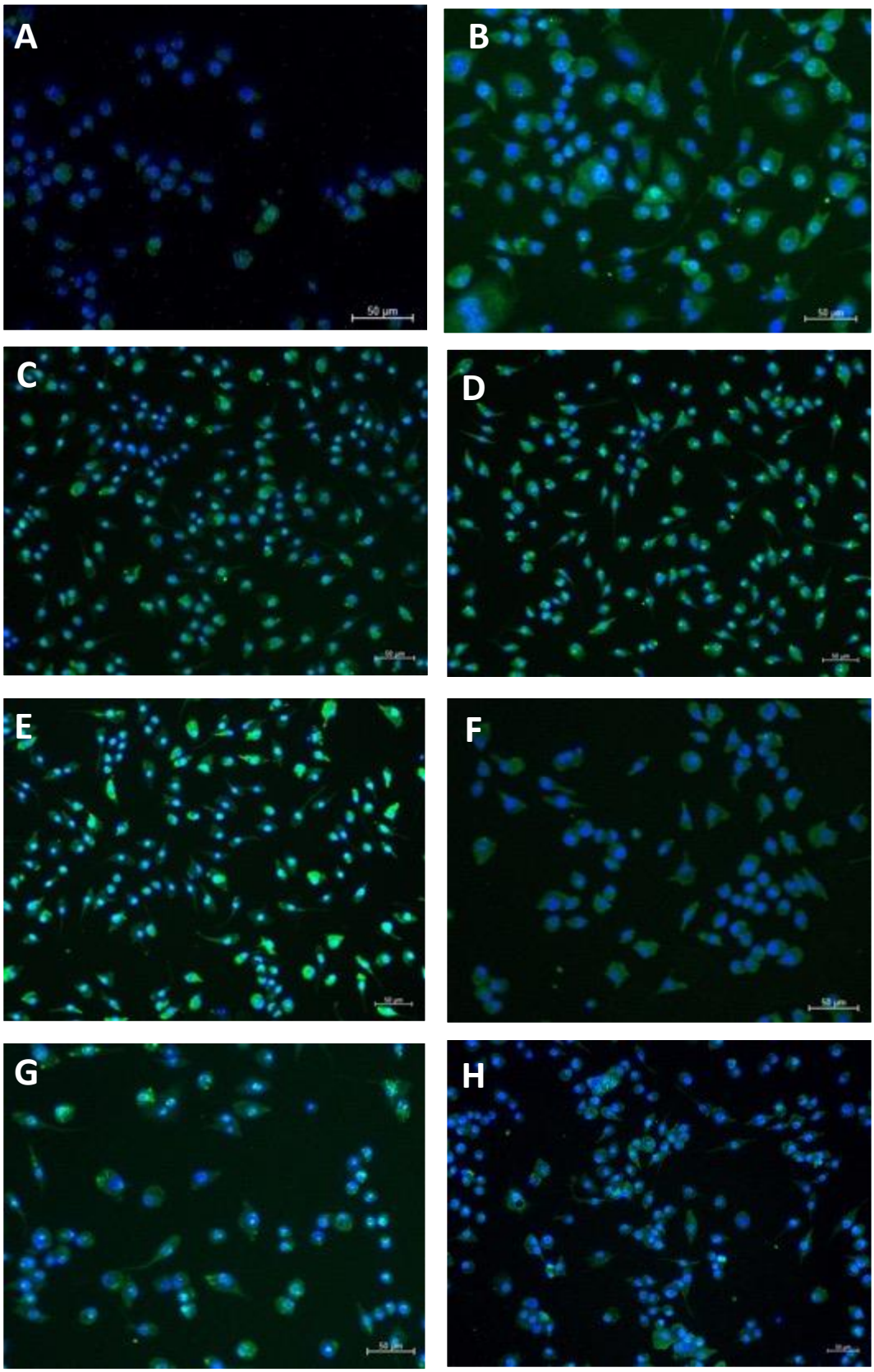
A
B
C
D
E
F
G
H

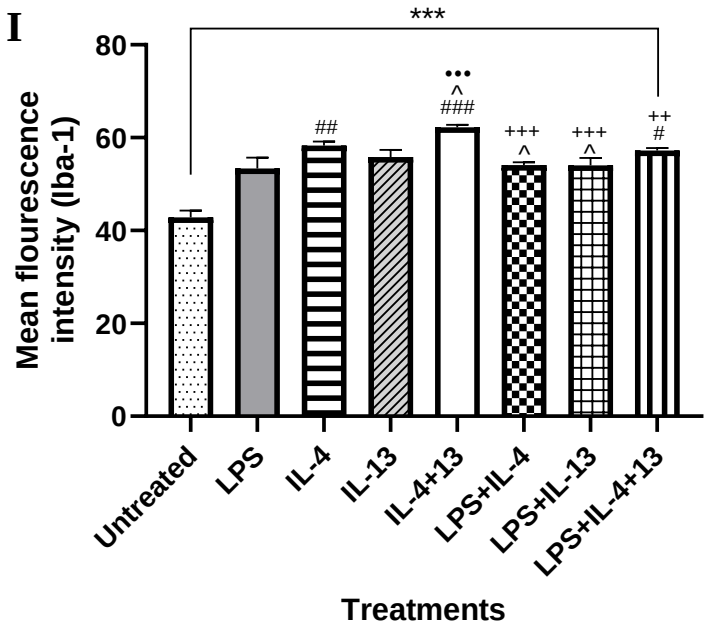


**Fig. 12: Immunofluorescence detection of Iba1 on C8-B4 microglia following LPS induction and IL-4/IL-13 stimulation.** *Representative of fluorescence images showing microglia activities in (A) Untreated M0 control, and (B) LPS, (C) IL-4, (D) IL-13, (E) IL-4+IL-13, (F) LPS+IL-4, (G) LPS+IL-13 and (H) LPS+IL-4+IL-13 treated cells (I) graph showing the mean fluorescence intensity of Iba1 in untreated vs. treated cells. Images were captured with a fluorescence microscope (Axio Vertical A1, Zeiss, USA) and analysed using the Zen Lite Blue version 3.8 program. Data are represented as the mean ± SEM of three independent experiments. Statistical significance was determined using One-Way ANOVA with Tukey's post hoc test. ***= p≤ 0.001, **=p<0.01 vs Untreated, ###= p≤0.001, ##=p<0.01 vs LPS; • =p≤ <0.05 vs IL-13.*

### 3.4 LPS-induced inflammatory changes marked by CD86 Immunoreactivity

CD86 is a co-stimulatory molecule expressed on the surface of antigen-presenting cells (APC) with counter receptors on T cells in response to pathogenic insults (Yang *et al.,* 2010). The expression of CD86 on these cells can reveal their means of activation and involvement in immune response, generally associated with inflammation. The use of CD86 as a pro-inflammatory marker in immunofluorescence has been widely used (Furgiuele *et al.,* 2022). In this study, CD86 was used to visually assess the effect of the LPS challenge on C8-B4 microglial cells and to examine changes in immunofluorescence intensity (Fig. 13). As expected, the LPS treated cells exhibited a peak fluorescence intensity when compared with the other cultures (LPS: Fig. 13B vs control/ treatments: Fig. 13A and 13C-H). These observations correlate to a significantly increased expression of CD86 in LPS-challenged microglial cells compared to the untreated control and other treated cells ($p<0.001$, Fig. 13I).

Furthermore, the morphological changes observed in the LPS treated cells were indicative of the M1 phenotype, as cells appeared rounder and amoeboid shaped. Cells treated with IL-4 and/or IL-13 only (Fig. 13C-E and 13I) indicated a significant downregulation in fluorescence intensity of CD86 when compared to cells co-stimulated with LPS and IL-4/13 ($p<0.001$, Fig. 13F-G), thus confirming possible mitigatory effects of IL-4 and IL-13 cytokines on LPS-induced inflammatory changes in the cultured cells (Fig. 13I). Morphological differences were examined in cells treated with IL-4 and IL-13 (Fig. 13E-G), which presented ramified processes appearing more branched, indicative of the M2 microglial phenotype.

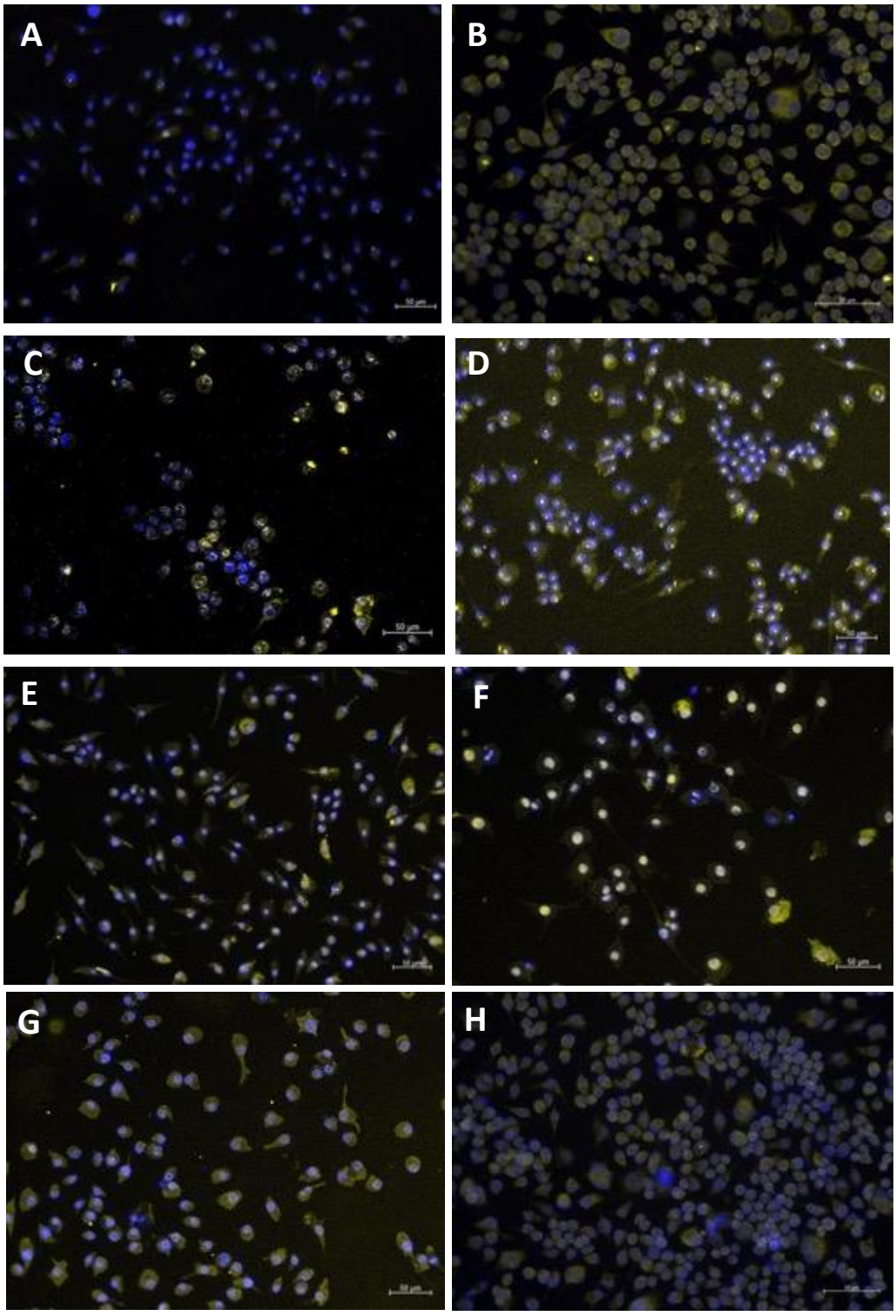

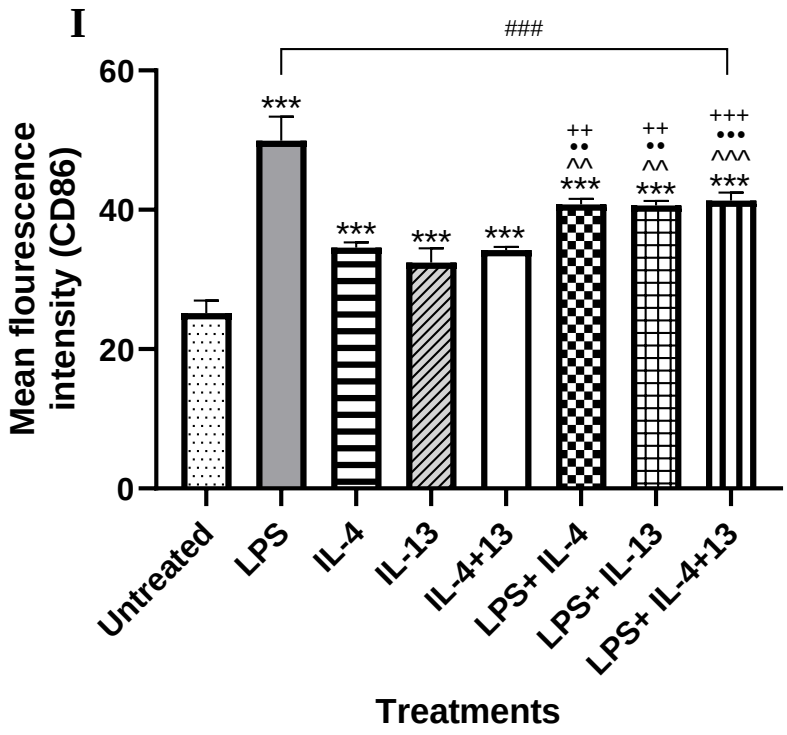


**Fig. 13: Immunofluorescence detection of CD86 on LPS-induced C8-B4 microglia with or without IL-4/IL-13 stimulation.** *Representative of fluorescence images showing microglia activities in (A) Untreated M0 control, (B) LPS, (C) IL-4, (D) IL-13, (E) IL-4+IL-13, (F) LPS+IL-4, (G) LPS+IL-13 and (H) LPS+IL-4+IL-13 treated microglial cells (I) showing the mean fluorescence intensity of CD86 in cultured microglial cells following LPS and IL-4/IL-13 treatments. Images were captured with a fluorescence microscope (Axio Vertical A1, Zeiss, USA) and analysed using the Zen Lite Blue version 3.8 program. Data are represented as the mean ± SEM of three independent experiments. Statistical significance was determined using One-Way ANOVA with Tukey's post hoc test. ***= p≤ 0.001, **=p<0.01 vs Untreated, ###= p≤0.001, ##=p<0.01 vs LPS; • =p≤ <0.05 vs IL-13*

### 3.5 IL-4/13-induced CD206 activation in LPS-challenged microglial cells confirms polarization to M2 anti-inflammatory phenotype.

CD206 is primarily expressed on the surface of alternatively activated M2 macrophages and microglial cells, which play a vital role in tissue repair, inflammatory resolution, and immune modulation (Suzuki *et al.,* 2018). Hence, CD206 is a common anti-inflammatory marker for immunofluorescence detection. In this study, CD206 expression was measured in the cell cultures to determine the involvement of this cell surface maker in neuroinflammation. The data revealed a marked increase in expression of CD206 in all cells that received separate or combined treatments of IL-4 and IL-13 (Fig. 14C-H), compared to decreased expression in the untreated and LPS-challenged cells (Fig. 14 B). These observations are further supported by significantly increased CD206 positive cells in IL-4/13 treated cells compared to both

control and LPS treated cells ($p<0.001$, Fig. 14). As shown in Fig. 14E, I, peak activation of CD206 in cells exposed to co-treatments of IL-4 and IL-13 confirms the anti-inflammatory potential of these cytokines and their abilities to act synergistically to polarise the cells to attain an M2 phenotype.

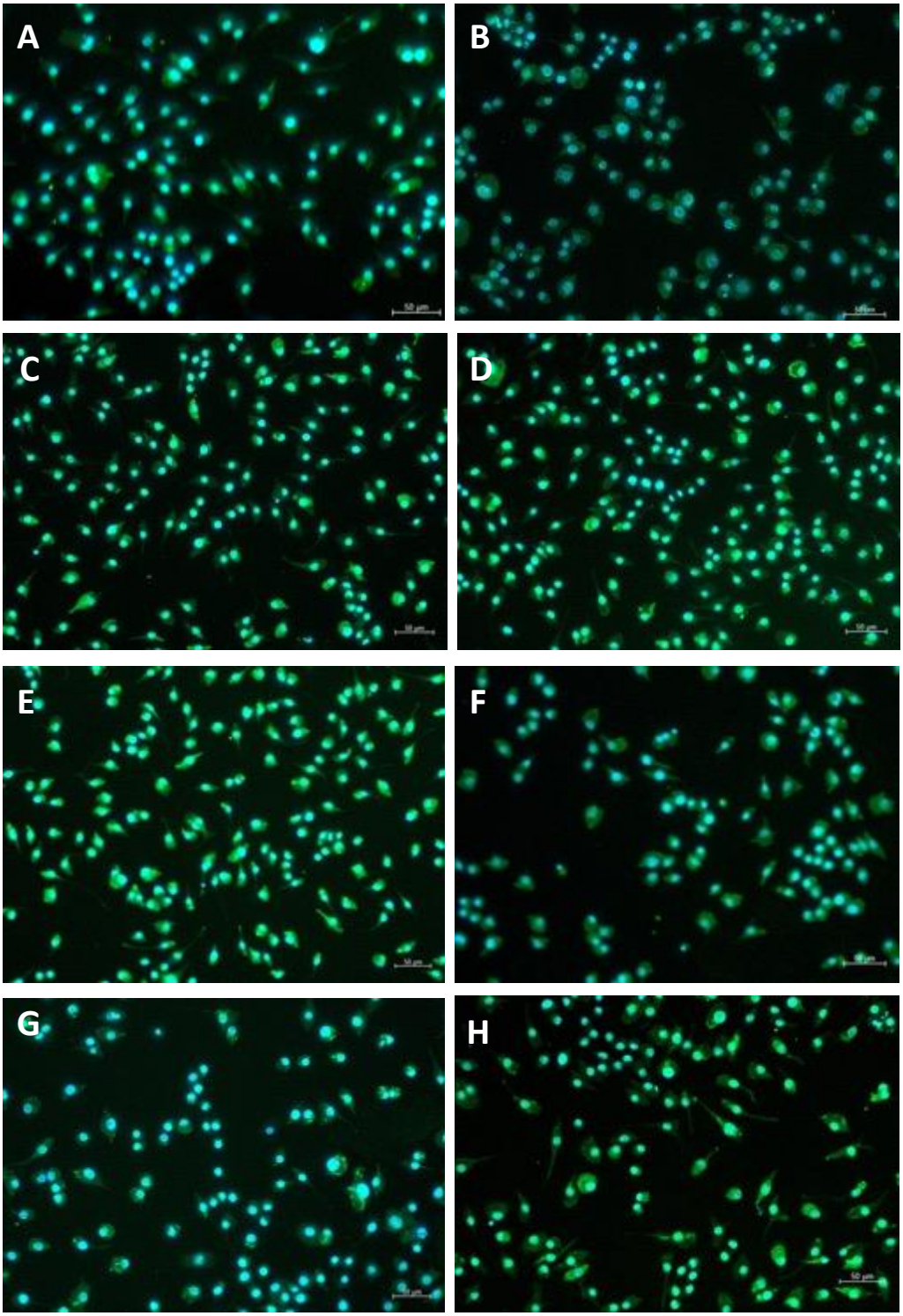

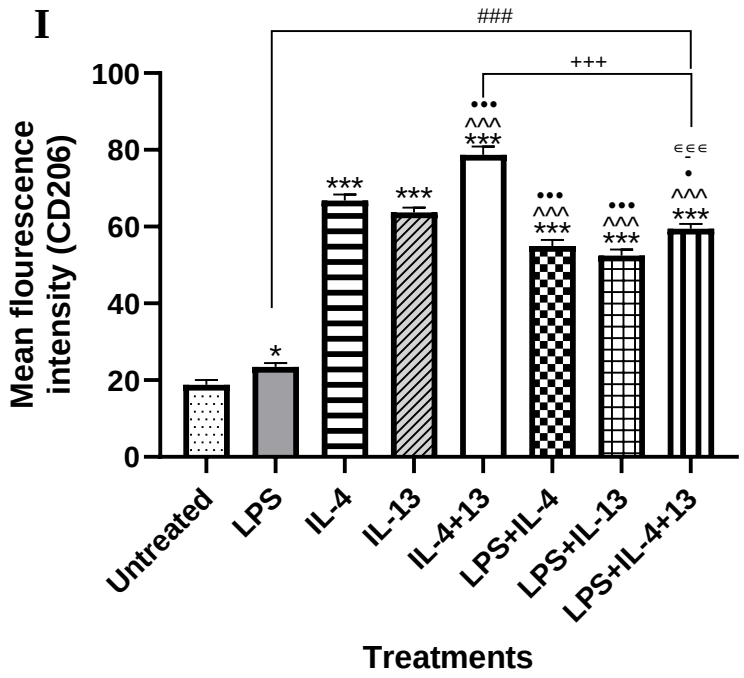


**Fig. 14: Immunofluorescence detection of CD206 on LPS induced C8-B4 microglia in the presence or absence of IL-4/IL-13.** *Representative of fluorescence images showing microglia activities in (A) Untreated M0 control, (B) LPS, (C) IL-4, (D) IL-13, (E) IL-4+IL-13, (F) LPS+IL-4, (G) LPS+IL-13 and (H) LPS+IL-4+IL-13 treated cells, (I) showing the mean fluorescence intensity of CD206 in microglial cells following LPS and IL-4/IL-13 treatments. Images were captured with a fluorescence microscope (Axio Vertical A1, Zeiss, USA) and analysed using the Zen Lite Blue version 3.8 program. Data are represented as the mean ± SEM of three independent experiments. Statistical significance was determined using One-Way ANOVA with Tukey's post hoc test. ***= p≤ 0.001, **=p<0.01 vs Untreated, ###= p≤0.001, ##=p<0.01 vs LPS; • =p≤ <0.05 vs IL-13*

### 3.6 Immunofluorescence analysis of STAT6 on microglia following LPS induction and IL-4/IL-13 stimulation

STAT-6 is one of the downstream molecules of the IL-4Rα signalling pathway that mediates cellular responses to IL-4 and IL-13 anti-inflammatory cytokines (McCormick & Heller, 2015). The immunofluorescence technique was used to determine the expression (Fig. 15 A-H) and intensity (Fig. 15I) of STAT-6 expression in IL-4 and IL-13 treated cells in response to LPS-induced inflammation. The data show that STAT-6 was greatly increased in expression in cells co-stimulated with IL4 and IL-13 (Fig. 15E) compared to the other cultures (15A-D, F-H). Statistical analysis further revealed significantly increased STAT6 mean fluorescence intensity in cells with all treatments compared to the control ($p<0.001$, Fig. 15I). However, peak intensity was observed in the cells exposed to co-treatment of IL-4 and IL-13, thus confirming an increased amount of the intracellular STAT6 downstream molecule (Fig. 15I).

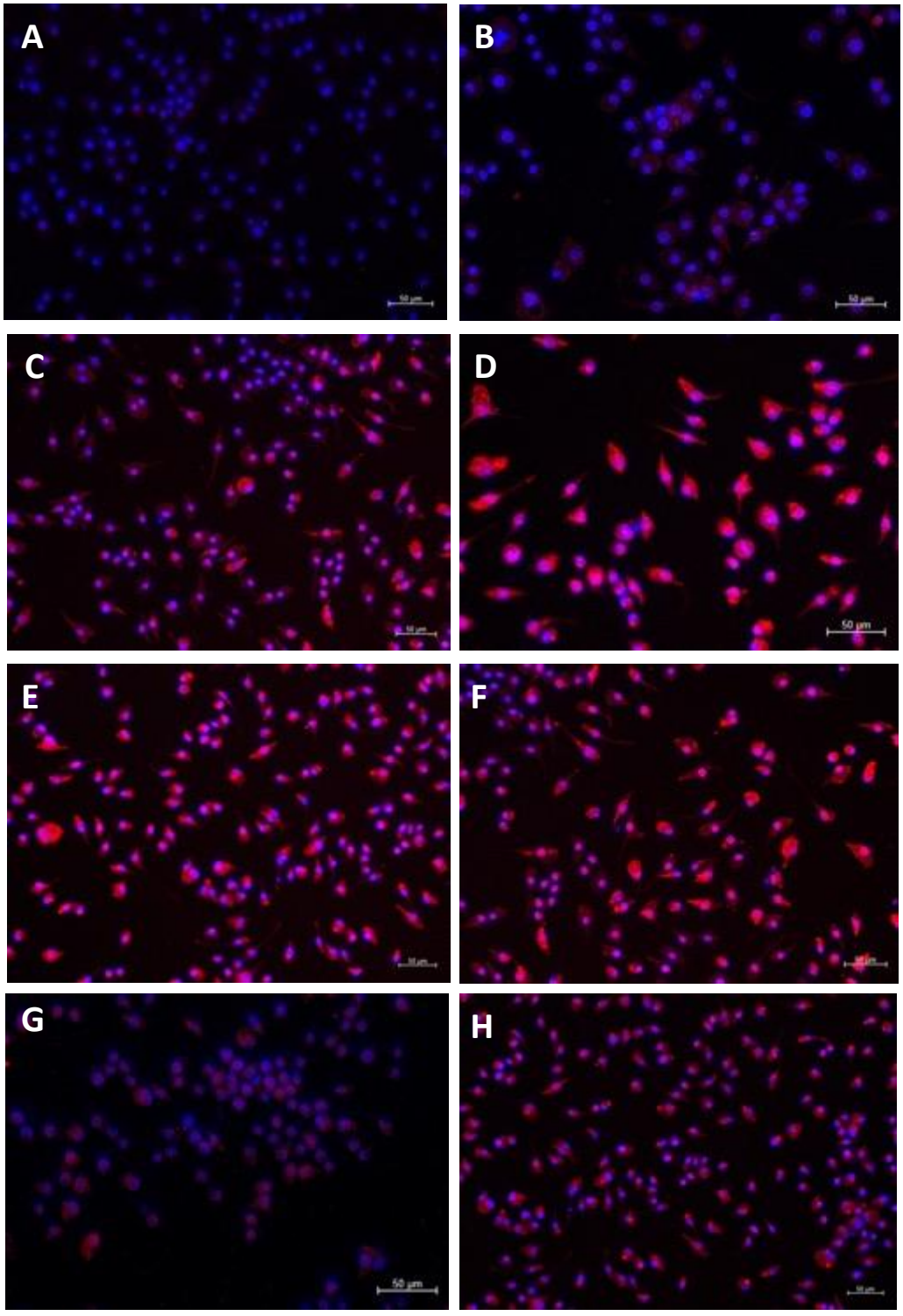
A
B
C
D
E
F
G
H

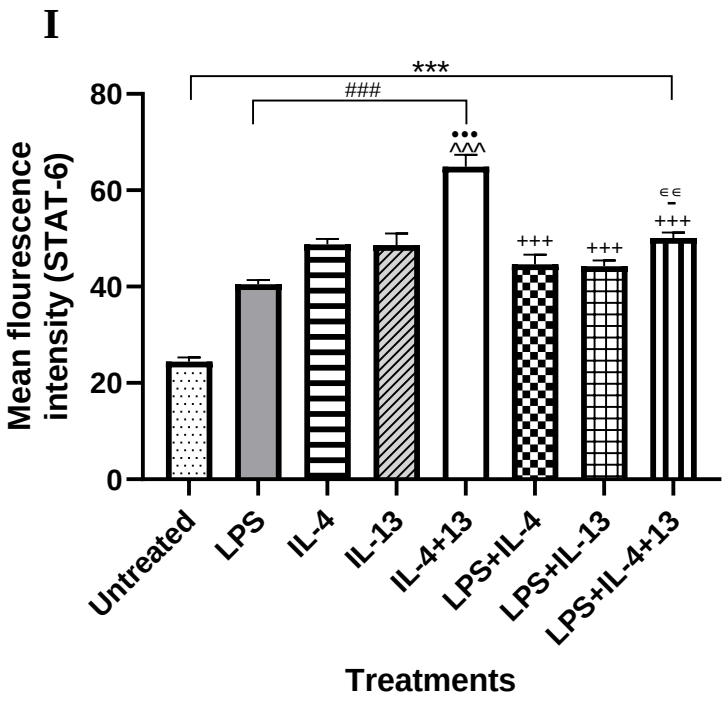


**Fig.15: Immunofluorescence detection of STAT-6 in C8-B4 microglia cells following LPS and IL-4/IL-13 treatment.** *Representative of fluorescence images showing microglia activities in (A) Untreated M0 control, (B) LPS, (C) IL-4, (D) IL-13, (E) IL-4+IL-13, (F) LPS+IL-4, (G) LPS+IL-13 and (H) LPS+IL-4+IL-13 treated cells, (I) showing the mean fluorescence intensity of CD206 in microglial cells following LPS and IL-4/IL-13 treatments. Images were captured with a fluorescence microscope (Axio Vertical A1, Zeiss, USA) and analysed using the Zen Lite Blue version 3.8 program. Data are represented as the mean ± SEM of three independent experiments. Statistical significance was determined using One-Way ANOVA with Tukey's post hoc test. ***= p≤ 0.001, **=p<0.01 vs Untreated, ###= p≤0.001, ##=p<0.01 vs LPS; • =p≤ <0.05 vs IL-13*

## 3.7 Gene expression changes influenced by LPS and IL-4/13 treatments

### 3.7.1 Amplification and Melt Curve Analysis

Following gene amplification, a melt curve analysis was performed, revealing distinct peaks highlighting the presence of individual products without the formation of primer dimers. Fig. 16 represents the melt curve analysis for the reference gene, GAPDH.

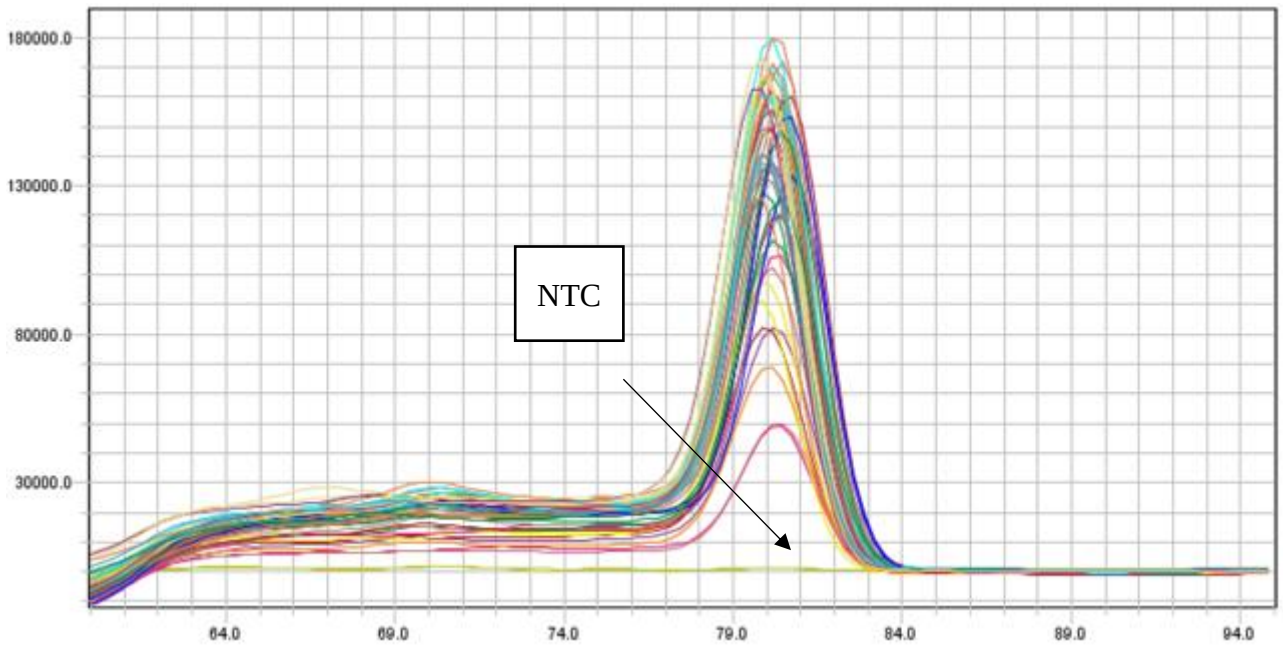


**Fig. 16: The amplification curve shows no amplification for the NTC**

### 3.7.2 PCR Efficiency

The PCR efficiency for both the reference gene and chosen target genes in the LPS induced and IL-4/IL-13 polarised samples was established from a four-parameter logistic standard curve (Fig. 17) generated by means of a 10-fold serial dilution of the cDNA cocktail mix. Beolw, Fig. 17 illustrates the standard curve for the reference gene, GAPDH.

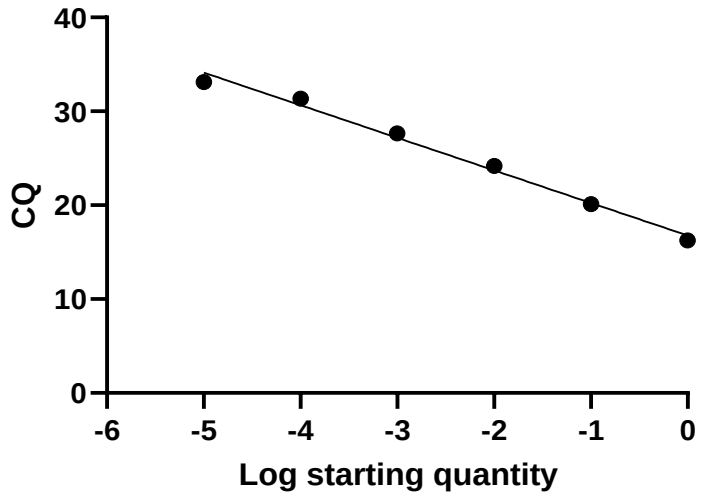


**Fig. 17: Representative standard curve generated for GAPDH. PCR efficiency was 91,56% which falls within the acceptable range of 90-110%.**

The PCR efficiencies for all genes fell within an acceptable range of 90-110% (Table 7).

**Table 7: qPCR efficiency and regression coefficient calculated from a standard curve of LPS-induced M1 and IL-4/IL-13 polarised microglia cDNA cocktail mix.**

| Gene Abbreviation | Ta (ºC) | Slope | $R^2$ | qPCR efficiency (%) |
|---|---|---|---|---|
| **GAPDH** | 60ºC | -3,5424 | 0,9939 | 91,56% |
| **TNFα** | 60ºC | -3,3710 | 0,9783 | 97,99% |
| **IL-1ß** | 60ºC | -3,4568 | 0,9825 | 94,68% |
| **Arg-1** | 60ºC | -3,3798 | 0,9906 | 97,7% |
| **IL4Rα** | 60ºC | -3,3991 | 0,9903 | 96,88% |
| **STAT6** | 60ºC | -3,4371 | 0,9857 | 95,41% |
| **CD206** | 60ºC | -3,5691 | 0,9832 | 98,59% |
| **BDNF** | 60ºC | 3,2996 | 0,9797 | 99,67% |

### 3.7.3 LPS-induced changes in TNFα and IL-1β gene expression

To further investigate LPS-induced inflammatory response changes in the cultured microglial cells, mRNA transcripts of TNFα and IL-1β were quantified in the samples 24 hours post treatment. The data show that the expression of TNFα mRNA in LPS-treated cells was significantly increased by 7-fold compared to the untreated M0 control group ($p<0.001$, Fig. 18A). It was also observed that the transcriptional expression of TNFα in the LPS-treated cells was significantly higher compared to other treatment groups ($p<0.001$, Fig. 18A). Expression of TNFα mRNA in cells treated with IL-4 alone or co-treated with IL-13 to initiate M2 microglia was significantly less when compared to the LPS-treated cells ($p<0.001$, Fig. 18A). Cells that were initially stimulated with LPS, and later received separate treatments of IL-4 or IL-13 or combined treatments exhibited significant 4-fold increases ($p<0.001$) in TNFα expression when compared to the untreated control, but in contrast, the treatments caused a significant decrease in LPS-induced changes in TNFα expression ($p<0.05$, Fig. 18A).

Similar to TNFα, IL-1β can activate and promote proliferation and differentiation of immune cells such as T and B cells (de Gruijter *et al.,* 2022). However, the excessive

production of IL-1β can result in chronic inflammatory diseases such as rheumatoid arthritis. Analysis of IL-1β mRNA expression showed a significant increase in all LPS treated groups when compared to the untreated control group ($p<0.001$, Fig. 18B). Microglial cells exposed to LPS exhibited a 15-fold increase in IL-1β mRNA expression compared to the control and groups treated with IL-4 and/or IL-13, where significant downregulation in IL-1β mRNA expression was found ($p<0.001$, Fig. 18B). It was also observed that co-treatments with IL-4 and/or IL-13 caused significant inhibition of LPS-induced transcriptional changes in the cells ($p<0.001$, Fig. 18B).

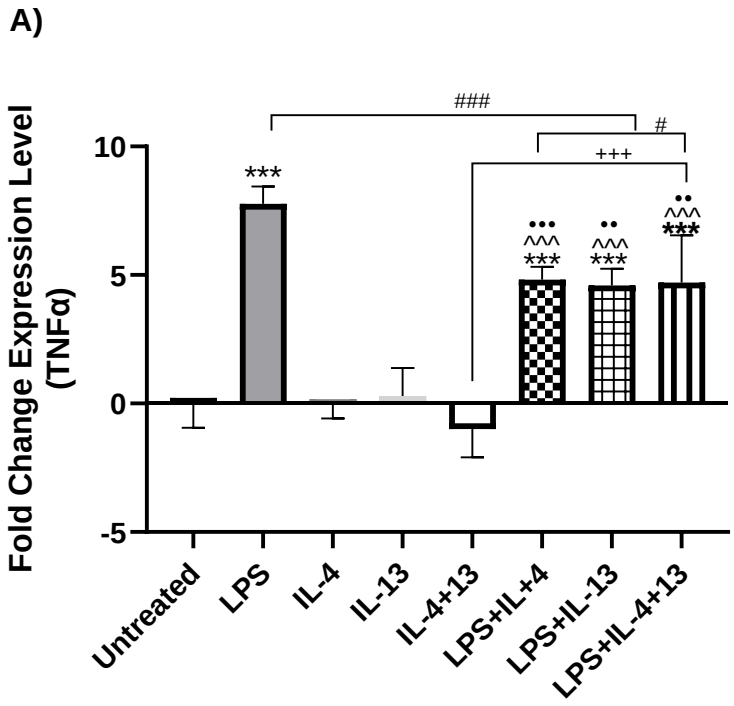

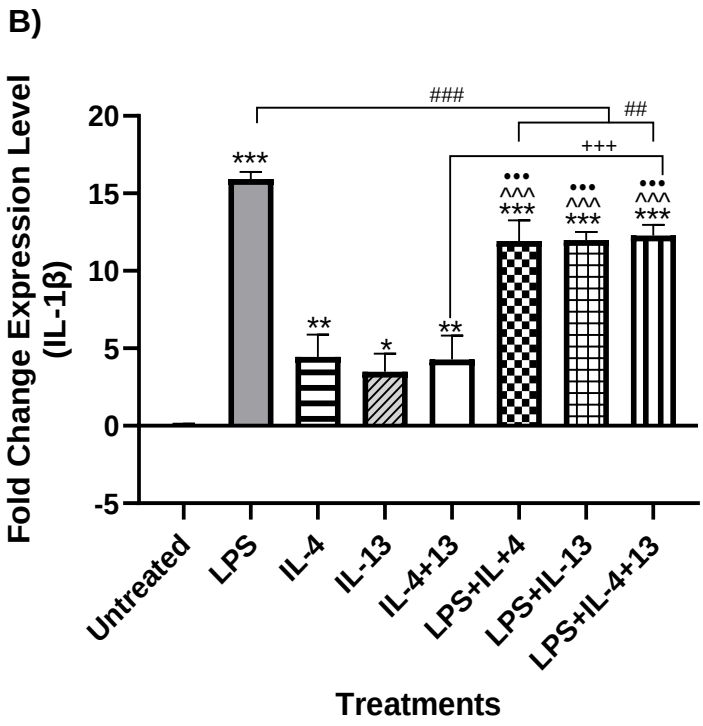


**Fig. 18: Gene expression analysis of (A) TNFα and (B) IL-1β completed using Log2 (ΔΔCt) normalized by GAPDH.** *Fold expression level of C8-B4 microglia (M0) with or without LPS, in the presence or absence of IL-4/IL-13. Data are represented as the mean ± SEM of three independent experiments. Statistical significance was determined using One-Way ANOVA with Tukey's post hoc test. ***= p≤ 0.001, **=p<0.01, *= p<0.05 vs Untreated, ###= p≤0.001, ##=p<0.01, vs LPS; ^^^=p≤ 0.001 vs IL-4;••• =p≤ 0.001 vs IL-13; +++=p≤ 0.001 vs IL-4+IL-13*

### 3.7.4 Anti-inflammatory roles of Arginase-1 and CD206

Arginase-1 is an enzyme that promotes metabolic activity by playing a vital role in the urea cycle and nitrogen metabolism. Furthermore, Arg-1 stimulates immune function and is associated with the M2 phenotypic profile of macrophages and microglial cells, which involves tissue repair and resolution of inflammatory responses (Clemente *et al.,* 2020). Another well-known M2 microglial marker that contributes to tissue repair, resolution of inflammation, and induction of immune tolerance is CD206 (Suzuki *et al.,* 2018). CD206, also known as the mannose receptor, plays a vital role in cellular functions such as pinocytosis and phagocytosis and interacts with glycoproteins and glycolipids found on the surfaces of pathogens. This suggests that CD206 release can contribute to the initial recognition and targeting of pathogens in neuronal tissues (Tanaka *et al.,* 2021).

On this premise, the anti-inflammatory roles of Arginase-1 and CD206 were investigated by quantifying the transcriptional changes in the expression of these molecules, influenced by LPS and IL-4/13 treatments. The findings revealed a significant upregulation in Arginase-1 mRNA across all treated cell cultures compared to the untreated M0 control ($p<0.01$, Fig. 19A). Within the treatment groups, Arginase-1 mRNA expression was greatly reduced in cells exposed to only LPS (M1 cells), meanwhile the cells exposed to separate or co-treatments of IL-4 and/ or IL-13 (M2 cells) exhibited 7 to 9-fold increases in the expression of Arginase-1 mRNA compared to the LPS-treated cells ($p<0.001$, Fig. 19A).

Further analysis shows a corresponding result of significant upregulation in CD206 mRNA across all treatments, when compared to the untreated control cells ($p<0.01$, Fig. 19b). CD206 mRNA expression was significantly upregulated in cells stimulated with IL-4 and IL-13 when compared to the LPS treated cultures, with a 6-fold increase in CD206 mRNA expression ($p<0.001$, Fig. 19B). Cultures treated with LPS and co-stimulated with IL-4 and IL-13 indicated a significant decrease in CD206 mRNA expression in comparison to the M2 IL-4 and IL-13 stimulated cultures.

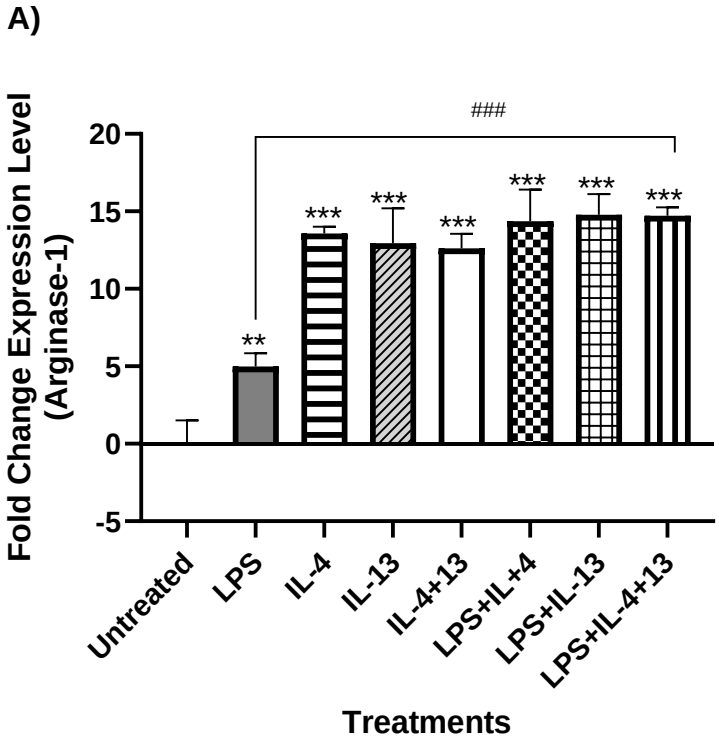

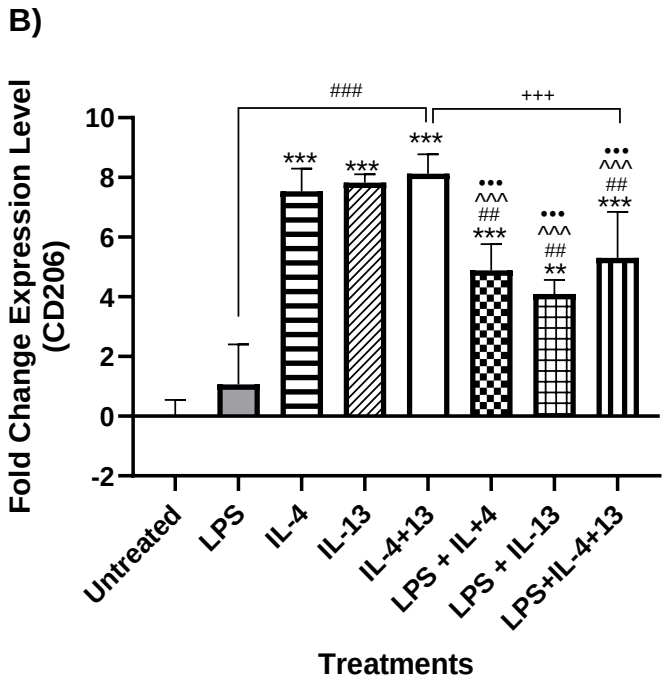


**Fig. 19: Arginase-1 and CD206 gene expression in microglial cells.** *Fold expression level of C8-B4 microglia (M0) with or without LPS, in the presence or absence of IL-4/IL-13. Data are represented as the mean ± SEM of three independent experiments. Statistical significance was determined using One-Way ANOVA with Tukey's post hoc test. ***= p≤ 0.001, **=p<0.01 vs Untreated, ###= p≤0.001, ##=p<0.01, vs LPS; ^^^=p≤ 0.001 vs IL-4;••• =p≤ 0.001 vs IL-13; +++=p≤ 0.001 vs IL-4+IL-13*

### 3.7.5 IL-4Rα mediates IL-4/13-induced phenotypic switching from M1 to M2

IL-4Rα is a component of both the IL-4 and the IL-13 receptor complexes. IL-4Rα is a type I transmembrane protein that can bind IL-4 and IL-13 to regulate IgE production, which can stimulate the isotype switching from IgM to IgE, promoting the differentiation to Th2 T cells (Isidoro-Garcia, 2005).

Next, the roles of IL-4Rα were investigated with respect to the polarizing and anti-inflammatory effects of IL-4 and IL-13 sister cytokines. Data obtained from qRT-PCR analysis indicates no significant differences in IL-4Rα mRNA expression in M1 cells exposed to LPS only, compared to the untreated control ($p>0.05$, Fig. 20). As expected, significant increases in IL-4Rα mRNA expression were observed in almost all cell cultures exposed to separate or combined treatments of IL-4 and IL-13, with or without LPS treatment, compared to the resting M0 untreated control cells ($p<0.001$, Fig. 20). Surprisingly, it was further observed that the M1 cells initially exposed LPS and later polarised to M2 cells via IL-4 or IL-13 stimulation only expressed a non-significant increase in IL-4Rα when compared to both untreated control and LPS treated cells ($p>0.05$, Fig. 20).

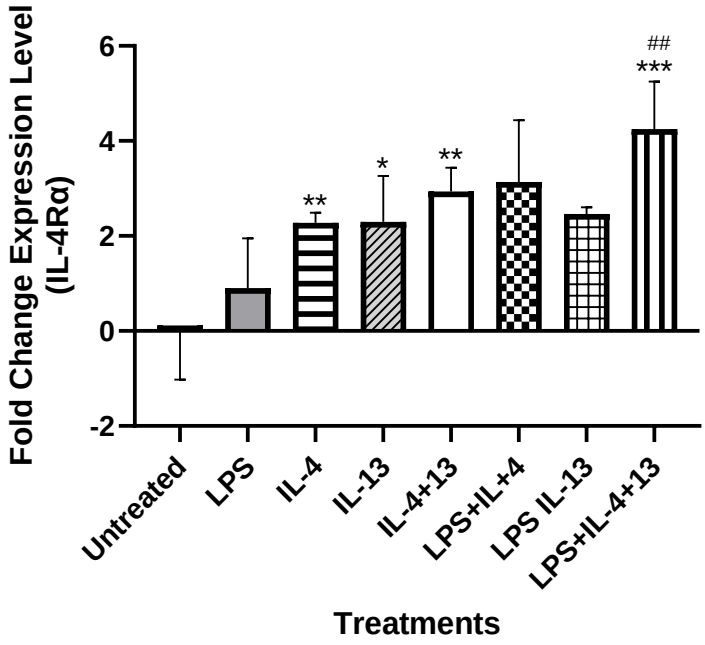


**Fig. 20: IL-4Rα gene expression in microglial cells.** *Fold expression level of C8-B4 microglia (M0) with or without LPS, in the presence or absence of IL-4/IL-13. Data are represented as the mean ± SEM of three independent experiments. Statistical significance was determined using One-Way ANOVA with Tukey's post hoc test. ***= p≤ 0.001, **=p<0.01, *= p<0.05 vs Untreated, ##=p<0.01, vs LPS*

### 3.7.6 Downstream activation of STAT-6 regulates microglial response to LPS-induced challenge.

STAT-6 belongs to a family of proteins that transmit signals from a receptor complex to the nucleus and activate mRNA expression. STAT-6 is activated by IL-4 and IL-13 and is a key element for various responses in T cells, such as the development of Th2 cells and IL-4-stimulated proliferative responses (Goenka & Kaplan, 2011).

Having established that IL-4Rα mediates the polarizing effects of IL-4/13 treatments in this study, the downstream activities of STAT6 were also investigated to ascertain the roles of this transcription factor in LPS-induced inflammation and the resolving potential of enhanced IL-4 and IL-13 signalling. STAT6 mRNA expression in the cell cultures that received only LPS treatment was not statistically different from the resting M0 control cells ($p>0.05$, Fig. 21). It was further observed that LPS treatment downregulated STAT6 mRNA expression in the cells when compared to separate or combined treatments with IL-4 or IL-13 that led to significant activation of STAT6 ($p<0.001$, Fig. 21). Moreover, greatest induction of STAT6 mRNA was evident in the cells that received co-treatments of IL-4 and IL-13 without LPS (Fig. 21).

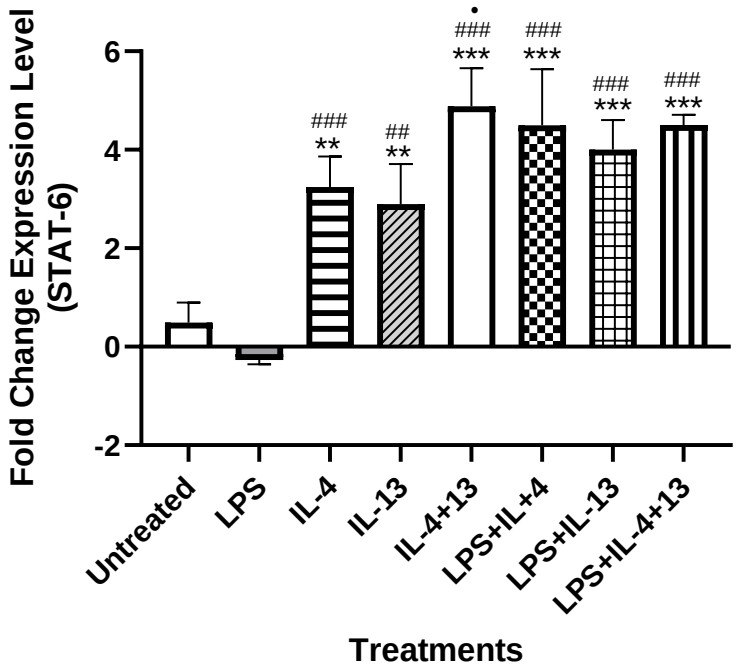


**Fig. 21: STAT-6 gene expression in microglial cells.** *Fold expression level of C8-B4 resting M0 microglia with or without LPS, in the presence or absence of IL-4/IL-13. Data are represented as the mean ± SEM of three independent experiments. Statistical significance was determined using One-Way ANOVA with Tukey's post hoc test. ***= p≤ 0.001, **=p<0.01 vs Untreated, ###= p≤0.001, ##=p<0.01 vs LPS; • =p≤ <0.05 vs IL-13*

### 3.7.7 Combined treatments with IL-4 and IL-13 promote BDNF gene expression in microglial cells.

BDNF is a multifunctional regulator of neuronal development, function, synaptic plasticity, and neuroprotection (Miranda *et al*., 2019). In this study enhanced BDNF mRNA expression was observed in all treated cells, when compared to the resting microglial control ($p<0.01$, Fig. 22). Cells treated with LPS and co-stimulated with IL-4 and IL-13 exhibited a significant increase in BDNF mRNA expression in comparison to both the untreated control and LPS treated cells, indicating that treatments with IL-4 and IL-13 induced a synergistic upregulation of BDNF expression in attempt to restore neural health or homeostasis.

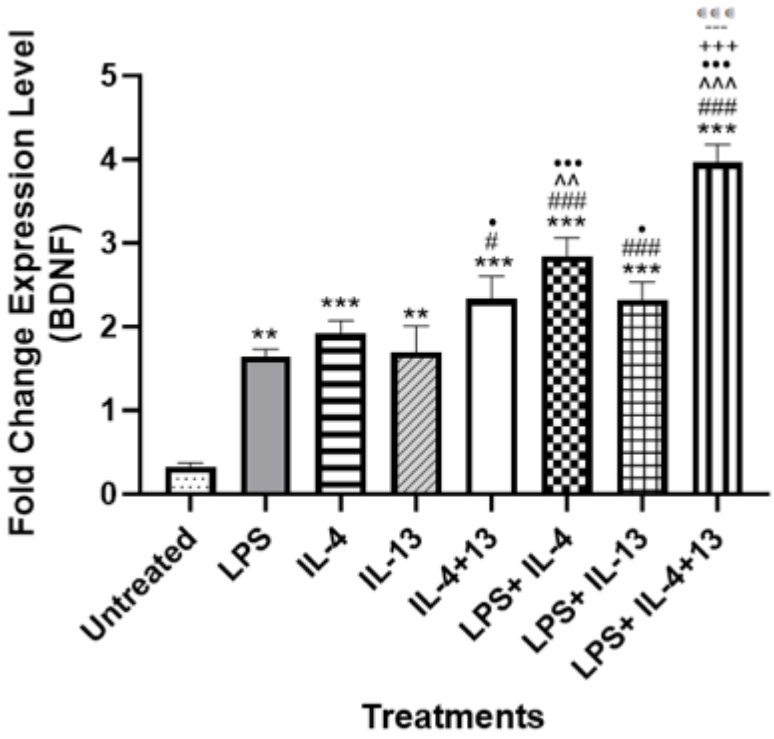


**Fig. 22: BDNF gene expression in microglial cells.** *Fold expression level of C8-B4 resting M0 microglia with or without LPS, in the presence or absence of IL-4/IL-13. Data are represented as the mean ± _SD of three independent experiments. Statistical significance was determined using One-Way ANOVA with Tukey's post hoc test. ***= p≤ 0.001 , **= p≤ 0.01 vs Untreated, ###= p≤0.001, ##= p≤ 0.01 vs LPS; ^^^=p≤ 0.001, ^^=p≤ 0.01 vs IL-4;••• =p≤ 0.001, • =p≤ <0.05 vs IL-13; +++=p≤ 0.001 vs IL-4+IL-13; --- = p ≤0.001 vs LPS+IL-4; € € € = p ≤ 0.001 vs LPS+IL-13*

# CHAPTER FOUR

# DISCUSSION AND CONCLUSION

## 4.1 Discussion

Neuroinflammation is characterized by a localized inflammatory response within the CNS. This involves intricate interactions between immune cells and glial cells, such as microglia, that stimulate the release of inflammatory molecules and induce cellular responses to varying infectious insults, injury, or chronic neurodegenerative diseases. As a result, activated immune cells secrete inflammatory mediators such as cytokines, chemokines, and ROS to eliminate pathogens, clear debris and initiate tissue repair (Shao *et al.,* 2022). However, prolonged exposure to inflammatory mediators can result in harmful effects on CNS function, which can lead to the onset of neurodegenerative diseases, autoimmune conditions, and neuroinflammatory syndromes (Eikelenboom *et al.,* 2010). Hence, it is important to understand the mechanisms and consequences of neuroinflammation for developing targeted therapeutic interventions to modulate these processes and potentially promote neuroprotection. Therefore, this study examined the effect of IL-4/IL-13-directed microglial activation and differentiation in response to LPS-induced neuroinflammation. This was completed by investigating the effect of IL-4 and IL-13 stimulation on LPS-treated and untreated C8-B4 microglial cells, by examining the cells' response through the endogenous production of TNFα, IL-1β, and BDNF. Furthermore, the LPS-induced inflammatory changes and the polarizing effect of exogenous IL-4 and IL-13 cytokines via the expression of Iba1, CD206, CD86, and STAT-6 cell surface markers were determined. Lastly, the molecular quantification of mRNA transcripts of TNFα, IL-1 β, Arg1, CD206, IL-4Rα, STAT-6, and BDNF were investigated by RT-PCR.

### 4.1.1 Effects of IL-4/IL-13 simulation on LPS-induced changes in cell viability

Neuroinflammation is associated with neuronal damage and altered biological mechanisms involving glial activation, proinflammatory molecule production, and increased oxidative stress (Shao *et al.,* 2022). Among these, microglia and infiltrating macrophages function in initiating and maintaining neuroinflammatory environment through changes in their morphology (Chen *et al.,* 2021). This means that microglia

can rapidly respond to changes by shifting from a surveillance model to numerous activation (Orihuela *et al,* 2016). Therefore, in this study, the murine C8-B4 microglial cell line was used.

Lively and Schlichter, (2018) highlighted that the reactive response to infection is characterized by a multi-faceted pro-inflammatory phenotype. This includes the release of cytokines or ROS that may inflict damage. LPS, which is the most well-known pro-inflammatory stimulus for microglia, was used to differentiate resting C8-B4 microglia into the classically activated M1 phenotypic microglia. Conversely, IL-4 and IL-13, well- studied anti-inflammatory cytokines, are known for aiding cellular repair and regeneration amid inflammatory conditions. These cytokines interact through a common receptor, IL-4Rα, by regulating the polarization of the microglial phenotype by activating STAT-6 (Biswas *et al.,* 2012). Since IL-4 and IL-13 are considered to express neuroprotective effects on neurons in animal models of experimental autoimmune AD, the resting C8-B4 microglial cells were stimulated with IL-4 and IL-13 to exhibit the alternatively activated M2 microglial phenotype, to determine if these cytokines can downregulate the production of inflammatory cytokines induced by LPS challenge. Furthermore, understanding the regulatory mechanisms governing the shift between M1 and M2 microglia can drive the understanding of developing novel therapies and restoring the homeostatic balance between these polarised states.

To establish if the stimulus used to promote the phenotypic switch between the M1 and M2 phenotype was safe to use in the C8-B4 cell line, a cell viability assay using the WST-1 reagent was conducted. Cell viability assays are performed to determine the health of the cells in a cultured sample to understand the effects of different treatments, conditions, and interventions on cell survival (Adan *et al.,* 2016). The results of this study show that C8-B4 cultures treated with 10 ng $mL^{-1}$ of LPS alone or combined treatments of LPS and IL-4 cultures (Fig. 8) exhibited moderate decreases in cell viability, compared to the untreated control that maintained 100% viability. A study conducted by Lively and Schlichter (2018) reported that a wide range of LPS concentrations can be used (10 ng $mL^{-1}$ – 2 ug $mL^{-1}$) but found that 10 ng $mL^{-1}$ is optimal for inducing inflammatory responses in cells without causing cytotoxicity, as was used in this study (Sivagnanam *et al.,* 2010). Furthermore, it was observed that treatments with IL-4 and IL-13 did not alter the cell viability, as compared to the

untreated microglial control. Thus, identifying that these cytokines are not cytotoxic in nature.

### 4.1.2 BDNF mediates the intracellular response to LPS-induced inflammation and the resolving potential of anti-inflammatory IL-4 and IL-13 cytokines.

It was previously mentioned that neuroinflammation can be considered as the initial response to harmful stimuli in order to restore CNS homeostasis. This process includes the synchronized action of resident CNS cells, namely microglia and astrocytes (Yang & Zhou, 2019). The development of the neuroinflammatory response can vary based on the diversity of the microglial activation states attained in response to differing detrimental stimuli (Prinz *et al.,* 2019). Additionally, the neuroinflammatory response is coordinated by a ubiquitous transcription factor, NFκB, which functions in inducing the expression of genes activated during the neuroinflammatory response, which include growth factors, cytokines, chemokines and cellular ligands. Among these regulatory cytokines are TNFα, which is a proinflammatory cytokine produced by microglia, astrocytes, and neurons in the CNS (Clark *et al.,* 2010). TNFα serves as a primary regulator of the initial phase of the inflammatory response, promoting the inflammatory cytokine signalling cascade (Jang *et al.,* 2021). TNFα further contributes to the regulation of synaptic plasticity, development, and homeostasis (Lui *et al.,* 2017). A study conducted by Olmos & Llado (2014) reported that under healthy conditions, TNFα has regulatory functions on central physiological processes such as synaptic plasticity, learning and memory, and astrocyte-mediated synaptic amplification. However, under pathological conditions microglia release excessive levels of TNFα, leading to a vital constituent of the neuroinflammatory response that marks a characteristic of numerous neurological conditions. Furthermore, it is well established that IL-1β is another proinflammatory cytokine that plays a key role in the neuroinflammatory response, such as in the CNS effects of peripheral LPS challenge (Zhao *et al*., 2020). Therefore, in this study, the expression of TNFα and IL-1β in LPS challenged and IL-4 and IL-13 stimulated microglia was determined. Culture supernatants of C8-B4 microglial cells treated with LPS, IL-4, and IL-13 individually or in combination were collected at 12 and 24 hours post-treatment to establish the endogenous production of TNFα and IL-1β.

It is well established that LPS is a potent mediator promoting the pro-inflammatory phenotype of microglia *in vivo* and *in vitro* (Lively & Schlichter, 2018). The current study revealed that C8-B4 cultures exposed to LPS challenge evoked high levels of TNFα and IL-1β within 12 and 24 hours of exposure (Fig. 9 and 10). This confirms that the LPS challenge induced an inflammatory response in the microglial cells. A study conducted by Rutten *et al.* (2016) highlights the importance of identifying peak cytokine expression at varying time points, and based on the ELISA results, we may deduce that 24 hours is the optimal time to observe TNFα secretion (Fig. 9). These findings are consistent with a similar study conducted by Mor *et al.* (2018) who focused on astrocyte activation, but measured TNFα at time points ranging from 6-48 hours following LPS stimulation. The authors concluded that 24 hours is the optimal time for supernatant collection to obtain the highest TNFα secretion over a 6-48 hour range. Another study that investigated LPS-induced inflammatory changes in mice by measuring the peripheral levels of IL-1β at 4,6,8 and 24-hour intervals found that observable changes are less detectable 24 hours after treatment (Mittli *et al.,* 2023). The findings of the current study agree with the report by Mittli and colleagues since increased levels of IL-1β secretion were apparent in the cell culture 12 hours post treatment (Fig. 10). Correlating results show that individual treatments of C8-B4 cell cultures with IL-4 and IL-13 did not alter the expressions of TNFα and IL-1β. However, when the cultures were treated with LPS and co-stimulated with IL-4 and IL-13, there was a significant increase in TNFα secretion ($p<0.001$) in comparison to the untreated control, but reduction in secretion of both TNFα and IL-1β compared to LPS treatment alone. This emphasizes the pro-inflammatory action of LPS and the counter effects of the anti-inflammatory cytokines IL-4 and IL-13. Similar findings were obtained by Bryant *et al*. (2017) who examined the downregulatory effect of IL-4 and IL-13 on LPS-mediated inflammatory response in human gestation and associated tissues and found that IL-4 and IL-13 retained inhibitory effects when added in conjunction with LPS. Bryant and colleagues further established no significant difference between IL-4 and IL-13 when treatments were administered individually (Bryant et al., 2017), which was also confirmed in our present study of microglia.

As mentioned previously, microglia, the brain's resident immune cells, play a vital role in immune surveillance, defence and aid in tissue repair in restoring CNS homeostasis (Hansen *et al*., 2018). Additionally, microglia functions in neurogenesis, synaptic pruning, and myelination, and are linked with higher cognitive function such as

learning and memory. This is facilitated by supporting the formation of learning-related synapses via BDNF signal transduction (Parkhurst *et al*., 2013; Pierre *et al*., 2017).

BDNF, an essential neurotrophin, is fundamental for neuronal survival, development, and function. BDNF contributes to synaptic plasticity crucial for learning and memory in the CNS, and supports microglial activation *in vivo* (Jiang *et al.,* 2011). In response to inflammatory insult, BDNF is released either through activity-dependent exocytosis or from microglial cells via the exocytotic pathway, both of which are inclined to modulation (Kuczewski *et al*., 2008). Hence, BDNF is seen as a potential mediator for moderating the shift between acute and unresolved chronic inflammation, believed to drive the progression of neurodegenerative diseases (Tansey & Goldberg, 2010). In response to noxious stimuli, microglial activation occurs through changes in their morphology, proliferation, and release of molecules that can be considered to be neuroprotective. Since IL-4 and IL-13 are considered to exert neuroprotective effects, the expression of endogenous production of BDNF in LPS challenged and IL-4 and IL-13 stimulated microglia to establish the link between the anti-inflammatory modality of microglia dependent on IL-4 and IL-13 stimulation and BDNF neuroprotective responses was determined.

As with the analysis of TNFα and IL-1β secretion, culture supernatants of C8-B4 microglial cells treated with LPS, IL-4, and IL-13 individually or in combination were collected at 12 and 24 hours post-treatment to establish the endogenous production of BDNF. At 12 hours post-treatment, a significant amount of BDNF was secreted by LPS-treated cell cultures (Fig. 11A). This result correlates to the findings by Gomes *et al.* (2013), who demonstrated that the activation of microglia with LPS triggers a release of BDNF, which functions in an autocrine/ paracrine role by stimulating microglial activation. Additionally, in the present study, the cultures treated with LPS and co-stimulated with IL-4 and IL-13 exhibited a highly significant increase in BDNF expression when compared to the untreated control and cultures treated with LPS alone ($p<0.001$), which further confirms the neuroprotective roles of IL-4 and IL-13 in this study, as these sister cytokines likely exhibited synergistic effects on BDNF gene expression in an attempt to restore homeostasis. Furthermore, the increases in BDNF secretion in cultures treated with IL-4 and IL-13 individually or combined observed at 24 hours post-treatment (Fig. 11B) validate the release of BDNF endogenously during phenotypic switching of microglial cells from resting M0 to alternatively activated M2

microglia. This observation is supported by a previous study that reported that IL-4 influenced microglia to adopt the alternative activation phenotypic state, which was associated with increased levels of BDNF release (Zang *et al.*, 2021). The current study provides further evidence that the neuroprotective BDNF secretion is associated with IL-4 and IL-13 anti-inflammatory potential, as cultures initially exposed to LPS challenge and later treated with IL-4 and IL-13 evoked significant upregulation in BDNF secretion (Fig. 11B).

Next, transcriptional changes in TNFα, IL-1β, and BDNF gene expression in response to LPS-induced neuroinflammation and IL-4/IL-13 polarisation were investigated to further confirm the neuroprotective roles of IL-13 and IL-4.

It was observed that LPS exposure upregulated TNFα gene expression, without significant change in IL-4/ IL-13 treated cultures (Fig. 18a) These findings are consistent with previous studies which reported that activated microglia produce and release TNFα as an initial or immediate response to injury to promote clearance of infiltrating immune cells and resolution of inflammation (Lombardi *et al*., 2019, Rodgers *et al.,* 2020, Veroni *et al.,* 2010).

Therefore, it can be deduced that cytokines are fundamental in orchestrating the inflammatory response following CNS infection or traumatic injury. After LPS administration, the innate immune response is triggered via TLR-4 activation, initiating the production of pro-inflammatory cytokines by activating transcription factors such as NFκB (Andreakos *et al.*, 2004). This response results in the synthesis and upregulation of IL-1β which further contributes to the inflammatory response. A significant upregulation of IL-1β mRNA expression was detected in LPS-treated cultures which further confirms the development of inflammatory responses in the microglia to LPS challenge (Fig. 18b). Interestingly, the LPS-induced inflammatory changes were suppressed by IL-4 and IL-13 treatments (Fig. 18b). These results coincide with previous findings by Bryant *et al.* (2017) who reported that IL-4 and IL-13 downregulated LPS-mediated inflammatory response in human-gestation-associated tissues.

It was found that LPS and IL-4 or IL-13 treatments alone or combined stimulation upregulated BDNF mRNA expression in the cultures, thus providing additional evidence for BDNF mediating the intracellular response to LPS-induced inflammatory

changes, as well as the resolving potential of the counter-inflammatory IL-4 and IL-13 cytokines. This further highlights that M2 microglial polarised phenotypes induced by IL-4 and IL-13, and the synergistic effect of these M2 cytokines increases BDNF expression in an attempt to restore homeostasis in response to LPS-inflammatory insult.

### 4.1.3 IL-4/13-induced STAT-6 activation mediates the development of anti-inflammatory microglial phenotype.

Iba-1 is a cytoplasmic, actin-binding protein that contributes to the reorganisation of the membrane cytoskeleton, vital to the dynamic properties of microglia (Ahmed *et al*., 2007). For this reason, Iba-1 has been widely reported as a microglial-specific marker, used commonly for microglial detection (Kanazawa *et al*., 2002). To confirm the presence of microglia, Iba-1 expression in cell cultures was determined by immunofluorescence staining following LPS challenge and/or IL-4/13 stimulation. The results show that untreated microglia exhibited a notably lower fluorescence intensity for anti-Iba-1 antibody binding when compared to the treated cells (Fig 12B-H), aligning with Fig 12I, where all treatments exhibited a significantly increased fluorescent intensity. The cellular morphology indicated that the microglial cells were activated in response to LPS treatment, as the cells appeared larger, and rounder, the protrusions decreased and appeared slightly thicker and were amoeba-shaped, in line with the characteristics of the M1 microglia phenotypic profile. This correlates to the findings of (Wu *et al*., 2019) who conducted a study to determine LPS-induced BV2 microglial activation and differentiation and reported that LPS-induced M1 microglia as more rounded and amoeba-like. In the IL-4/IL-13 treated cells, minute filopodial finger-like projections were observed (Fig. 12 D-F). Kress *et al*. (2007) measured the three-dimensional dynamics of microglia filopodia and determined that the filopodial projections act as cellular “tentacles”, and after binding to a particle, the filopodia retracted and bound the particle towards the cell for phagocytosis. This is indicative of the plasticity of microglial phenotypes, as well as their functional role in the CNS, and confirms the phenotypic switch to M2 microglial differentiation. It was further noted that the untreated C8-B4 microglial cells appeared less dense in the population when compared to the remaining cell treatments, further confirming the larger appearance of the M1 phenotype and the increased projections of the M2 phenotypic profile. Interestingly, the cultures stimulated with LPS and co-stimulated with IL-4 and IL-13

presented an elongated morphology as opposed to the rounded M1 characteristic, confirming the anti-inflammatory M2 phenotypic profile of the IL-4/IL13 treatments on LPS-induced microglia.

The presence of microglial M1 and M2 phenotypes was confirmed by the immunofluorescence analysis. Classically activated microglia are associated with the expression of the surface antigen CD86 (Zhou *et al.,* 2017), therefore, to confirm the pro-inflammatory action of LPS, the C8-B4 microglia were stained with anti-CD86. The immunofluorescence analysis revealed a distinct upregulation of CD86 expression in microglial populations following treatment with LPS (Fig. 13B), which correlates to the significantly increased fluorescent intensity (Fig. 13 I) observed in the LPS-treated cells when compared to the untreated control. Also, distinctive morphological changes were observed in the cultures treated with LPS when compared to the resting, untreated microglia. The cell bodies presented larger and rounded shapes, and the protruding processes appeared shorter, indicative of an amoeboid-like morphology. Similar findings were observed by Wu *et al.* (2019) who described LPS-treated microglia as amoeba-shaped and described similar morphological changes in LPS-induced microglia. Furthermore, it was evident as shown in Fig. 13B that the LPS-induced M1 microglia displayed reduced ramification when compared to the resting M0 microglial cells (Fig. 13A). The LPS-treated cells also portrayed a significant increase in CD86 fluorescence intensity when compared to the cells treated with IL-4 and/or IL-13 (Fig. 13 C-E, Fig. 13 I) and it was evident that when cells were stimulated with combined treatments of IL-4 and IL-13, a morphological change exhibiting the M2 phenotype was observed. Intriguingly, the cultures co-stimulated with LPS, IL-4, and IL-13 exhibited a significant reduction in their fluorescence intensity in comparison to the LPS-treated cells but were significantly upregulated in comparison to IL-4/Il-13 stimulated cultures ($p<0.01$), which provided evidence for the role of CD86 as a M1 microglial marker. The pronounced increase in cell densities in the LPS-treated cultures and distinctive amoeboid morphology of the CD-86 positive microglia highlights their activation in response to LPS treatments.

The M2 phenotypic state of microglia, also known as the alternative activation state, is known for its anti-inflammatory and tissue-repairing functions (Guo *et al.,* 2022). CD206, a member of the transmembrane protein family, is expressed in macrophages, dendritic cells neural tissue, astrocytes, and microglia (Kobayashi *et*

*al*., 2013). To confirm the M2 polarizing action of IL-4 and IL-13, anti-CD206 was used to analyse the C8-B4 microglial cell line. This is supported by numerous studies in which CD206 is widely recognised as a M2 microglial marker (Durafourt *et al.,* 2012). A study conducted by Régnier-Vigouroux (2003) reported that CD206 is involved in numerous cellular functions such as phagocytosis and is suggested to contribute to the first step of cell recognition and capture of pathogens in neural tissues. Fig 14I illustrates a significant upregulation of CD206 fluorescence intensity in microglial cells following IL-4 and/or IL-13 treatments, which confirms the reliability of CD206 as a marker for M2 polarization. Furthermore, distinct morphological features were exhibited in the cultures treated with IL-4 and or IL-13, as seen in Fig 14C-E. The ramified processes presented a slightly more branched morphology and appeared as thin elongated processes. Additionally, the cell size was visibly reduced in comparison to the M1-activated (LPS stimulated) microglia (Fig. 14B), which is indicative of the anti-inflammatory phenotype as previously described (Tanaka *et al.,* 2021). Cells treated with LPS and co-stimulated with IL-4 and IL-13 displayed a significant increase in fluorescence intensity when compared to the cultures treated with LPS alone, further indicating the use of CD206 as a reliable marker to confirm the M2 polarised state of the microglial cells, validating their activation in response to IL-4 and IL-13 treatments.

As mentioned previously, both IL-4 and IL-13 cytokines are secreted by T cells, macrophages, and microglia to mediate inflammatory response (May & Fung, 2015). They share a receptor, IL-4Rα, that upon activation, initiates a transduction signal leading to an anti-inflammatory response (Suzuki *et al.,* 2015). Both cytokines utilize JAKs to induce the signalling and activate STAT-6, which translocate to the nucleus and regulates gene expression (Jiang *et al.,* 2000). Therefore, the nuclear translocation of STAT-6 was observed following IL-4 and IL-13 treatments in LPS-induced and untreated microglial cells. Cultures treated with IL-4 or IL-13 exhibited an increase in fluorescence intensity when compared to the untreated cells and LPS-treated cells. A prominent nuclear localization of STAT-6 was observed in the cells co-treated with IL-4 and IL-13, with increased fluorescence intensity. This alludes to the synergistic effects of IL-4 and IL-13 cytokines which likely provoke the intracellular activation of the JAK-STAT signalling pathway.

### 4.1.4 Expression of cell surface receptors activated during M2 polarisation in response to IL-4 and IL-3 treatment

The M2-microglial related phenotypes in response to LPS-induced inflammation was further examined and found that Arg-1 (Fig. 19a) and CD206 (Fig. 19b) expression were significantly increased in cultures treated either individually with IL-4 and IL-13, co-treated with IL-4 and IL-13, and co-stimulated with LPS. The increased Arg-1 expression in IL-4 and IL-13 treated microglia suggests that Arg-1 plays a role in regulating the M2 microglial response. It was also noted that IL-4 and IL-13 treated cells co-stimulated with LPS significantly increased the expression of Arg-1 compared to the untreated and LPS-treated cells, thus confirming the ant-inflammatory cytokine action in response to LPS challenge. These findings correlate to the study conducted by Ishida *et al.* (2023) who showed that LPS and IL-4 induced macrophages showed an upregulation of Arg-1 compared to the M2 IL-4 induced cells. The anti-inflammatory modality of IL-4 and IL-13 cytokines was further confirmed by the upregulation of CD206 expression in the cultures treated with the M2 cytokines (Stein *et al.,* 1992). The expression levels of CD206 remained unchanged in response to the LPS treatment, while a significant upregulation of CD206 expression in cultures stimulated with IL-4 and/or IL-13 was established in comparison to the untreated control (Fig. 19b). Cultures co-stimulated with LPS, IL-4 and IL-13 significantly increased CD206 mRNA transcripts when compared to the untreated control and LPS treated cells, but CD206 transcripts were significantly reduced by IL-4 and IL-13 lone treatments. This may suggest that LPS triggers the signalling cascade through TLR4 leading to the activation of the pro-inflammatory response and the effect of IL-4 and IL-13 in the polarization of microglia to exhibit the M2 phenotype. LPS therefore suppressed the expression of CD206 in the M2 phenotype. However, cultures exposed to LPS in the presence of IL-4 and IL-13 stimulation exhibited upregulation in CD206 expression, thus highlighting the anti-inflammatory modality of the IL-4 and IL-13 cytokines.

Having established that IL-4 and IL-13 stimulation activates STAT-6 signalling to evoke an anti-inflammatory response by microglia to LPS challenge, it is therefore imperative to delineate the roles of IL-4Rα receptor in neuroinflammation as a heterodimer complex that mediates the action of IL-4/13 cytokines. Therefore, the IL-4 and IL-13 induced STAT-6 phosphorylation in response to LPS induced

neuroinflammation was examined. The findings revealed that IL-4Rα expression was upregulated in cultures stimulated alone with IL-4 and IL-13 or exposed to both LPS and IL-4/13 treatments. This confirms that IL-4 and IL-13 cytokines and their receptors are dynamic mediators of type II immunity and anti-inflammatory processes. This relates to the findings of Ranasinghe *et al*. (2018) who reported that the IL4 and IL-13 receptor complex serves as a regulator of Th2 immunity development and M2 polarization, highlighting that IL-4 and IL-13 receptors are vital for inducing the polarized type II immunity required for the resolution of neuroinflammation. Furthermore, as has already been established, the activation of STAT-6, a transcription factor, occurs through phosphorylation in the presence of cytokines such as IL-4 and IL-13, therefore changes in the mRNA transcripts of STAT-6 following LPS-induction and IL-4/IL-13 polarization of microglia were determined. Upon activation, STAT-6 is vital for numerous T cell responses, comprising the development of Th2 cells and IL-4-stimulated proliferative responses. A study by Cao *et al.* (2016) demonstrated that IL-13 upregulated stem cell markers and assisted cell migration and invasion via the STAT-6 signalling pathway, providing a link between IL-13 and STAT-6 signalling. The link between STAT-6 signalling and IL-4 and IL-13 cytokines was confirmed in the present study (Fig. 21), as mRNA transcripts of STAT-6 were significantly upregulated in IL-4 and IL-13 treated cells in comparison to the untreated control ($p<0.01$). However, the combined treatment of IL-4 and IL-13 had a greater impact on the expression of STAT-6 when compared to the untreated control and LPS-treated samples ($p<0.001$), confirming that IL-4 and IL-13 act synergistically in the activation of the JAK/STAT signalling pathway. Cells stimulated with LPS and IL-4 and/or IL-13 significantly increased STAT-6 mRNA expression in comparison to the untreated and LPS-treated cells, indicating that STAT-6 is a vital downstream mediator of both IL-4 and IL-13 cytokines. From the findings shown in Fig. 20 and Fig. 21, it can be confirmed that IL-4 and IL-13 influence the microglial cells to M2 polarization in response to the LPS challenge, and binding to the IL-4Rα subunit can initiate the signalling cascade and activate nuclear translocation of STAT-6.

## 4.2 Conclusion

Neuroinflammation has been identified as a key process in driving the pathogenesis related to various neurodegenerative diseases, including Alzheimer's disease, Parkinson's disease, and brain injury. Microglia play a fundamental role in driving this process, due to the plasticity in their functional activity in the CNS, in which they release inflammatory mediators to promote inflammation or alter their phenotypic heterogeneity to stimulate the M2 anti-inflammatory, wound healing response.
The current study aimed to investigate how IL-4/IL-13 and STAT-6 signalling orchestrates the microglial response, activation, and differentiation to LPS-induced neuroinflammation. Further, the molecular mechanisms involved in the resolution of LPS-induced neuroinflammation and neural protection through IL-4/13- enhanced BDNF signalling were examined.

The findings confirm that LPS is a potent pro-inflammatory stimulus that alters the microglial phenotypic switch to resemble the M1-activated microglial state. This was characterized by the upregulation of key pro-inflammatory cytokines such as TNFα and IL-1β in the treated cell cultures. It was further confirmed that the expression of CD86 significantly increased in the M1 microglial phenotype cells of LPS treated cultures and that the cells appeared larger, rounder, and amoeba-shaped (Fig. 13), thereby confirming the M1 microglial polarised state.

IL-4 and IL-13 are vital components of the Th2-mediated immune response and play a functional role in the alleviation of LPS-induced neuroinflammation. Treatments with IL-4 and IL-13 elicited the anti-inflammatory response by inducing phenotypic switching in activated microglia to an alternative M2 phenotype. This was illustrated by the upregulation of Arg-1 and CD206 expression in IL-4 and IL-13 treated cultures (Fig. 19 a-b). Additionally, immunofluorescence analysis established distinct morphological features typical of the M2 microglial phenotype, where the ramified processes were presented as more branched, and the shape of the cell body appeared elongated (Fig. 14). Furthermore, the anti-inflammatory action of IL-4 and IL-13 was indicated in the downregulation of TNFα and IL-1β secretion and mRNA transcripts when C8-B4 cells were induced with LPS and co-stimulated with IL-4 and IL-13, in comparison to the cultures treated with LPS alone.

The microglial M2 polarized state was confirmed by activation with IL-4 and - IL-13, and the effect of these cytokines in the resolution of LPS-induced neuroinflammation was established by observing the activation of the IL-4Rα receptor and STAT-6 initiating the downstream intracellular signalling cascade. The findings demonstrate that in the presence of LPS-induced neuroinflammatory stimuli, the expression of IL-4Rα is significantly upregulated when microglia cells are co-stimulated with IL-4 and IL-13 (Fig. 20). This observed activation of IL-4Rα represents a pivotal shift inducing the anti-inflammatory phenotype, counteracting the pro-inflammatory changes induced by LPS. Furthermore, the findings provide evidence of the activation by IL-4 and IL-13 of STAT-6 as a downstream effector of IL-4Rα. The phosphorylation and nuclear translocation of STAT-6 was significantly upregulated in the cultures treated with IL-4 and IL-13 (Fig. 21). Cultures treated with LPS and co-stimulated with IL-4 and IL-13 were significantly upregulated in comparison to the cells treated with LPS alone, further indicating the activation of the STAT-6 signalling cascade by IL-4 and IL-13. Activated STAT-6 serves as a transcriptional regulator, modulating the expression of genes associated with immunomodulation, tissue repair, and anti-inflammatory responses.

Lastly, the central role of IL-4 and IL-13 enhanced BDNF secretion in the resolution of neuroinflammation has been highlighted. The findings demonstrated that 24 hours post-treatment with IL-4 and IL-13 a significant increase in BDNF secretion occurs in microglial cells (Fig. 11). Cultures treated with LPS and co-stimulated with IL-4 and IL-13 significantly upregulated BDNF secretion in comparison to the cultures stimulated with LPS independently, confirming that the combined treatments of IL-4 and IL-13 promote BDNF secretion in response to neuroinflammation. It was further established that BDNF mRNA transcripts were significantly increased in all treated cells, however, BDNF was significantly upregulated in cultures treated with combined IL-4 and IL-13 compared to the cells treated with IL-4 or IL-13 alone. Interestingly, the most significant upregulation of BDNF expression was observed in the cultures stimulated with LPS, IL-4, and IL-13, revealing the synergistic effects of IL-4 and IL-13 on BDNF expression in response to LPS-mediated inflammatory insult. This enhanced secretion of BDNF suggests a BDNF neuroprotective response aimed at counteracting the detrimental effects of neuroinflammation on neuronal health, viability, and function.

In summary, this study further increases our understanding of the anti-inflammatory roles of IL-4 and IL-13 in the downstream activation of the STAT-6 signalling cascade and provides insights into the neuroprotective effects of IL-4 and IL-13 through the expression of BDNF.

### 4.3 Limitations and recommendations for future studies

Since this study highlighted the anti-inflammatory modality of IL-4 and IL-13 in stimulating the downstream signalling of STAT-6, further investigations can examine potential interactions with other signalling pathways implicated in the activation of the M2 microglia. IL-4 and IL-13 share functional characteristics through the IL-4Rα and share the JAK signalling pathway to activate STAT-6. Since it has previously been reported that STAT-6 and IRS-2 are recognized as the primary pathways involved in IL-4 and IL-13 responsiveness (Ruckerl *et al*., 2012) and it is known that IL-13 binds via IL-13Rα-1 receptor, targeting the expression of JAK, IRS-2 signalling, and 13Rα-1 receptor through IL-13 should be investigated in future. Moreover, the cytokine release in response to the inflammatory and anti-inflammatory stimulus was limited in this *in vitro* setting, therefore it would be insightful to explore the effect of NFκB in initiating the TLR-4 as it induces pro-inflammatory cytokines via the activation of transcription factors, NFκB (Andreakos *et al.,* 2004). Furthermore, to better understand the neuroprotective effects of BDNF, the use of an anti-inflammatory therapeutic agent that could be administered *in vivo* and *in vitro* would be beneficial and could provide a more comprehensive understanding of the roles of BDNF. The use of a microglial cell line limits analysis of the complexity of *in vivo* microglial responses in the natural brain environment, therefore it would be valuable to extend this informative cell culture study to an animal model.

## References


Abbott NJ (2013). Blood-brain barrier structure and function and the challenges for CNS drug delivery. J. Inherit. Metab. Dis. 36, 437-449.

Abdul Y, Jamil S, He L, Li W & Ergul A (2020). Endothelin-1 (ET-1) Promotes a Proinflammatory Microglia Phenotype in Diabetic Conditions. Can J Physiol Pharmacol. 98(9), 596-603.

Abraham J, Jang S, Godbout J, Chen J, Kelley K, Dantzer R & Johnson RW (2008). Aging sensitizes mice to behavioral deficits induced by central HIV-1 gp120. Neurobiol. Aging 29(4), 614-621.

Adan A, Kiraz Y & Baran Y (2016). Cell proliferation and Cytotoxicity Assays. NIH 17(14), 1213-1221.

Ahmed Z, Shaw, G, Sharma VP, Yang C, McGowan E & Dickson DW (2007). Actin-binding proteins coronin-1a and IBA-1 are effective microglial markers for immunohistochemistry. J Histochem Cytochem 55(7), 687-700.

Alvares MM, Lui JC, Santigago GT, Cha BH, Vishwakarma A ... et al (2016) Delivery strategies to control inflammatroy response: Modulating M1 and M2 polarisation in tissue engineering applications. J Control Release 240, 349-363.

Andreakos E, Sacre SM, Smith C, Lundberg A, Kiriakidis S, Stonehouse T, Monaco C, Feldmann M & Foxwell BM (2004). Distinct pathways of LPS-induced NF-kappa B activation and cytokine production in human myeloid and nonmyeloid cells defined by selective utilization of MyD88 and Mal/TIRAP. Blood. 103, 2229–2237.

Andrews AL, Holloway JW, Holgate ST & Davies DE (2006). IL-4 receptor a is an important modulator of IL-4 and IL-13 receptor binding: im- plications for the development of therapeutic targets. J. Immunol. 176, 7456– 7461.

Aoki M, Yamaguchi R, Yamamoto T, Ishimaru Y, Ono T, Sakamoto A, ...et al.. (2015). Granulocyte-macrophage colony-stimulating factor primes interleukin-13 production by macrophages via protease-activated receptor-2. Blood Cells, Mol Dis. 54, 353–9.

Archie SR, Al Shoyaib A & Cucullo L (2021). Blood Brain Barrier Dysfunction in CNS Disorders and Putative Therapeurtic Trargets: An Overview. Pharmaceutics, 13 (11), 1779-82.

Avraham S, Lu TS & Avraham HK (1970). Blood–brain barrier. SpringerLink.

Bao K & Reinhardt RL (2015). The differential expression of IL-4 and IL-13 and its impact on type-2 immunity. Cytokine, 75(1), 25–37.

Bathina S & Das UN (2015). Brain-derived neurotrophic factor and its clinical implications. Archives of medical science: AMS, 11(6), p.1164.

Biswas SK, Chittezhath M, Shalova IN & Lim JY (2012). Macrophage polarization and plasticity in health and disease. Immunol. Res. 53, 11–24

Bivins A, Kaya D, Bibby K, Simpson SL, Bustin SA, Shanks OC & Ahmed W (2021). Variability in RT-qpcr assay parameters indicates unreliable SARS-COV-2 RNA quantification for wastewater surveillance. Water research. 203(2021), 1-8.

Brombacher TM, Nono JK, DeGouveia KS, Makena N, Darby M, Womersley J, Tamgue O & Brombacher F (2017). IL-13-mediated regulation of learning and memory. J Immunol. 198, 2681-2688.

Bustin SA, Benes V, Nolan T & Pfaffl M (2005). Quantitative real-time RT PCR – a perspective. Review, 34, 597-601.

Bustin, S. A. (2000). Absolute quantification of mRNA using real-time reverse transcription polymerase chain reaction assays. J Mol Endocrin, 25(2), 169-193.

Caballero-Herrero M, Jumilla E, Buitrago-Ruiz M, Valero Navarro & Cuevas M (2023). Role of Damage- Associated Molecular Patters (DAMPS) in the Postoperative Period after Colorectal Surgery. Int J Mol Sci 24(4) 3862-70.

Cai W, Dai X, Chen J, Zhao J, Xu M, Zhang, L, Tang B, Zhang W, Rocha M, Nakao T, Kofler J, Shi Y, Stetler RA, Hu X & Chen J (2019). STAT6/Arg1 promotes microglia/macrophage efferocytosis and inflammation resolution in stroke mice. JCI Insight 4(20).

Cao H, Zang J, Lui H, Wan L, Zhang H, Huang Q, Xu E & Lai M (2016). IL-13/STAT6 signaling plays a critical role in the epithelial-mesenchymal transition of colorectal cancer cells. Oncotarget. 7(38), 61183- 61198.

Casli BT & Reed-Gaeghan EG (2021). Microglial Function and Regulation during Development, Homeostasis and Alzheimer's Disease. Cells 10(4), 957-960.

Chen O, Luo X & Ji RR (2021). Macrophages and microglia in inflammation and neuroinflammation underlying different pain states. Med Rev 3(5) 381-407.

Chen S, Saeed A, Liu Q, Jiang Q, Xu H, Xia GG, Rao L & Duo Y (2023). Macrophages in immunoregulation and therapeutics. Signal Transduct Target Ther 8, 207-210.

Chen WW, Zhang X & Huang WJ (2016). Role of neuroinflammation in neurodegenerative diseases (review). Mol. Med. Rep. 13, 3391-3396.

Clemente GS, van Waarde A, Antunes IF, Domling A & Elsinga PH (2020). Arginase as a Potential Biomarker of Disease Progression: A Molecular Imaging Perspective. Int. J. Mol. Sci. 21(15), 52-69

Cobb CA & Cole MP (2015). Oxidative and Nitrative Stress in Neurodegeneration. Neurobiol Dis. 84, 4-21.

Derecki NC, Cardani AN, Yang CH, Quinnies KM, Crihfield A, Lynch KR & Kipnis J (2010). Regulation of learning and memory by meningeal immunity: a key role for IL-4. J. Exp. Med. 207,1067–1080.

Dimou L & Gallo V (2015). NG2-glia and their functions in the Central Nervous System. Glia 63, 1429–1451.

DiSabato D, Quan N & Godbout JP (2016). Neuroinflammation: the devil is in the details. J Neurochem. 139(2), 136-153.

Doorn KJ, Breve JJ, Drukarch B, Boddele HW, Huitinga I, Lucassen PJ & van Dam AM (2015). Brain region-specific gene expression profiles in freshly isolated rat microglia. Front Cell Neurosci. 9, 1-18.

Drokhlyansky E, Go¨z Aytu€rk D, Soh, TK, Chrenek R. O'Loughlin E, Madore C, Butovsky O, & Cepko CL(2017). The brain parenchyma has a type I interferon response that can limit virus spread. Proc. Natl. Acad. Sci. 114, 95–104.

Du L, Zhang Y, Chen Y, Zhu J, Yang Y & Zhang HL (2017). Role of microglia in neurological disorders and their potentials as a therapeutic target. Mol. Neurobiol. 54, 7567–7584.

Duan L, Chen BY, Sun XL, Luo ZJ, Rao ZR, Wang JJ & Chen LW (2013). LPS-induced proNGF synthesis and release in the N9 and BV2 microglial cells: a new pathway underling microglial toxicity in neuroinflammation. PloS 8(9).

Durafourt BA, Moore CS, Zammit DA, Johnson TA, Zaguia F, Guiot MC ... et al., (2012). Comparison of Polarization Properties of Human Adult Microglia and Blood-Derived Macrophages. Glia 60(5), 717–27.

Eikelenboom P, van Exel E, Hoozemans JJ, Veerhuis R, Rozemuller AJ & van Gool WA (2010). Neuroinflammation—An early event in both the history and pathogenesis of Alzheimer's disease. Neurodegener. Dis. 7, 38–41.

Engelhardt B & Ransohoff RM (2012).Capture, crawl, cross: the T cell code to breach the blood-brain barriers. Trends Immunol. 33, 579–589.

Figuera-Losada M, Rojas C & Slusher BS (2014). Inhibition of Microglial Activation as a Phenotypic Assay in Early Drug Development. J Biomol Screen 19(1), 17-31.

Franco-Bocangegra D, McAuley C, Nicoll JAR & Boche D (2019). Molecular Mechanisms of Microglial Motility: Changes in Aeging and Alzheimer's Disease. Cells 8(6), 639-643.

Frank-Cannon TC, Alto LT, McAlpine FE & Tansey MG (2009). Does neuroinflammation fan the flame in neurodegenerative diseases? Mol Neurodegener 4, 47.

Furgiuele S, Descamps G, Cascarano L, Boucq A, Dubois C, Journe F & Saussez S (2022). Dealing with Marophage Pasticity to Adress Theraputic Challenges in Head and Neck Cancers. Int J Mol Sci. 23(12)63-85

Gadani SP, Cronk JC, Norris GT & Kipnis J (2012). IL-4 in the brain: a cytokine to remember. J Immunol 189(9), 4213–4219.

Geier EG, Chen EC, Webb A, Papp AC, Yee SW, Sadee W & Giacomini KM (2013). Profiling solute carrier transporters in the human blood- brain barrier. Clin. Pharmacol. Ther. 94, 636–639.

Geissmann F, Jung S & Littman DR (2003). Blood monocytes consist of two principal subsets with distinct migratory properties. Immunity. 19, 71–82.

Goenka S & Kaplan MH (2011). Transcriptional regulation by STAT6. Immunol Res. 50(1), 87-96.

Gorman A & Golovanov AP (2022). Lipopolysaccharide structure and the phenomenon of low endotoxin recovery, Eur J Pharm Biopharm. 180, 289-307

Gour N & Wills-Karp M (2015). IL-4 and IL-13 Signalling in Allergic Airway Disease. Cytokine 75(1), 68-78.

Greenlee JE (2023). Introduction to meningitis - brain, spinal cord, and nerve disorders, MSD Manual Consumer Version. MSD Manuals

Guo S, Wang H & Yin Y (2022). Microglia Polarization from M1 to M2 in Neurodegenerative Diseases. Front Aging Neurosci 14, 23-30.

Hansen DV, Hanson JE & Sheng M (2018). Microglia in Alzheimer's disease. J. Cell. Biol. 217, 459-472

Heller NM, Dasgupta P, Dorsey N, Chapoval SP & Keegan AD (2012). The Type I and Type II Receptor Complexes for IL-4 and IL-13 Differentially Regulate Allergic Lung Inflammation. Allergic Diseases 44-62.

Heller NM, Qi X, Junttila IS, Shirey KA, Vogel SN, Paul WE ... et al., (2008). Type I IL-4Rs selectively activate IRS-2 to

Henry CJ, Huang Y, Wynne A, Hanke M, Himler J, Bailey MT, Sheridan F & Godbout JP (2008). Minocycline attenuates lipopolysaccharide (LPS)-induced neuroinflammation, sickness behavior, and anhedonia. J Neuroinflammation 5(1), 15.

Hu X, Li J, Fu M, Zhao X & Wang W (2021). The JAK.STAT signaling pathway: from bench to clinic. Signal Trasduct Target Ther 6, 402-420.

Ishida K, Nagatake T, Saika A, Kaeai S, Node E, Hosomi K & Kunisawa J (2023). Induction of unique macrophages subset by simultaneuous stimulation with LPS and IL-4. Front. Immunol. 14, 1-10.

Isidoro-Garcia M, Davila I, Laffond E, Moreno E, Lorente F & González-Sarmiento R (2005). Interleukin-4 (IL4) and interleukin-4 receptor (IL4RA) polymorphisms in asthma: A case control study - clinical and molecular allergy. BMC 3(15), 1-11

Jäkel S & Dimou L (2017). Glial cells and their function in the Adult Brain: A journey through the history of their ablation', Front Cell Neurosci. 11.

Jang D-I, Lee A-H, Shin H-Y, Song H-R, Park J-H, Kang T-B, Lee S-R & Yang S-H (2021). The role of tumor necrosis factor alpha (TNF-α) in autoimmune disease and current TNF-α inhibitors in therapeutics. Int. J. Mol. Sci. 22(5), 19-27.

Jeong HK, Ji K, Min K & Joe EH (2013). Brain inflammation and microglia: facts and misconceptions. Exp. Neurobio 22(2), 59-67.

Jessen, KR (2004). Glial cells. The international journal of biochemistry & cell biology, 36(10), 1861-1867.

Jiang H, Harris MB & Rothman P (2000). IL-4/IL-13 signaling beyond JAK/STAT. J Allergy Clin Immunol. 105, 1063–70

Jiang Y, Wei N, Lu T, Zhu J, Xu G &Liu X (2011). Intranasal brain-derived neurotrophic factor protects brain from ischemic insult via modulating local inflammation in rats. Neurosci. 172, 398-401

Jurga AM, Paleczna M & Kuter KZ (2020). Overview of general and discriminating markers of differential microglial phenotypes. Front Cell Neurosci. 14, 1-18.

Kaminska B, Mota M & Pizzi M (2016). Signal transduction nad epigenetic mechanisms in the control of microglia activation during neuroinflammation. BBA 1862, 339-351.

Kanazawa H, Ohsawa K, Sasaki Y, Kohsaka S & Imai Y (2002). Macrophage/microglia-specific protein Iba1 enhances membrane ruffling and Rac activation via phospholipase C-gamma-dependent pathway. J Biol Chem. 277(22), 20026–20032

Kany S, Vollrath JT & Relja B (2019). Cytokines in Inflammatory Disease. Int J Mol Sci. 20(23), 10-21.

Keegan AD, Zamorano J, Keselman A & Heller NM (2018). IL-4 and IL-13 Receptor Signaling from 4PS to Insulin Receptor Substrate 2. Front Immunol 9, 87-91.

Kempuraj, D, Thangavel R, Natteru PA, Selvakumar GP, Saeed D, Zahoor H, Zaheer S, Lyser SS & Zaheer A (2016). Neuroinflammation induces neurodegeneration. J. Neurol. Neurosurg. Spine 1(1),1003.

Kobayashi K, Imagama S, Ohgomori T, Hirano K, Uchimura K, Sakamoto K ... et al., (2013). Minocycline Selectively Inhibits M1 Polarization of Microglia. Cell Death 10, 1-12

Kuczewski N, Porcher C, Ferrand N, Fiorentino H, Pellegrino C, Kolarow R, Lessmann V, Medina I & Gaiarsa JL (2008). Backpropagating action potentials trigger dendritic release of BDNF during spontaneous network activity. J Neurosci. 28, 7013

Landis J & Shaw LM (2014). Insulin Receptor Substrate-2 Mediated Phosphatidylinositol-3-kinase Signaling Selectively Inhibits Glycogen Synthase Kinase-3β to Regulate Aerobic Glycolysis J. Biol. Chem. 289, 18603–18613.

Larionov A, Krause A & Miller W (2005). A standard curve based method for relative real time PCR data processing. BMC bioinformatics, 6(62), 1-16

Li H, Jiang T, Li MQ, Zheng XL & Zhao GJ (2018). Transcriptional Regulation of Macrophages Polarization my MicroRNA's. Front Immunol 9, 1175-1183.

Liu Y, Zhou LJ, Wang J, Li D, Ren WJ, Peng J .., et al (2017). TNF-α differentially regulates synaptic plasticity in the hippocampus and spinal cord by microglia-dependent mechanisms after peripheral nerve injury. J. Neurosci. 37, 871- 881.

Lively S & Schlichter LC (2013). The microglial activation state regulates migration and roles of matrix-dissolving enzymes for invasion. J. Neuroinflammation 10, 75.

Lombardi M, Parolisi R, Scaroni F, Bonfanti E, Gualerzi A, Gabrielli M, Kerlero de Rosbo N, Uccelli A, Giussani P, Viani P... et al., (2019). Detrimental and protective action of microglial extracellular vesicles on myelin lesions:

Astrocyte involvement in remyelination failure. Acta Neuropathol. 138, 987–1012.

Ludwig PE, Reddy V & Varacallo M (2022). Neuroanatomy, neurons. NLM

Maguire E, Connor-Robson NC, Shaw B, O'Donoghue R, Stoberl N & Hall-Roberts H (2022). Assaying Microglial Functions In Vitro. Cells 11(21), 4-18.

Maldonado RF, Correira I & Valvano M (2016). Lipopolysaccaride modification in Gram-Negative bacteria during CHrinic Infection. FEMS Microbiol Rev 40(4), 480-493.

Martinez FO & Gordon S (2014). The M1 and M2 paradigm of macrophage activation: time for reassessment. F1000 Prime Rep 6, 13.

May RD & Fung M (2015). Strategies targeting the IL-4/IL-13 axes in disease. Cytokine. 75, 89–116.

Mazuir E, Fricker D & Sol-Foulon N (2021). Neuron–oligodendrocyte communication in myelination of cortical GABAergic cells. Life 11, 216.

McCormick SM & Heller NM (2015). Commentary: IL-4 and IL-13 receptors and signaling. Cytokine, 75(1), 38–50.

Mencel M, Nash M & Jacobson C (2013). Neuregulin upregulates microglial α7 nicotinic acetylcholine receptor expression in immortalized cell lines: implications for regulating neuroinflammation. PloS 8(7).

Miranda M, Morici JF, Zanoni MB & Bekinschtein P (2019). Brain-derived neurotrophic factor: A key molecule for memory in the healthy and the pathological brain. Front. 13, 1-6.

Mittli D, TukacsV, Ravasz L, Csosz E, Kizma T, Kardos J, Juhasz G & Kekesi KA (2023). LPS- induced acute neuroinflammation involving IL-1B signaling leads to proteomic, cellular and network-level changes in the prefrontal cortex of mice. Brain Behav Immun Health. 28 (2023) 1-15.

Mizobuchi H, Yamamoto K, Tsutsui S, Yamashita M, Nakata Y, Inagawa ... et al., (2020). A unique hybrid characteristic having both pro and anti-inflammatory phenotype transformed by repetitive low dose lipopolysaccharide in C8-B4 microglia Sci Rep. 10, 45-89

Mor E, Cabilly Y, Goldshmit Y, Zalts H, Modai S, Edry L, Elroy-Stein O & Shomron N (2011). Species-specific microrna roles elucidated following astrocyte activation. Nucleic Acids Res. 39 (9), 3711-3721

Nair S & Diamond, MS (2015). Innate immune interactions within the central nervous system modulate pathogenesis of viral infections. Curr. Opin. Immunol. 36, 47–53.

Nakagawa Y & Chiba K (2014). Role of microglial M1/M2 polarization in relapse and remission of psychiatric disorders and diseases. MDPI 12,28-48.

Neill DR, Wong SH, Bellosi A, Flynn RJ, Daly M, Langford TK ... et al., (2010). Nuocytes represent a new innate effector leukocyte that mediates type-2 immunity. Nature. 464, 1367-70.

Nelms K, Keegan AD, Zamorano J, Ryan JJ & Paul WE (1999). The IL-4 receptor: signaling mechanisms and biologic functions. Annu Rev Immunol 17, 701-738.

Norden DM, Muccigrosso MM & Godbout JP (2016). Microglial priming and enhanced reactivity to secondary insult in aging, and traumatic CNS injury, and neurodegenerative disease. Neuropharmacology, 96, 29-41.

Ochocka N & Kaminska B (2021). Microglia Diversity in Health and Diseased Brain: Insights from Single-Cell Omics. Int J Mol Sci. 22(6), 32-45.

Oh C, Geba G. & Molfino N. (2010). Investigational therapeutics targeting the IL4/IL13/STAT6 pathway for the treatment of asthma. Eur Respir Rev. 115, 46-54

Ohgidani M, Kato T A, Haraguchi Y, Matsushima T, Mizoguchi Y... et al (2017). Microglial CD206 gene has potential as a state marker of bipolar disorder. Front. Immunol. (7), 676.

Olmos G & Llado J (2014). Tumour necrosis factor alpha: A link between neuroinflammation and excitotoxicity. Mediators Inflamm. 1-24

Orihuela R, McPherson CA & Harry GJ (2016). Microglial M1/M2 polarization and metabolic states. Br. J. Pharmacol. 173, 649–665.

Park HJ, Oh SH, Kim HN, Jung YJ & Lee PH (2016). Mesenchymal stem cells enhance α-synuclein clearance via M2 microglia polarization in experimental and human parkinsonian disorder. Acta Neuropathol. 132, 685–701.

Parkhurst CN, Yang G, Ninan I, Savas JN, Yatwa JR III, Lafaille JJ.., et al (2013). Microglia promote learning-dependent synapse formation through brain-derived neurotrophic factor. Cell 155, 333-345

Peri F & Calabrese V (2014). Toll-like Receptor 4 (TLR4) modulation by synthetic and natural compounds: an update. J Med Chem. 57(9), 3612-3622.

Pierre WC, Smith PLP, Londono I, Chemtom S, Mallard C & Lodygensky GA (2017). Neonatal microglia: the cornerstone of brain fate. Brain Behave. Immun. 59, 333-345

Prinz M, Jung S & Priller J (2019). Microglia Biology: One Century of Evolving Concepts. Cell. 179, 292–311.

Quirié A, Demougeot C, Bertrand N, Mossiat C, Garnier P, Marie C... et al. (2013). Effect of stroke on arginase expression and localization in the rat brain. Eur. J. Neurosci. 37, 1193–1202.

Ranasinghe C, Li SRZ, Khanna M & Jackson RJ (2018). IL-4 and IL-13 Receptors. Encyclopaedia of Signalling Molecules. Pp 2549-2557.

Ranoa DRE, Kelley SL & Tapping RI (2013).Human Lipopolysaccharide-binding Protein (LBP) and CD14 Independently Deliver Triacylated Lipoproteins to Toll-like Receptor 1 (TLR1) and TLR2 and Enhance Formation of the Ternary Signaling Complex. J BiolChem. 288(14), 9729-9741.

Régnier-Vigouroux A (2003). The Mannose Receptor in the Brain. Int Rev Cytol 226, 321–42.

Reinert LS, Lopusna K, Winther H, Sun C, Thomsen MK, Nandakumar R, Mogensen TH, Meyer M, Vaegter C... et al. (2016). Sensing of HSV-1 by the cGAS-STING pathway in microglia orchestrates anti- viral defence in the CNS. Nat. Commun. 7, 13348.

Rodgers KR, Lin Y, Langan TJ, Iwakura Y & Chou RC (2020). Innate Immune Functions of Astrocytes are Dependent Upon Tumor Necrosis Factor-Alpha. Sci. Rep. 10, 1–15.

Rossi C, Cusimano M, Zambito M, Finardi A., Capotondo A., Garcia-Manteiga JM, Comi G, Furlan R, Martino G & Muzio L (2018). Interleukin 4 modulates microglia homeostasis and attenuates the early slowly progressive phase of amyotrophic lateral sclerosis. Cell Death Dis 9(2), 1-16.

Rückerl D, Jenkins S, Laqtom N, Gallagher I, Sutherland T, Duncan S, Buck A & Allen J (2012). Induction of IL-4Rα–dependent microRNAs identifies PI3K/Akt signaling as essential for IL-4–driven murine macrophage proliferation in vivo. Blood 120, 2307-2316.

Rutten S, Schusser GF, Abraham G & Schrodl W (2016). Release kinetics of tumor necrosis factor-alpha and interleukin-1 receptor antagonist in the equine whole blood. BMW Vet. Res. 12, 1-17

Rychlik W (1995) Selection of primers for polymerase chain reaction, Mol. Biotechnol, 3(2)129-134.

Schafer D P, Lehrman EK & Stevens B (2013). The “quad-partite” synapse: microglia-synapse interactions in the developing and mature CNS. Glia 61, 24–36.

Scott TE, Lewis CV, Zhu M, Wang C, Samuel CS, Drummond GR & Kemp- Harper BK (2023). IL-4 and IL-13 induce equivelant expression of traditional M2 markers and modulation of reactive oxygen species in human macrophages. Scientific Reports 13, 2-10.

Seif F, Koshmirsafa M, Aazami H, Mohsenzadegan M, Sedighi G & Bahar M (2017). The role of JAK-STAT signaling pathway and its regulators in the fate of T helper cells. Cell Commun. Signal. 15(23), 1-13.

Sevenich L (2018). Brain-Resident Microglia and Blood-Borne Macrophages Orchestrate Central Nervous System Inflammation in Neurodegenerative Disorders and Brain Cancer. Front. Immunol. 9(697), 1-16.

Shao F, Wang X, Wu H, Wu Q & Zhang (2022). Microglia and Neuroinflammation: Crucial Pathological Mechanisms in Traumatic Brain Injury induced Neurodegenration. Front Agiing Neurosci. (14), 1-11.

Sharma, A., & Changotra, H. (2018). Autophagy Genes (ATG16L1 and IRGM) Variants and Hepatitis B Virus Infection Susceptibility (Doctoral dissertation, Jaypee University of Information Technology, Solan, HP).

Sica A & Mantovani A (2012). Macrophage plasticity and polarization: in vivo veritas. J Clin Invest 122(3), 787–795.

Sivagnanam V, Zhu X & Schlichter LC (2010). Dominance of E. coli phagocytosis over LPS in the inflammatory response of microglia. J. Neuroimmunol. 227, 111–119.

Slanzi A, Lannoto G, Rossi B, Zenaro E & Constantin G (2020). In vitro Models of Neurodegenerative diseases. Front. Cell. Dev. Biol. 1-13.

Stein M, Keshav S, Harris N & Gordon S (1992). Interleukin 4 potently enhances murine macrophage mannose receptor activity: a marker of alternative immunologic macrophage activation. J. Exp. Med. 176, 287–292.

Suzuki A, Leland P, Joshi BH & Puri RK (2015). Targeting of IL-4 and IL-13 receptors for cancer therapy. Vol. 75, Cytokine. 75, 79–88.

Suzuki Y, Shirai M, Asada K, Yasui H, Karayama M, Hozumi H, Furuhashi K, Enomoto N, Fujisawa T, Nakamura Y, Inui N, Shirai T, Hayakawa H & Suda T (2018).

Macrophage mannose receptor, CD206, predict prognosis in patients with pulmonary tuberculosis. Nature News, 1-16

Takeshita Y & Ransohoff RM (2012). Inflammatory cell trafficking across the blood-brain barrier: chemokine regulation and in vitro models. Immunol Rev. 248, 228–239.

Tanaka S, Ohgidani M, Hata N, Inamine S, Sagata N, Shirouzu N, Mukae N, Suzuki SO, Hamasaki H, Hatae R, Sangatsuda Y, Fujioka Y, Takigawa K, Funakoshi Y, Iwaki T, Hosoi M, Iihara K, Mizoguchi M & Kato TA (2021). CD206 expression in induced microglia-like cells from peripheral blood as a surrogate biomarker for the specific immune microenvironment of neurosurgical diseases including glioma. Front. Immunol. 12, 1-5.

Tansey MG & Goldberg MS (2010). Neuroinflammation in Parkinson's disease: its role in neuronal death and implications for therapeutic intervention. Neurobiol Dis. 37(3), 510-521

Veroni C, Gabriele L, Canini I, Castiello L, Coccia E, Remoli ME, Columba-Cabezas S, Aricò E, Aloisi F & Agresti C (2010). Activation of TNF receptor 2 in microglia promotes induction of anti-inflammatory pathways. Mol. Cell. Neurosci. 45, 234–244.

Weller RO (2013). Anatomy of the meninges: structural and functional aspects, p 17–30. In Christodoulides M (ed), Meningitis: cellular and molecular basis. CAB International, Wallingford, Oxfordshire, United Kingdom.

Werner C & Engelhard K (2007). Pathophysiology of traumatic brain injury. Br J Anaesth. 99, 4–9.

Wu J, Ding D, Li Q, Wang X, Sun Y & Li L (2019). Lipoxin A4 Regulates Lipopolysaccharide- Induced BV2 Microglial Activation and Differentiation via the Notch Signalling Pathway. Front. Cell. Neurosci. 13, 19-29.

Yang I, Han SJ, Kaur G, Crane C & Parsa AT (2010). The role of microglia in central nervous system immunity and Glioma Immunology. J Clin Neurosci. 17(1), 6-10.

Yang QQ & Zhou JW (2019). Neuroinflammation in the central nervous system: Symphony of glial cells. Glia. 67,1017–1035

Ye, J., Coulouris, G., Zaretskaya, I., Cutcutache, I., Rozen, S., & Madden, T. L. (2012). Primer-BLAST: a tool to design target-specific primers for polymerase chain reaction. BMC bioinformatics, 13(134), 1-11.

Yin J, Valin KL, Dixon ML & Leavenworth JW (2017). The role of microglia and macrophages in CNS homeostasis, autoimmunity and cancer. J Immunol. Res. 1-12.

Zainuddin A, Chua KH, Abdul Rahim N & Makpol S (2010). Effect of experimental treatment on GAPDH mRNA expression as a housekeeping gene in human diploid fibroblasts. BMC Mol. Biol. 11-59.

Zhang J-M & Jianxiong A (2007). Cytokines, inflammation, and pain. Int Anesthesiol Clin, 45(2), 27-37

Zhou T, Huang Z, Sun X, Zhu X, Zhou L, Li M, Cheng B Lui X & He C (2017). Microglia Polarisation with M1/M2 Phenotype Changes in rd1 Mouse Model of Retinal Degeneration. Front Neuroanat. 11, 77-89.